Systems Biology Determinants of Motor Behavior in Humans

I n a u g u r a l - D i s s e r t a t i o n

zur

Erlangung des Doktorgrades

der Mathematisch-Naturwissenschaftlichen Fakultät

der Universität zu Köln

vorgelegt von

Eva-Maria Pool

aus Kevelaer

2014

Berichterstatter/in: (Gutachter)	Prof. Dr. Ansgar Büschges Prof. Dr. Christian Grefkes
Tag der mündlichen Prüfung:	14. Januar 2015

Table of Content

Zusammenfassung

Die Ausführung von Bewegungen beruht auf einem fein regulierten und dynamischen Zusammenspiel zwischen dem primären motorischen Kortex (M1) und anderen kortikalen und subkortikalen Hirnregionen. Eine Reihe von funktionellen Bildgebungsstudien konnte bereits einen Zusammenhang zwischen dem Grad der Komplexität einer Handbewegung und der neuralen Aktivität innerhalb des sensomotorischen Kortex nachweisen. Neben extrinsisch vorgegebenen Modulationen der motorischen Performanz hängt das Aktivitätsniveau zerebraler Areale auch von intrinsischen Faktoren wie beispielsweise der Händigkeit ab. Händigkeit bezeichnet hier die individuelle Prädisposition, die linke oder rechte Hand bei alltäglichen Bewegungen kontinuierlich der anderen Hand gegenüber vorzuziehen.

Motorisches Verhalten wird jedoch nicht allein durch die Aktivität einzelner zerebraler Areale vermittelt, sondern basiert vielmehr auf der Interaktion dieser Regionen innerhalb des motorischen Netzwerkes. Konnektivitätsanalysen für funktionelle Bildgebungsdaten stellen eine Möglichkeit dar, diese neuralen Prozesse, die dem motorischen Verhalten zu Grunde liegen, auf Netzwerkebene zu betrachten. So erlauben uns Modelle der "effektiven Konnektivität", den Einfluss zu schätzen, den eine neuronale Einheit auf eine andere neuronale Einheit ausübt. Dagegen bezeichnet "funktionelle Konnektivität" die zeitliche Korrelation (oder Kohärenz) zwischen räumlich segregierten neurophysiologischen Prozessen.

Ziel der Dissertation ist es zu untersuchen, wie sich verschiedene Aspekte der Motorik auf die Aktivität und Konnektivität des motorischen Netzwerkes auswirken. In der ersten Studie wurde mittels funktioneller Magnetresonanztomographie (fMRT) und Dynamic Causal Modelling (DCM) die effektive Konnektivität zwischen Schlüsselregionen des motorischen Systems untersucht. Gesunde, rechtshändige Probanden (n=36) hatten dabei die Aufgabe, Faustschlussbewegungen in verschiedenen Frequenzen mit der rechten oder linken Hand durchzuführen. Das aufgestellte Netzwerkmodell setzte sich aus motorischen Regionen beider Hemisphären zusammen, bestehend aus M1, dem supplementär-motorischen Areal (SMA), dem ventrolateralen Prämotorkortex (PMv), dem motorischen Anteil des Putamen sowie dem motorischen Zerebellum. Die Konnektivitätsanalyse zeigte, dass eine Zunahme der Bewegungsfrequenz mit einer linear ansteigenden neuronalen Kopplung der kontralateralen prämotorischen Arealen (SMA, PMv) sowie des ipsilateralen Zerebellums mit dem kontralateralen, “aktiven“ M1 einherging. Andere Verbindungen wurden durch die Veränderung der Bewegungsfrequenz nicht moduliert. Diese Ergebnisse lassen vermuten, dass eine stärkere Kopplung, besonders zwischen prämotorischen Arealen und M1, eine Steigerung der motorischen Leistung einfacher Handbewegungen ermöglicht.

In der zweiten Studie wurde mittels fMRT und DCM die effektive Konnektivität zwischen Schlüsselregionen des motorischen Systems bei Faustschlussbewegungen der dominanten und nicht-dominanten Hand an 18 Rechts- und 18 Linkshändern untersucht. Die Händigkeit wurde mittels des “Edinburgh Händigkeitsinventar“ (EHI) nach Oldfield (1971) erhoben. Das aufgestellte Netzwerkmodell setzte sich, analog zur ersten Studie, aus denselben motorischen Regionen beider Hemisphären zusammen. Die Konnektivitätsanalyse dieser Daten zeigte, dass Rechtshänder bei Bewegung der dominanten Hand eine signifikant stärkere Kopplung der kontralateralen (linken, d.h., dominanten) SMA mit der ipsilateralen SMA, dem ipsilateralem PMv, dem kontralateralem Putamen und dem kontralateralem M1 aufwiesen verglichen mit äquivalenten Verbindungen bei Linkshändern. Darüber hinaus korrelierte die Stärke der Händigkeit, repräsentiert durch die individuellen Lateralitätsquotienten des EHI, mit den Kopplungsparametern dieser Verbindungen. Hingegen waren Frequenzeffekte auf die neuronale Kopplung nicht unterschiedlich zwischen Rechts- und Linkshändern. Zusammenfassend zeigen die Daten, dass Händigkeit mit Unterschieden in der effektiven Konnektivität innerhalb des motorischen Netzwerkes assoziiert ist, wobei die SMA

rechtshändiger Probanden hier eine besondere Rolle einnimmt. Linkshänder weisen eine schwächere Asymmetrie im Hinblick auf die effektive Konnektivität auf. Dies weist auf unterschiedliche Mechanismen der dominanten Hemisphäre zur Kontrolle der motorischen Handfunktion bei Links- im Vergleich zu Rechtshändern, hin.

Allerdings können individuelle Unterschiede bei der Durchführung motorischer Aufgaben möglicherweise auch Störgrößen für aufgabenbasierte fMRT-Studien sein. So kann beispielsweise eine motorische Aufgabe weniger anstrengend für den Probanden sein, wenn diese mit der dominanten Hand anstatt mit der nicht-dominante Hand durchgeführt werden soll, was letztlich durch die neurale Aktivität widergespiegelt wird. “Resting-State“ fMRT bietet eine attraktive Möglichkeit, diese Störgrößen zu umgehen, da Netzwerke unabhängig von einer spezifischen Aufgabe untersucht werden können. In der dritten Studie wurde daher die funktionelle Konnektivität von 18 Rechts- und 18 Linkshänder mittels “Resting-State“ fMRT untersucht. Die Händigkeit wurde mit Hilfe des EHI erhoben. Daraufhin haben wir funktionelle Konnektivitätskarten zwischen dem linken und rechte M1 und allen anderen Regionen berechnet (“seed-based whole-brain functional connectivity maps“). Um den Effekt von Händigkeit auf die funktionelle Konnektivität zu untersuchen, wurden differentielle Kontraste und Regressionsanalysen, in denen der EHI als Kovariate eingeschlossen wurde, berechnet. Darüber hinaus haben wir einen multivariaten linearen “Support Vector Machine“ (SVM) Klassifikations-Algorithmus angewandt, um die individuelle Spezifität der Hirnregionen zu untersuchen, die einen Unterschied zwischen den Resting-State-Karten der Rechts- und Linkshänder zeigen. Die Ergebnisse zeigen, dass Rechtshänder im Vergleich zu Linkshändern, eine stärkere funktionelle Konnektivität zwischen linkem M1 und dorsolateralen Prämotorkortex (PMd), aufweisen. Die Konnektivität mit dem rechten PMd konnte einzelne, unbekannte Rechts- und Linkshänder mit einer Genauigkeit von 86,2% richtig klassifizieren. Kontrollanalysen, in denen nicht-motorische Netzwerke, wie das Broca-Sprachnetzwerk und das visuelle Netzwerk, berücksichtigt wurden, ergaben keine signifikanten Unterschiede in Abhängigkeit der Händigkeit. Eine höhere Konnektivität bei Rechtshändern spiegelt daher einen systematischen Einfluss von Händigkeit auf intrinsischer Ebene wider und könnte erklären, dass Rechtshändigkeit häufig mit einer stärkeren Lateralisierung des Verhaltens einhergeht als Linkshändigkeit. Darüber hinaus dient die erhöhte Konnektivität zwischen M1 und PMd als ein individuelles Klassifikationsmerkmal / Endophenotyp für Händigkeit.

Zusammengefasst zeigen die Ergebnisse, dass die dynamische Modulation im motorischen System sowohl bei Rechts- als auch bei Linkshändern durch den Einfluss prämotorischer Areale auf den M1 kontralateral zur bewegten Hand vermittelt wird. Darüber hinaus zeigen die Daten, dass Unterschiede in der Kopplungsstärke zwischen Rechts- und Linkshändern den Einfluss der Händigkeit sowohl auf die funktionellen als auch auf die effektiven Konnektivität widergespiegeln.

Abstract

Motor skills are mediated by a dynamic and finely regulated interplay of the primary motor cortex (M1) with various cortical and subcortical regions engaged in movement preparation and execution. Several neuroimaging studies already demonstrated that increasing motor performance in simple motor tasks is associated with higher activation levels in the motor system. Additional to the extrinsic modulation of motor performance, neural activity is also influenced by intrinsic factors such as handedness. Handedness – defined as the preference to use one hand over the other – is associated with differences in activation levels in various motor tasks performed with the dominant or non-dominant hand.

However, motor actions are implemented in a distributed network of motor regions rather than a single cortical area. For that reason, it is important to consider the neural processes underlying motor behavior from a network perspective that is offered by connectivity analyses. Models of effective connectivity allow the estimation of the influence that areas exert over each other while functional connectivity is defined as temporal coherence between remote, segregated neurophysiological events.

The present thesis aimed to investigate how the dynamic modulation of motor performance and connectivity is mediated by extrinsic and intrinsic factors in the human motor system. In the first study, we used functional magnetic resonance imaging (fMRI) and dynamic causal modeling (DCM) to investigate effective connectivity of key motor areas at different movement frequencies performed by right-handed subjects (n=36) with the left or right hand. The network of interest consisted of motor regions in both hemispheres including M1, supplementary motor area (SMA), ventral premotor cortex (PMv), motor putamen, and motor cerebellum. The connectivity analysis showed that performing hand movements at higher frequencies was associated with a linear increase in neural coupling strength from premotor areas (SMA, PMv) contralateral to the moving hand and ipsilateral cerebellum towards contralateral, active M1. In addition, we found hemispheric differences in the amount by which the coupling of premotor areas and M1 was modulated, depending on which hand was moved. Other connections were not modulated by changes in motor performance. The results suggest that a stronger coupling, especially between contralateral premotor areas and M1, enables increased motor performance of simple unilateral hand movements.

In the second study, we used fMRI and DCM to investigate effective connectivity between key motor areas during fist closures of the dominant or non-dominant hand performed by 18 right- and 18 left-handers. Handedness was assessed employing the Edinburgh-Handedness-Inventory (EHI). The network of interest consisted of key motor regions in both hemispheres including M1, SMA, PMv, motor putamen and motor cerebellum. The connectivity analysis revealed that in right-handed subjects movements of the dominant hand were associated with significantly stronger coupling of contralateral (left, i.e., dominant) SMA with ipsilateral SMA, ipsilateral PMv, contralateral motor putamen and contralateral M1 compared to equivalent connections in left-handers. The degree of handedness as indexed by the individual EHI scores also correlated with coupling parameters of these connections. In contrast, we found no differences between right- and left-handers when testing for the effect of movement speed on effective connectivity. In conclusion, the data show that handedness is associated with differences in effective connectivity within the human motor network with a prominent role of SMA in right-handers. Left-handers featured less asymmetry in effective connectivity implying different hemispheric mechanisms underlying hand motor control compared to right-handers.

However, differences in task performance are inherent putative confounds for all task based fMRI studies. For example, performing a standard motor task might be less demanding when using the dominant hand compared to the non-dominant hand, which may also affect

neural activation levels, e.g., in frontoparietal areas. Thus, resting-state fMRI seems an attractive approach to overcome these putative confounds as it allows investigating networks independent from performance. In the third study, we, therefore, scanned 18 right- and 18 left-handers with resting-state fMRI. Handedness was assessed by the EHI. We computed whole-brain functional connectivity maps of the left and right M1. To test for the effect of handedness, we computed differential contrasts and regression analyses including EHI as a covariate. We further used a multivariate linear support vector machine (SVM) classifier algorithm to reveal the individual specificity of brain regions showing differences between the resting-state maps of right- and left-handers. Using left M1 as a seed region revealed stronger interhemispheric functional connectivity between M1 and dorsolateral premotor cortex (PMd) in right-handers as compared to left-handers. Furthermore, this individual cluster in right PMd classified right- and left-handers with 86.2% accuracy. Control analyses using non-motor resting-state networks, including the (Broca) speech and the visual network, revealed no significant differences in functional connectivity related to handedness. Higher connectivity in right-handers might, therefore, reflect a systematic impact of handedness on an intrinsic functional level and might explain the observation that right-handedness is usually more lateralised than left-handedness. Furthermore, enhanced connectivity between M1 and PMd serves as an individual marker / endophenotype of handedness.

In summary, the present thesis demonstrates that the dynamic modulation of the motor system during motor performance is mediated by a specific set of brain regions in both right- and left-handers. Furthermore, the results indicate that differences in coupling strength between right- and left-handers reflect the impact of handedness on both functional and effective connectivity.

I Introduction

1.1 The human motor system

Voluntary movements depend on the well-tuned interplay of excitatory and inhibitory influences between neurons of cortical and subcortical structures within the human motor system. The primary motor cortex (M1) corresponds to Brodmann Area (BA) 4 (Brodmann, 1909) and is located in the anterior wall of the central sulcus. Cytoarchitectonically, BA4 is characterized by absence of lamina IV and presence of giant Betz pyramidal cells in cortical layer V (Brodmann, 1909; Vogt and Vogt, 1919), whose axons bend down in the precentral gyrus and form the cortico-spinal tract (CST) (Strick, 1988). The CST passes through the posterior limb of the internal capsule before 70-90% of the fibres cross below the medullary pyramids in the brain stem to the contralateral side, referred to as lateral CST. The remaining fibers cross further caudal at the level of the spinal cord segment of their target cells, referred to as ventral CST. The pyramidal cells innervate motor neurons, directly or indirectly via interneurons, in the anterior horn of the spinal cord whose motoneurons finally terminate onto skeletal muscles. The human extra-pyramidal motor system is composed of the basal ganglia, cerebellum, and extra-pyramidal fibre tracts connecting the motor cortex with motor brain stem nuclei and the spinal cord, respectively. M1 has a somatotopic organization, with different regions of the cortex engaged in the control of face, arm, and leg movements. Accordingly, foot and leg representations are located in the mesial wall of the precentral gyrus followed by trunk, arm, hand, fingers (from little finger to thumb), face, lips, and tongue representations from dorsomedial to ventrolateral (Penfield and Rasmussen, 1950).

The premotor cortex (BA6) is an important cortical motor area located anterior to M1. BA6 can be subdivided into three distinctive functional areas, the supplementary motor area (SMA), the dorsal premotor cortex (PMd), and the ventral premotor cortex (PMv). Cytoarchitectonic and histochemical data from macaque monkeys allow a modern parcellation of the agranular frontal isocortex in seven subregions (F1-F7; “F” for “frontal”) (Matelli et al., 1985, 1991) (Figure 1). The mesial part of BA6 is subdivided into F3 (SMA) and F6 (pre-SMA). F2 and F7 are located in the superior part of BA6 (PMd) while F4 and F5 are located in the inferior BA6, (PMv). Finally, F1 basically corresponds to BA4 (M1).

Invasive studies further investigated the functional properties of these areas. For example, tract tracing studies in macaques showed that the premotor areas (SMA, PMd, PMv) have extensive projections to the hand area in M1 (Dum and Strick, 2005; Shimazu et al., 2004)

and are hence important network nodes in the cortical motor system enabling hand movements (Dum and Strick, 2002, 2005). Single-cell recording data further showed that a large proportion of SMA neurons solely respond to contralateral hand movements (Kazennikov et al., 1999), thereby suggesting a specific role for lateralized hand movements. There is also evidence from lesion studies in monkeys that a damage of SMA is associated with deficits in internally remembered motor sequences and the generation of self-initiated hand movements (Halsband and Passingham, 1985). Likewise, neuroimaging studies in humans described the involvement of SMA in many unimanual tasks, especially for movement sequencing and internal pacing (Jakobs et al., 2009; Jenkins et al., 2000; Passingham, 1989).

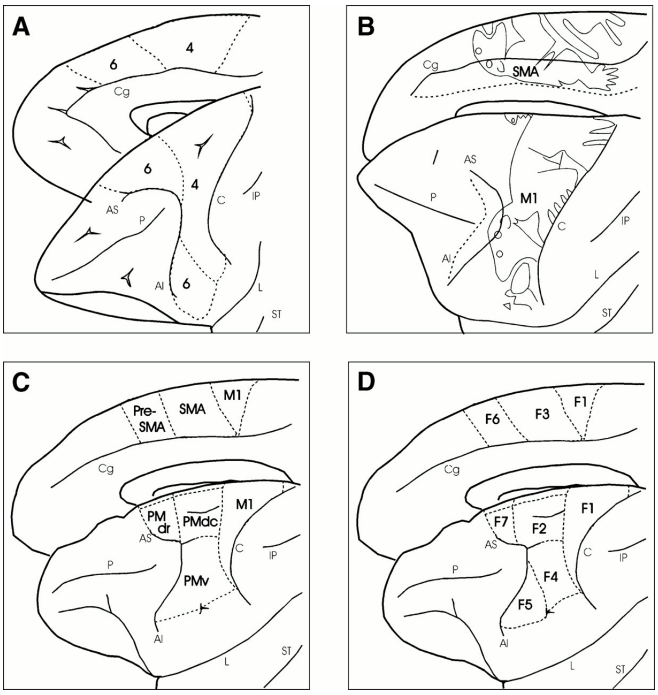

Figure 1. Comparative view of subdivisions of the agranular frontal cortex of the monkey **A:** cytoarchitectonic map of Brodmann (1909) **B:** functional map of Woolsey et al. (1952) **C:** modern, functional subdivision of Matelli et al. (1985) **D:** histochemical and cytoarchitectonic map of Matelli et al. (1985).
AI=inferior arcuate sulcus; AS=superior arcuate sulcus; C=central sulcus; Cg=cingulate sulcus; F1–F7=agranular frontal areas; IP=intraparietal sulcus; L=lateral fissure; M1=primary motor cortex; P=principal sulcus; PMdc=dorsal premotor cortex, caudal; PMdr=dorsal premotor cortex, rostral; PMv=ventral premotor cortex; SMA=supplementary motor area; ST=superior temporal sulcus.
Source: Luppino & Rizzolatti 2000

The premotor cortex (PM) is involved in the preparation and organization of movements (Wise, 1985). Direct comparisons of neuronal activity in PMd and PMv further revealed a fundamental difference in their functional properties. Several tract-tracing studies provide

evidence that the preparatory activity facilitates the initiation of arm movements according to predetermined motor parameters (Churchland and Shenoy, 2007; Churchland et al., 2006; Hoshi and Tanji, 2006). This is also supported by animal lesion studies revealing deficits in selecting correct movements when conditional but not spatial cues were presented after muscimol, a potent agonist of $GABA_A$ receptors, was injected (Kurata and Hoffman, 1994), indicating that PMd contributes to both preparation and selection of movements. In contrast, PMv neurons reflect the visuospatial information of a visual cue and are involved in the visual guiding of movements for reaching a target in space or grasping an object (Hoshi and Tanji, 2006; Kubota and Hamada, 1978; Raos et al., 2006). Furthermore, a lesion of PMv induces deficits in grasping objects without an impairment of finger movements (Fogassi et al., 2001). Several neuroimaging studies in humans supported the functional relevance of premotor cortex in movement planning and execution of externally triggered movements, especially in transforming external sensory stimuli into motor programs (Johnson et al., 1996; Kawashima et al., 1994; Schubotz and von Cramon, 2001).

Beside these cortical areas, subcortical brain regions such as basal ganglia and cerebellum are regarded as motor structures as well. The basal ganglia include the striatum consisting of caudate nucleus and putamen, the external and internal segment of the globus pallidus, the subthalamic nucleus and the substantia nigra (Smith et al., 1998). The projections of the motor circuit to the basal ganglia are focused on the motor putamen which play as central role in the facilitation and inhibition of motor actions (Alexander and Crutcher, 1990). The putamen receives somatotopic projections from the sensorimotor cortex (Alexander and Crutcher, 1990). Lesion studies suggested a role of the putamen in the selection and automatic performance of previously learned movements (Griffiths et al., 1994).

The cerebellum is linked to the cerebral cortex via two-stage feedforward and feedback systems. It receives input from the motor cortex via the pontine nuclei (Alexander and Crutcher, 1990; Stoodley and Schmahmann, 2010). In contrast, the motor modules in the anterior part of the cerebellum project back to M1 via the ventrolateral thalamus (Ramnani, 2006; Stoodley and Schmahmann, 2010). Several lesion studies in animals and humans demonstrated that the cerebellum is essential for the integration of isolated movements into a skillfully executed and timely coordinated ensemble (Goodkin et al., 1993; Hardiman et al., 1996; Ramnani, 2006). The cerebellar nuclei further influence lower centres via the rubrospinal tract, a major descending pathway that begins in the red nucleus and terminates on the motoneurons in the spinal cord (Cheney et al., 1991; Ramnani, 2006). Thus, cerebellar output influences spinal mechanisms involved in motor control (Ramnani, 2006).

Structural connectivity between these cortical and subcortical motor regions was validated by invasive tracer studies in macaque monkeys revealing both homotopic and heterotopic transcallosal connections between M1, SMA, PMv and PMd, putamen and cerebellum in macaque monkeys (Akkal et al., 2007; Boussaoud et al., 2005; Hoshi et al., 2005; Kelly and Strick, 2003; Luppino et al., 1993; McGuire et al., 1991; Middleton and Strick, 2000; Rouiller et al., 1994).

1.2 Neural coupling within the human motor network

Motor actions are mediated by interplay of various brain regions engaged in different aspects of movement preparation and execution. As demonstrated by several previous neuroimaging studies, increasing motor performance in simple motor tasks is associated with higher activation levels in motor areas (Dettmers et al., 1995; Dettmers et al., 1996; Jäncke et al., 1998a; Jäncke et al., 1998b; Nakai et al., 2003; Rao et al., 1996; Schlaug et al., 1996; Witt et al., 2008). For example, Jäncke and colleagues found a linear relationship between BOLD response within the left sensorimotor cortex and movement frequency when investigating the effects of different movement speeds on neural activity changes in the sensorimotor cortex (Jäncke et al., 1998a). Lutz and colleagues revealed rate-dependent effects on neural activity not only for M1 but also for the cerebellum (Lutz et al., 2000). However, motor actions are implemented in a distributed network of motor regions rather than a single cortical area (Boudrias et al., 2012; Eickhoff and Grefkes, 2011; Grefkes et al., 2008). That is why in the last decades, connectivity analyses offering a network perspective on the neural processes underlying motor behavior became more and more important in order to reveal the physiological correlates of motor behavior. Especially models of effective connectivity allow the estimation of the influence that areas exert over each other (Friston, 1994). For example, effective connectivity studies using fMRI and DCM demonstrated that performing fist closures with the right or left hand increases neural coupling between premotor areas and M1 contralateral to the moving hand (Boudrias et al., 2012; Eickhoff et al., 2008; Grefkes et al., 2008). Consistently, the analysis of effective connectivity in electroencephalographic (EEG) data confirmed that finger movements elicit a context-specific increase in neuronal coupling in the gamma band, especially among premotor regions and between premotor cortex and M1 (Herz et al., 2012). Lin and colleagues investigated regional interactions in a network including M1, SMA, cerebellum, thalamus and basal ganglia using fMRI and showed that both the left and the right corticocerebellar and corticostriate circuits are modulated by different movement rates (Lin et al., 2009). These findings suggest that motor behavior also

depends on how effectively higher motor areas interact with M1 (i.e., the primary motor output region of the cerebral cortex). However, to date we still know very little about the network interactions that enable the modulation of motor performance in healthy subjects.

1.3 Anatomical and functional brain asymmetry

Almost 90% of the people exhibit a bias to use their right hand for most activities that is consistent across the historical record and across cultures (Annett, 1985; Porac and Coren, 1981). Interestingly, preferred hand use can be observed at embryonic and fetal stages in humans, long before language ability is developed. Ultrasound studies have shown that most fetuses prefer to suck their right thumb at 15 weeks (Hepper et al., 1991). Heppner and colleagues followed up this study of 75 individuals and found that the 60 fetuses that preferred to suck their right thumb were right-handed as teenagers, whereas 10 of the 15 fetuses that preferred to suck their left thumb, were left-handed as teenagers (Hepper, 2013; Hepper et al., 2005b). Hence, brain asymmetry is present as soon as the fetus engages in behavior that could exhibit laterality suggesting a regulation by intrinsic controls at early stages of life. Experimental evidence further suggests that this intrinsic behavioral phenomenon is associated with asymmetries in the structural and functional organization of the cerebral cortex. For example, Amunts and colleagues investigated morphometric differences in the adult brain using magnetic resonance imaging (MRI), and demonstrated a deeper central sulcus in the left compared to the right hemisphere in both right- and left-handers (Amunts et al., 1996). Interhemispheric comparisons further revealed a significantly larger M1 representation of the hand and finger area contralateral to the preferred hand (Volkmann et al., 1998). Solodkin and colleagues mapped brain activation patterns in right- and left-handers during single and sequential finger movements and found larger volumes of activation and less hemispheric lateralization in left-handers (Solodkin et al., 2001). The latter finding is compatible with behavioral data demonstrating that hand preference in left-handers is often expressed to a lesser degree than in right-handers (Borod et al., 1984).

However, hemispheric asymmetry of the brain is not only limited to handedness. Since Paul Broca described left-hemisphere language regions in right-handed patients in the 1860s, lesions to this area produce a wide range of deficits known collectively as Broca's aphasia. This brain area that is mostly located on the posterior region of the left inferior frontal gyrus (Brodmann areas 44 & 45) and controls speech is today known as *Broca's area*. Several neuroimaging studies already observed that approximately 95% of healthy right-handed subjects show a left-hemispheric dominance for language. Whereas the hand preferred for

manual skills is contralateral to the dominant language hemisphere in most of the right-handers, this relation cannot be commonly observed in left-handers. Several studies early demonstrated a reduced functional asymmetry for language in left-handers (Goodglass and Quadfasel, 1954; Ratcliff et al., 1980; Satz, 1979; Steinmetz et al., 1991). Pujol and colleagues used fMRI to define the occurrence of left-hemisphere, bilateral, and right-hemisphere language activation during a word generation task in 100 healthy right- and left-handers (Pujol et al., 1999). The authors observed that 70% of the left-handers have left cerebral dominance while 30% show a right hemisphere dominance or a bilateral pattern of language dominance (Pujol et al., 1999). Furthermore, Knecht and colleagues revealed that a large majority of humans show a left-hemispheric dominance for the control of speech functions, independent of whether they prefer the right or left hand for manual skills (Knecht et al., 2000).

A quantitative evaluation method of handedness is the Edinburgh Handedness Inventory (EHI) according to Oldfield (1971). This 10-item questionnaire is designed to assess handedness by self-report of the preferred hand for carrying out common activities such as writing and drawing, striking a match, and using utensils such as a toothbrush, knife, and spoon. Subjects are asked to place either one (+) or two (++) check marks under "left" or "right" indicating the strength of preference for each activity. In case that the subject "would never try to use the other hand unless absolutely forced to" for the given activity, two checks have to be placed. As some activities require the use of both hands, the directions specify which movement component reflects hand preference (e.g., striking a match: the hand that holds the match). In the next step, a laterality quotient (LQ) can be calculated as followed, based on the number of checks for right or left hand preference:

$$LQ = \frac{\sum right - \sum left}{\sum right + \sum left}$$

The LQ ranges from a score of 100 (completely right-handed) to a score of −100 (completely left-handed). An LQ > 25 indicates right-handedness, and an LQ < −25 indicates left-handedness (Pujol et al., 1999).

1.4 Functional magnetic resonance imaging (fMRI)

Functional magnetic resonance imaging (fMRI) is a non-invasive brain-mapping method that makes use of the blood-oxygenation-level-dependent (BOLD) effect (Ogawa et al.,

1990). The BOLD signal that is usually measured in fMRI studies is determined by hemodynamic changes. Activated neurons induce a regional increase in cerebral blood flow (CBF) and that exceeds the concomitant increase in oxygen consumption rate ($CMRO_2$) since oxygen uptake is diffusion-limited (Fox et al., 1988). The magnetic susceptibility of blood is influenced by the concentrations of diamagnetic oxyhemoglobin and paramagnetic deoxyhemoglobin (Figure 2).

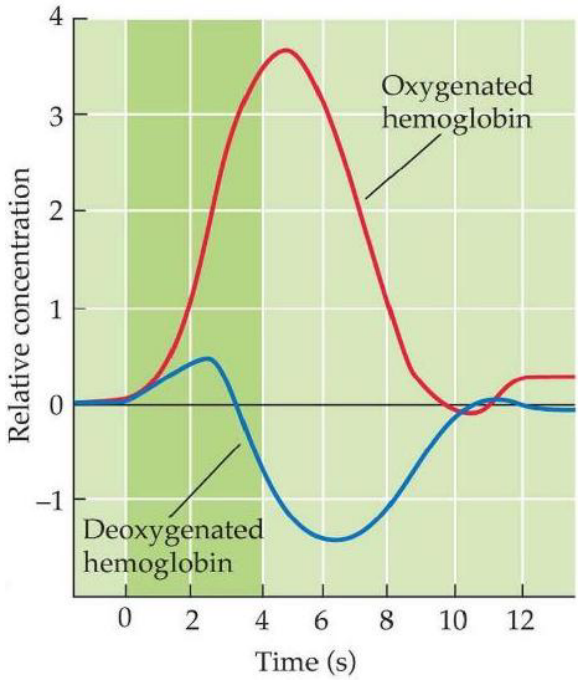

Figure 2. Changes in oxyhemoglobin and deoxyhemoglobin. After stimulus presentation, oxyhemoglobin concentration increases. Changes in deoxyhemoglobin concentration are biphasic displaying a small early increase shortly after stimulus onset, followed by a decrease below pre-stimulus baseline.
Source: © Psychology Press.

After a neuronal event, deoxyhemoglobin initially increases slightly and, therefore, causes the "initial dip" of the hemodynamic response function (HRF), followed by an increase of oxygen delivery ($CMRO_2$), cerebral blood flow (CBF), and cerebral blood volume (CBV). The CBF increases by a larger fraction than the $CMRO_2$ (Fox et al., 1988), resulting in a decrease of the oxygen extraction fraction and, thereof, a decrease of local deoxyhemoglobin.

Thus, the fMRI BOLD signal slightly increases, as a result of an oversupply of oxyhemoglobin relative to deoxyhemoglobin. The blood oxygenation level finally returns to its initial baseline level and the BOLD signal decays to levels slightly below baseline (undershoot) before returning to its initial baseline level (Heeger and Ress, 2002). This

neurovascular response has a delay of 3-6s and is regionally variable. When investigating the neuronal origin of the BOLD signal, Logothetis and colleagues demonstrated that the BOLD effect directly reflects the neuronal response evoked by a sensory stimulus (Logothetis et al., 2001). The authors observed that the BOLD signal was more related to local field potentials (LFPs) representing the dendro-somatic components of the input signals in neuronal populations rather than spiking activity (Logothetis et al., 2001).

The analysis of fMRI data comprises data preprocessing and statistical analysis. The data preprocessing usually consists of (1) spatial realignment to correct for spatial displacements induced by head movements during scanning, (2) spatial co-registration to link functional scans to a high-resolution anatomical scan, (3) spatial normalization to fit images to the standard brain template of the Montreal Neurological Institute (MNI, Canada) which allows for group comparisons, and finally (4) spatial smoothing to increase the signal-to-noise ratio (i.e., a measure of signal strength relative to background noise) and, therefore, to increase the statistical power (Smith, 2001).

For the statistical analysis of each individual subject (first-level analysis), the variation of fMRI signal in each voxel is modelled as a linear combination of experimental conditions and an error term by using a mass-univariate General Linear Model (GLM) (Kiebel and Holmes, 2007). The experimental regressors consist of onsets of experimental conditions convolved with an HRF model to account for the temporal delay of the hemodynamic response. The regression weights are parameters that are separately estimated for each voxel and experimental condition. Statistical analyses on estimated parameters are performed based on T- or F-contrasts. The result is a statistical map showing significantly activated voxels given a certain linear combination of regressors. The individual contrast parameters estimates of the first level analysis then serve as the new dependent variable, instead of the raw data, and are entered into a multi-subject second-level analysis (group-analysis). Since the analysis at the second level explicitly models the variability of the estimated effects across subjects, the obtained significant results can be generalized to the population from which subjects were drawn as a random sample.

1.5 Brain connectivity

Specific ways of analysing BOLD fMRI data also allows us to compute how anatomically connected areas functionally or effectively interact with each other. Functional connectivity is defined as temporal correlation between spatially remote neurophysiological events (Friston, 1994) and is usually computed from low-frequency (<0.1Hz) resting-state fMRI data, that is,

during wakeful rest, but in the absence of active task performance. Resting-state fMRI is, therefore, an independent modality and an attractive approach to understand networks in the human brain, independent of an overt motor task. In contrast to this non-directional, correlative nature of functional connectivity, effective connectivity refers to the causal influences that brain areas exert over another under the assumptions of a given system theoretic perspective (Friston, 1994; Stephan et al., 2007). Effective connectivity is usually employed for active tasks as opposed to resting states although there are recent applications of DCM for resting-state fMRI (Friston et al., 2014). One method to investigate effective connectivity is dynamic causal modeling (DCM), a hypothesis-driven approach that estimates interactions in a pre-defined network of brain regions based on anatomically motivated hypotheses about their connections (Penny et al., 2004). DCM uses a biophysically validated hemodynamic forward model to explain changes in neural activity evoked by a given task where the changes in neuronal states over time are modelled as

$$\frac{dx}{dt} = (A + \sum_{j=1}^{m} u_j B^{(j)})x + Cu$$

where x is the state vector, A represents the endogenous (intrinsic) connectivity, B(j) represent the condition-specific modulations of the region driven by the input function u, and C represents the influence of direct inputs to the system. When combining DCM with fMRI both the neuronal and the hemodynamic parameters are estimated from the measured BOLD data using an iterative Bayesian algorithm to optimize an approximation of both the model evidence (i.e. likelihood of the model given the data) and the posterior density (i.e. likelihood of the data given the parameters for a particular model) (Friston et al., 2003). Statistical inference is drawn from the maximum *a posteriori* estimates and posterior covariances of the posterior density function. A recent study reported moderate to excellent test–retest reliability of DCM coupling parameters (Schuyler et al., 2010).

II Objectives

The present thesis aimed to investigate how the dynamic modulation of motor performance and connectivity is mediated by extrinsic and intrinsic factors in the human motor system. Three studies were performed to answer the following questions.

(i) How does the brain modulate motor performance?

Different fMRI studies demonstrated that an increasing movement frequency is associated with stronger neural activity, especially in the contralateral primary sensorimotor cortex (Jäncke et al., 1998a; Sadato et al., 1996). Lesion studies already revealed that motor impairments are related to reduced coupling between premotor and primary motor cortex (Fridman et al., 2004; Johansen-Berg et al., 2002; Rehme et al., 2011a; Wang et al., 2011). Therefore, we hypothesized that the frequency-dependent modulation of motor performance is associated with an increase of the neural coupling within the motor system, especially between contralateral premotor areas and M1.

(ii) Is the preference to use the right or left hand in everyday life reflected by systematic differences in network interactions during unimanual movements?

Handedness is an important intrinsic factor that determines motor skills of the hands. Several neuroimaging studies already investigated handedness effects and observed differences in neural activity related to the dominance of the moving hand (Jäncke et al., 1999; Kloppel et al., 2007). However, to date little is known about hand preference and the dynamics of the motor network. In order to investigate the effect of handedness on network dynamics, we compared a group of right-handed with a group of left-handed subjects in neural activity, connectivity and motor performance. We assumed a difference between the neural couplings of the motor network during dominant as compared to non-dominant hand movements that might explain the behavioural notion that left-handers tend to be more flexible in the use of both the dominant and non-dominant hand.

(iii) Does handedness influence resting-state functional connectivity?

When comparing two groups, putative differences in task performance (either in absolute performance measures or in hidden parameters like attention and effort) are inherent confounds in basically all task-dependent fMRI studies (Lowe et al., 1998; Yan et al., 2012).

Resting-state fMRI is an attractive approach to investigate networks in the human brain as it is independent from such performance confounds. It allows us to focus on differences between right- and left-handers in neural states that are not – or at least partially – influenced by differences in demands or performance imposed by the respective task. According to previous studies revealing a hemispheric asymmetry related to handedness during motor performance (Haaland et al., 2004; Jäncke et al., 1998a; Solodkin et al., 2001), we hypothesized that these differences within the human motor network between right- and left-handers are already represented on an intrinsic functional level of the brain and might, therefore, reflect biological markers of handedness.

In the first study (Pool et al., 2013), we scanned a group of healthy right-handed subjects (n=36) using fMRI to assess the interactions among motor areas during the execution of fist closures with the right or left hand at three different frequencies: (i) 0.75 Hz, (ii) 1.5 Hz, and (iii) 3.0 Hz, yielding six experimental conditions. Effective connectivity, i.e., the causal influence that one area exerts upon activity of another (Friston et al., 2003), was estimated by means of DCM for a bihemispheric network consisting of key areas of the cortical motor system engaged in hand movements, i.e., M1, SMA and PMv as well as subcortical motor areas including the putamen and cerebellum (Witt et al., 2008).

In the second study (Pool et al., 2014a), we investigated whether there are differences in neural activity and interregional interaction of key motor regions between right- (n=18) and left-handers (n=18), as assessed by the EHI (Oldfield, 1971). Again, subjects were asked to perform fist closures with the right or left hand at different movement frequencies (0.75 Hz, 1.5 Hz, and 3.0 Hz). DCM was used to assess effective connectivity during unimanual movements of the dominant and non-dominant hands at different frequencies for a bihemispheric network consisting of key motor areas that were already included in Pool et al., 2013.

In the third study (Pool et al., 2014b), we scanned 36 healthy volunteers (18 right-handers, 18 left-handers) with resting-state fMRI. To test whether effects were specifically related to the motor system, we also investigated resting-state connectivity maps of the visual system and the language system using the primary visual cortex (V1) and the pars triangularis of the inferior frontal gyrus (IFG) as seed regions. According to previous studies revealing a hemispheric asymmetry related to handedness during motor performance (Haaland et al., 2004; Jäncke et al., 1998a; Solodkin et al., 2001), we hypothesized that differences within the human motor network between right- and left-handers can already be detected in absence of

an overt motor task. Furthermore, we used a multivariate linear support vector machine (SVM) classifier algorithm (Chang and Lin, 2011) to reveal the individual specificity of brain regions showing differences between the resting-state maps of right- and left-handers.

III Publications

3.1 Network dynamics engaged in the modulation of motor behavior in healthy subjects.
Eva-Maria Pool, Anne K. Rehme, Gereon R. Fink, Simon B. Eickhoff, Christian Grefkes
Neuroimage (2013). 82C, 68-76.

3.2 Handedness and effective connectivity of the motor system.
Eva-Maria Pool, Anne K. Rehme, Gereon R. Fink, Simon B. Eickhoff, Christian Grefkes
Neuroimage (2014). 99, 451-460.

3.3 Functional resting-state connectivity of the human motor network: Differences between right- and left-handers
Eva-Maria Pool, Anne K. Rehme, Gereon R. Fink, Simon B. Eickhoff, Christian Grefkes
(under review)

3.1

Network dynamics engaged in the modulation of motor behavior in healthy subjects.

Eva-Maria Pool, Anne K. Rehme, Gereon R. Fink, Simon B. Eickhoff, Christian Grefkes

Neuroimage (2013). 82C, 68-76.

NeuroImage 82 (2013) 68–76

Contents lists available at SciVerse ScienceDirect

NeuroImage

journal homepage: www.elsevier.com/locate/ynimg

Network dynamics engaged in the modulation of motor behavior in healthy subjects

Eva-Maria Pool [a], Anne K. Rehme [a], Gereon R. Fink [b,c], Simon B. Eickhoff [c,d], Christian Grefkes [a,b,*]

[a] Neuromodulation & Neurorehabilitation, Max Planck Institute for Neurological Research, 50931 Cologne, Germany
[b] Department of Neurology, University of Cologne, 50931 Cologne, Germany
[c] Institute of Neuroscience and Medicine (INM-1, INM-3), Jülich Research Centre, 52428 Jülich, Germany
[d] Institute of Clinical Neuroscience and Medical Psychology, Heinrich Heine University, 40225 Düsseldorf, Germany

ARTICLE INFO

Article history:
Accepted 29 May 2013
Available online 6 June 2013

Keywords:
Dynamic causal modeling
Effective connectivity
Movement frequency
Premotor cortex
Cerebellum

ABSTRACT

Motor skills are mediated by a dynamic and finely regulated interplay of the primary motor cortex (M1) with various cortical and subcortical regions engaged in movement preparation and execution. To date, data elucidating the dynamics in the motor network that enable movements at different levels of behavioral performance remain scarce. We here used functional magnetic resonance imaging (fMRI) and dynamic causal modeling (DCM) to investigate effective connectivity of key motor areas at different movement frequencies performed by right-handed subjects (n = 36) with the left or right hand. The network of interest consisted of motor regions in both hemispheres including M1, supplementary motor area (SMA), ventral premotor cortex (PMv), motor putamen, and motor cerebellum. The connectivity analysis showed that performing hand movements at higher frequencies was associated with a linear increase in neural coupling strength from premotor areas (SMA, PMv) contralateral to the moving hand and ipsilateral cerebellum towards contralateral, active M1. In addition, we found hemispheric differences in the amount by which the coupling of premotor areas and M1 was modulated, depending on which hand was moved. Other connections were not modulated by changes in motor performance. The results suggest that a stronger coupling, especially between contralateral premotor areas and M1, enables increased motor performance of simple unilateral hand movements.

Introduction

Motor actions are based upon an interplay of brain regions engaged in different aspects of movement preparation and execution. Several neuroimaging studies demonstrated that increasing motor performance in simple motor tasks is associated with higher activation levels in the motor system (Dettmers et al., 1995; Dettmers et al., 1996; Jancke et al., 1998a; Jancke et al., 1998b; Jancke et al., 1999; Nakai et al., 2003; Rao et al., 1996; Schlaug et al., 1996; Witt et al., 2008). For example, Jancke and colleagues investigated the effects of different movement speeds on neural activity changes in the sensorimotor cortex and found a linear relationship between blood oxygen level dependent (BOLD) response within the left sensorimotor cortex and movement frequency (Jancke et al., 1998a). In a more recent study, Lutz and colleagues reported movement rate effects at the neural activity level not only for the primary motor cortex (M1) but also for the cerebellum (Lutz et al., 2005). However, motor actions are implemented in a distributed network of motor regions rather than a single cortical area (Boudrias et al., 2012; Eickhoff and Grefkes, 2011; Grefkes et al., 2008a; Jancke et al., 1998a; Jancke et al., 1998b). A network perspective on the neural processes underlying motor behavior is offered by connectivity analyses. Especially models of effective connectivity allow the estimation of the influence that areas exert over each other (Friston, 1994). For example, effective connectivity studies using functional magnetic resonance imaging (fMRI) and dynamic causal modeling (DCM, Friston et al., 2003) demonstrated that performing fist closures with the right or left hand increases neural coupling between premotor areas and M1 contralateral to the moving hand (Boudrias et al., 2012; Eickhoff et al., 2008; Grefkes et al., 2008a). Consistently, analysis of effective connectivity of electroencephalographic (EEG) data confirmed that finger movements elicit a context-specific increase in neuronal coupling in the gamma band, especially among premotor regions and between premotor cortex and M1 (Herz et al., 2012). Moreover, Lin and colleagues used fMRI data to investigate regional interactions in a network including M1, supplementary motor area (SMA), cerebellum, thalamus and basal ganglia, and showed that both the left and the right corticocerebellar and corticostriate circuits are modulated by different movement rates (Lin et al., 2009). These findings suggest that motor behavior also depends on how effectively higher motor areas interact with M1 (i.e., the primary motor output region of the cerebral cortex). However, to date we still know very little about the network interactions that enable the modulation of

* Corresponding author at: Department of Neurology, University Hospital Cologne, Kerpener Straße 62, 50937 Cologne, Germany. Fax: +49 221 478 7005.
E-mail address: christian.grefkes@uk-koeln.de (C. Grefkes).

1053-8119/$ – see front matter © 2013 Elsevier Inc. All rights reserved.
http://dx.doi.org/10.1016/j.neuroimage.2013.05.123

motor performance in healthy subjects. This information is important not only to further our understanding of the neural mechanisms underlying motor behavior, but also from a clinical point of view in order to identify new potential targets in neurorehabilitation, e.g., for non-invasive brain stimulation (Grefkes and Fink, 2012).

We, therefore, scanned a group of healthy right-handed subjects (n = 36) using fMRI to assess the interactions among motor areas during the execution of unimanual hand movements consisting of visually paced fist closures at different movement frequencies. Effective connectivity was estimated by means of DCM for a bihemispheric network consisting of key areas of the cortical motor system engaged in hand movements, i.e., M1, SMA and the ventrolateral premotor cortex (PMv) as well as subcortical motor areas including the putamen and cerebellum (Witt et al., 2008). According to previous neuroimaging studies, we hypothesized that higher movement speed evokes a stronger BOLD signal especially in the contralateral primary sensorimotor cortex (Jancke et al., 1998b; Sadato et al., 1996). Furthermore, given the role of the premotor cortex for better motor skills in patients with brain lesions, we assumed that higher task performance was associated with stronger connectivity of premotor areas (SMA, PMv) with M1 (Fridman et al., 2004; Johansen-Berg et al., 2002; Rehme et al., 2011; Wang et al., 2011).

Material and methods

Subjects

The study was approved by the ethics committee of the Medical Faculty, University of Cologne, Germany, and performed in accordance with the Declaration of Helsinki. Thirty-six right-handed subjects (14 males; 22–34 yrs old; mean age 26.2 ± 2.7 SD) with no history of neurological or psychiatric diseases gave written informed consent. Handedness was assessed by the Edinburgh-Handedness-Inventory (EHI) (Oldfield, 1971).

fMRI design

For motor system activation, we used a block-design task where subjects were asked to perform fist closures with their right or left hand at three different frequencies: (i) 0.75 Hz, (ii) 1.5 Hz, and (iii) 3.0 Hz, yielding six experimental conditions. Our pre-experimental tests showed that fist closure frequencies higher than 3.0 Hz are often beyond the motor skills of the subjects, while movement frequencies lower than 0.75 only yield very weak levels of BOLD activity. However, robust activation on a single subject level is an important technical prerequisite for region-of-interest based approaches like DCM.

The task was presented on a shielded thin-film transistor (TFT) screen at the rear end of the scanner which was visible via a mirror mounted on the MR head coil. Written instructions ("right hand" or "left hand") were displayed for 2 s indicating which hand had to be moved in the upcoming block of trials. Then, the instruction text was replaced by a white circle which started to blink in red color at one of the three frequencies (i.e., 0.75 Hz/1.5 Hz/3.0 Hz) and the subjects were asked to perform fist closures at that frequency until the circle disappeared. Blocks of fist closures (15 s) were separated by resting baselines (15 s plus a temporal jitter of 1–2.5 s) in which a black screen instructed the subjects to rest until the next instruction text appeared. Each condition was repeated five times throughout the experiment. The sequence of blocks was pseudo-randomized for each subject. The whole experiment consisted of 30 blocks and lasted ~18 min. Compliance of the subjects in the scanner was documented by an experimenter standing next to the subject and counting the number of fist closures per block. Subjects were familiarized with the task twice, first outside the scanner, then inside the scanner. Each subject was able to perform the task without difficulties after a few practice trials due to the relative simplicity of the motor task (excluding relevant learning effects).

Image acquisition and processing

Functional MR images were acquired on a Siemens Trio 3.0 T scanner using a gradient single-shot echo planar imaging (EPI) sequence with the following parameters: repetition time (TR) = 2000 ms, echo time (TE) = 3.0 ms, field of view (FOV) = 220 × 220 mm, flip angle = 90°, voxel size = 3.4 × 3.4 × 3.4 mm^3, volumes = 550 (3 dummy images), slices = 32, and interslice gap = 1 mm. Image slices were acquired in ascending order covering the whole brain from the cerebellum to vertex. In addition, high-resolution T1-weighted structural images were acquired (TR = 2250 ms, TE = 3.93 ms, FOV = 256 mm, voxel size = 1.0 × 1.0 × 1.0 mm^3, slices = 176).

All analyses (fMRI, DCM) were carried out using SPM8 (http://www.fil.ion.ucl.ac.uk; release 2009). After realignment of the EPI volumes and co-registration with the anatomical T1-weighted image, all volumes were spatially normalized to the standard template of the Montreal Neurological Institute employing the unified segmentation approach (Ashburner and Friston, 2005). Finally, data were smoothed using an isotropic Gaussian kernel of 8 mm full-width-at-half-maximum.

For the statistical analysis, box-car vectors for each condition were convolved with a canonical hemodynamic response function as implemented in SPM8 to create the regressors of interest in the framework of the general linear model (GLM). We pursued a parametric analysis approach in order to identify neural activity that was modulated by different levels of movement frequency. Accordingly, SPMs were computed on a single subject level with onset regressors for each hand (right hand, left hand) and respective parametric regressors (1st order polynomial expansion) coding the frequency of a given condition (0.75 Hz, 1.5 Hz, and 3.0 Hz). The time series in each voxel was high-pass filtered at 1/128 Hz to remove low frequency drifts. Movement parameters as assessed by the realignment algorithm were treated as covariates to exclude movement-related variance from the image time series. Furthermore, the temporally jittered instruction period was separately modeled as an additional regressor (thus separated from all the resting and the movement conditions), but not further analyzed in the group analysis. The parameter estimates for all four conditions (main effect "right hand movements", parametric modulation "right hand movements", main effect "left hand movements", parametric modulation "left hand movements") were subsequently compared between subjects (n = 36) in a full factorial analysis of variance (ANOVA). Voxels were considered significant when passing a height threshold of $T > 4.7$ ($P < 0.05$, family wise error (FWE)-corrected at the voxel level).

Dynamic causal modeling

We used deterministic bilinear DCM (Friston et al., 2003) to assess effective connectivity between the regions activated by the motor task. DCM is a hypothesis-driven approach to model effective connectivity between distinct brain regions, resulting in three sets of parameters: (i) the endogenous coupling irrespective of the actual experimental condition (DCM A-matrix), (ii) parameters for context-dependent changes in coupling evoked by the experimental condition (here: the 2 main effects of hand movements (left, right) and the 2 parametric conditions) (DCM B-matrix), and (iii) the direct experimental input to the system that drives regional activity (DCM C-matrix).

As DCMs are computed on the single subject level, we extracted the first eigenvariate of the BOLD time-series, adjusted for effects of no interest, from 10 regions-of-interest (ROIs) at subject specific coordinates. ROIs were defined as spheres (radius: 4 mm) centered upon individual activation maxima based on individually normalized SPMs. Left hemispheric ROIs were identified by using a conjunction analysis across all three movement frequencies of the right hand, while ROIs in the right hemisphere were identified in a conjunction

analysis of the corresponding left hand conditions. The ROIs consisted of M1, SMA, PMv, motor putamen and motor cerebellum, representing core regions of the motor system (Witt et al., 2008). We chose PMv as ROI rather than PMd as PMv neurons are especially engaged in grasping hand movements, while PMd neurons are predominantly engaged in arm/reaching movements (Grefkes and Fink, 2005; Rizzolatti and Luppino, 2001; Rottschy et al., 2012). The preference of PMv for hand motor function was also reflected by the BOLD fMRI data of the present study which clearly showed a separable PMv cluster while PMd was only weakly activated, and the area of activation extended typically into the M1 activation cluster (Fig. 1A).

As individual activation maxima may vary across subjects (Eickhoff et al., 2009), we ensured comparability by selecting coordinates according to the following anatomical constraints: M1 on the rostral wall of the central sulcus at the "hand knob" formation (Yousry et al., 1997), SMA on the mesial wall within the interhemispheric fissure between the paracentral lobule (posterior landmark) and the anterior commissure (Picard and Strick, 2001), PMv situated in the precentral sulcus close to the inferior precentral gyrus and pars opercularis (Rizzolatti et al., 2002), the mediolateral central part of the putamen (Put) (Nambu et al., 2002) and the superior part of the anterior lobe of the cerebellum (Cb) (Diedrichsen et al., 2009). All ROIs were extracted in each subject from both hemispheres using a threshold of $P < 0.001$ (uncorrected). The coordinates of all individual ROIs are given in Supplemental Table 1. Based on structural connectivity data derived from invasive studies in macaque monkeys (Akkal et al., 2007; Boussaoud et al., 2005; Hoshi et al., 2005; Kelly and Strick, 2003; Luppino et al., 1993; Middleton and Strick, 2000; Rouiller et al., 1994), we assumed endogenous connections (DCM A-matrix) as specified in Table 1. Note that connections between the cerebellum and cortical areas are relayed via the thalamus, and hence the coupling parameters from and to the cerebellum reflect the 'net effect' of this disynaptic connection. This notion also applies for any other indirect connection captured by the coupling parameters. We furthermore assumed a direct effect of the motor task (DCM C-matrix, input regions) on the activity of all premotor regions (left/right SMA, left/right PMv) (Goldman-Rakic et al., 1992; Wang et al., 2011).

Table 1
Anatomical references for endogenous connectivity (DCM A-matrix).

Connection	Reference
SMA → PMv	Luppino et al. (1993)
SMA → M1	Rouiller et al. (1994)
SMA → Put	Akkal et al. (2007)
SMA → Cb	Akkal et al. (2007)
PMv → SMA	Boussaoud et al. (2005)
PMv → M1	Rouiller et al. (1994)
PMv → Put	Middleton and Strick (2000)
PMv → Cb	Middleton and Strick (2000)
M1 → SMA	Rouiller et al. (1994)
M1 → PMv	Rouiller et al. (1994)
M1 → Put	Middleton and Strick (2000)
M1 → Cb	Middleton and Strick (2000)
Put → SMA	Kelly and Strick (2003)
Put → PMv	Middleton and Strick (2000)
Put → M1	Middleton and Strick (2000)
Put → Cb	Hoshi et al. (2005)
Cb → SMA	Akkal et al. (2007)
Cb → PMv	Middleton and Strick (2000)
Cb → M1	Middleton and Strick (2000)
Cb → Put	Hoshi et al. (2005)

SMA = supplementary motor area, PMv = ventral premotor cortex, M1 = primary motor cortex, Put = putamen, Cb = cerebellum.

Bayesian model selection

Based on the DCM A-matrix, we set up alternative models of varying complexity representing biologically plausible hypotheses on interregional coupling among ROIs during movements of the right or left hand at different frequencies (DCM B-matrix). Starting from a fully connected DCM B-matrix with 90 connections, we constructed 31 models according to (i) the presence of interhemispheric connections, and (ii) the lateralization of coupling towards M1 contralateral to the moving hand (Supplemental Fig. 1). At first, we omitted heterotopic interhemispheric connections between the premotor areas, putamen, cerebellum and M1 (models 2–5), then we successively removed heterotopic interhemispheric connections between the cortical and subcortical motor areas (models 6–11) as well as homotopic connections between the motor areas (models 12–16). Finally, all interhemispheric connections were removed (model 16), resulting in very simple models with only a few connections. Afterwards, the same strategy was applied to lateralized models which contained connections only towards M1 contralateral to the moving hand (models 17–31). We then used random effects Bayesian model selection (BMS) to identify the model with the highest posterior evidence, that is, the model which is the most likely generative model given the data (Stephan et al., 2009).

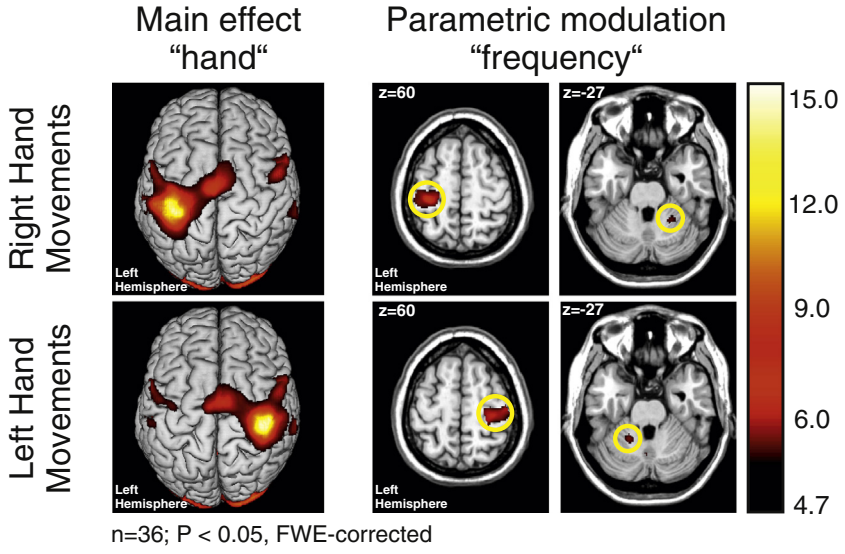

Fig. 1. Neural activity for visually paced fist closures (main effect "hand") and the parametric modulation of "frequency" (n = 36; $P < 0.05$, FWE-corrected).

Statistical analysis of DCM coupling parameters

The resulting DCM coupling parameters were tested for statistical significance using a one sample *t*-test ($P < 0.05$, Bonferroni-corrected for multiple comparisons). Connections that were linearly modulated by different hand movement frequencies were identified in the DCM B-matrix representing parametric modulation effects for movements of the right or left hand (separately). In order to test whether there was a difference in movement-dependent modulation between the left and the right hand, coupling strengths of corresponding connections were compared using paired t-tests.

Results

Neural activity during unilateral hand movements

Visually paced fist closures of the right or left hand (independent of movement frequency) were associated with enhanced BOLD activity in a network of cortical and subcortical areas comprising the contralateral primary motor cortex (M1), bilateral supplementary motor area (SMA), bilateral ventral and dorsal premotor cortex (PMv), bilateral basal ganglia, bilateral anterior lobe of the cerebellum, and bilateral primary visual cortex (V1) ($P < 0.05$, FWE-corrected, Fig. 1). Furthermore, activity was detected in somatosensory regions (S1, S2), thalamus, and extrastriate cortex.

When testing for the effect of different movement frequencies (0.75 Hz, 1.5 Hz, and 3.0 Hz) on BOLD activity levels during movements of the right and the left hand, we found significant effects for clusters of voxels situated in contralateral M1 as well as in ipsilateral cerebellum. Hence, activity in these areas positively correlated with higher movement frequencies (Fig. 1; $P < 0.05$, FWE-corrected on the voxel level). There were no significant negative correlations between BOLD activity and different hand movement frequencies.

Connectivity analysis

Model selection

According to the random-effects Bayesian model selection, the fully connected model (model 1) showed the highest exceedance probability of all tested models and was hence considered the most likely generative model given the data (Fig. 2).

Endogenous coupling (DCM A-matrix)

Fig. 3 displays the coupling parameters for the endogenous (i.e., movement-independent) part of connectivity among the motor areas of interest ($n = 36$; $P < 0.05$, Bonferroni-corrected; see also Supplemental Table 2). The coupling parameters represent connection strengths, describing how fast and strong a response occurs in the target region (Friston et al., 2003). Positive coupling parameters (green arrows) suggest a facilitation of neural activity, whereas negative coupling parameters (red arrows) can be interpreted as inhibition of neural activity.

The endogenous coupling of neural activity among the motor areas was symmetrically organized across both hemispheres for most of the regions of interest (Fig. 3, Supplemental Table 2). The most pro-minent positive influence on intrinsic M1 activity was exerted by SMA. In contrast, the endogenous coupling between PMv, putamen, cerebellum, and ipsilateral M1 was less pronounced. Transcallosal interactions between both M1 revealed a negative coupling in both directions.

Task-dependent coupling (DCM B-matrix)

Fig. 4 depicts the effect of unilateral fist closures on the interregional coupling in the motor system (DCM B-matrix) ($P < 0.05$, Bonferroni-corrected; see also Supplemental Table 3). When subjects moved their right hand, neural activity in the contralateral "active" M1 was driven by stronger bilateral coupling with SMA, PMv, putamen, and cerebellum. In contrast, the influence of contralateral SMA to M1 ipsilateral to the moving hand was negative suggesting that activity of the "inactive" M1 was inhibited. Movements of the left hand evoked a similar but mirror-reversed pattern of motor network modulations. Note that putative differences between corresponding connections in the figures result from threshold effects due to the Bonferroni correction procedure (but which were present at uncorrected *P*-values, e.g., the "missing" coupling between contralateral PMv and ipsilateral M1 during left hand movements).

Frequency-dependent changes of neural coupling

Fig. 5 summarizes connections that were frequency-dependent, i.e., for which coupling strengths co-varied with different movement frequencies ($P < 0.05$, Bonferroni-corrected; see also Supplemental Table 3). Here, green arrows indicate a positive correlation with higher movement frequencies while red arrows denote a negative correlation. The DCM analysis revealed that higher frequencies were associated with a stronger coupling exerted from contralateral SMA, contralateral PMv and ipsilateral PMv on the contralateral "active" M1 during right hand movements. Moreover, we found a frequency-dependent effect for the interhemispheric, excitatory influence from ipsilateral cerebellum on M1. In contrast, the inhibitory influence from contralateral SMA towards the ipsilateral "inactive" M1 decreased with higher movement frequencies, suggesting disinhibition of M1 activity with higher demands on motor performance. During left hand movements, a similar albeit mirror-reversed pattern of modulation within the motor network was observed.

Testing for differences in the amount by which these connections were modulated revealed that frequency-dependent increases in M1 coupling were stronger for the left SMA compared to the left PMv for movements of the right hand ($P = 0.012$). In contrast, there was no significant difference for the equivalent connections during movements of the left hand. This can be explained by a statistical trend of a stronger parametric coupling between the right PMv and right M1 during movements of the left hand compared to the coupling between the left PMv and left M1 during right hand movements ($P = 0.058$). Therefore, our data suggest that hemispheric effects impact on frequency-dependent modulations of connectivity in the motor system.

Discussion

The aim of the present study was to investigate the impact of movement speed on effective connectivity within the human motor system. The DCM analysis suggests that stronger activation levels in M1 observed at faster hand movements are driven by stronger driving influences exerted by the premotor regions (SMA, PMv) and cerebellum. In addition, we found hemispheric differences such that moving the right hand with higher frequency was associated with a stronger increases in SMA–M1 coupling compared to PMv–M1 coupling, while those effects were absent for movements of the left hand in our sample of right-handed subjects. In summary, these data suggest that increases of movement speed are mediated by increases in M1 connectivity with a few but specific areas within the motor system with changes in both facilitatory and inhibitory neural coupling across the two hemispheres.

Neural activity and frequency dependence

In line with previous studies, our fMRI data revealed a movement rate-dependent increase of neural activity within the contralateral M1 and the ipsilateral cerebellum during both right and left hand movements (Jancke et al., 1998a; Rao et al., 1996; Sadato et al., 1997; Schlaug et al., 1996). This increase in activity can be attributed to a recruitment of more motor units with higher movement frequency which will result in a stronger BOLD signal in the respective regions (Jancke et al., 1998b). In addition, more sensory feedback from muscle spindles and joint receptors also contribute to higher

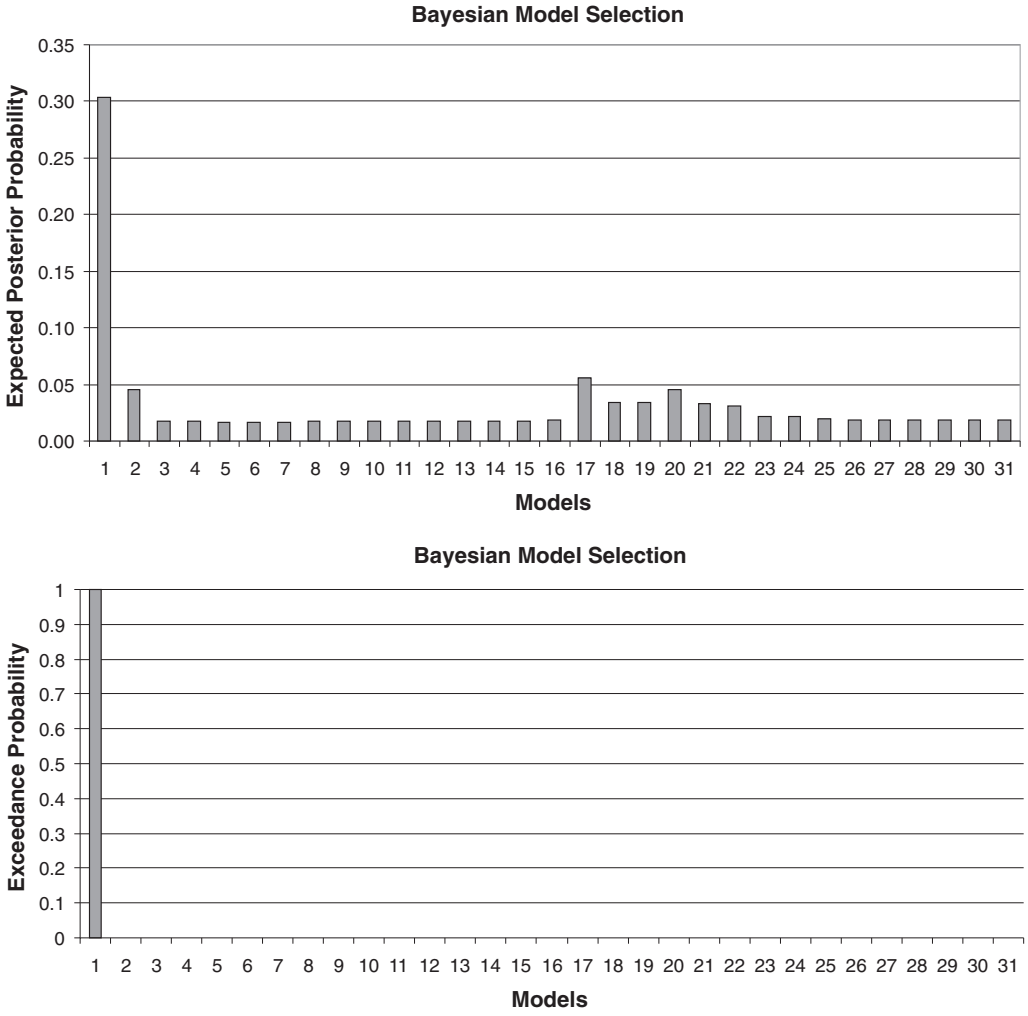

Fig. 2. Bayesian model selection: results.

BOLD signal in M1 (mediated by projections from the somatosensory cortex to Brodmann area 4 neurons; Geyer et al., 2000; Grefkes et al., 2001) and the cerebellum with faster hand movements (Fig. 1).

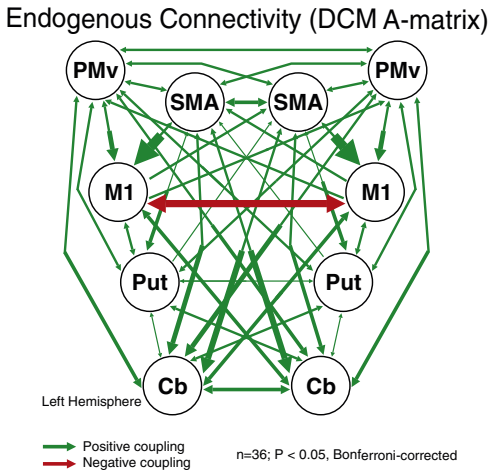

Fig. 3. Endogenous connectivity (DCM A-matrix; n = 36; $P < 0.05$, Bonferroni-corrected). Green arrows = positive coupling rates and red arrows = negative coupling rates. The width of each arrow corresponds to the coupling strength. For mean coupling parameters and *P*-values (one-sample *t*-test against zero) see Supplemental Table 2.

Neural coupling and frequency dependence

SMA and PMv

The studies discussed above suggest that increases in movement speed (i.e., increased movement frequencies) are driven by stronger activity in the primary sensorimotor cortex. In the present study, we pursued a systems perspective approach in order to provide a mechanistic explanation of such frequency-dependent effects found for M1 activity (and cerebellar activity, respectively). Therefore, we focused our analysis on core regions of the motor system activated by the motor paradigm including M1, premotor areas (SMA, PMv) as well as subcortical motor regions (putamen and cerebellum). Tract tracing studies in macaques showed that both PMv and SMA have extensive projections to the hand area in M1 (Dum and Strick, 2005; Shimazu et al., 2004) and are hence important network nodes in the cortical motor system enabling hand movements (Dum and Strick, 2002, 2005). Invasive cell recordings in macaque monkeys demonstrated that a majority of SMA neurons are selective for the use of either the ipsilateral or contralateral arm (Hoshi and Tanji, 2004). Single-cell recording data further showed that a large proportion of SMA neurons solely respond to contralateral hand movements (Kazennikov et al., 1999), thereby suggesting a specific role for lateralized hand movements. Neuroimaging experiments with human subjects described the involvement of the SMA in many unimanual tasks, especially for movement sequencing and internal pacing (Jakobs et al., 2009; Jenkins et al., 2000; Passingham, 1989). Transcranial magnetic stimulation (TMS)

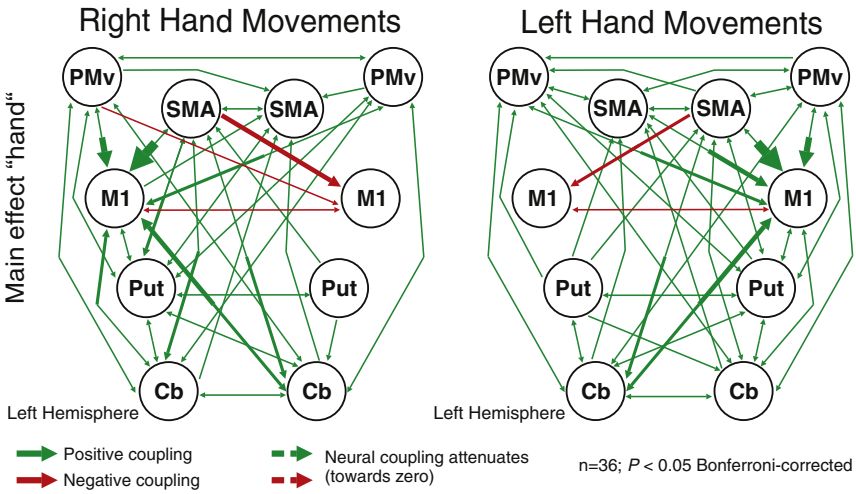

Fig. 4. Modulatory effects on effective connectivity (main effect "hand") during right and left hand fist closures (DCM B-matrix; n = 36; $P < 0.05$, Bonferroni-corrected). Green arrows = positive coupling rate and red arrows = negative coupling rates. The width of each arrow corresponds to the coupling strength. For mean coupling parameters and *P*-values (one-sample *t*-test against zero) see Supplemental Table 3.

studies using a double-pulse protocol revealed an excitatory influence from SMA on M1 activity, reflected by a higher motor evoked potential (MEP) amplitude during M1 stimulation after pre-conditioning SMA activity with TMS (Arai et al., 2012). These findings suggest a direct influence of the SMA on the recruitment of motor units in M1, which is compatible with the driving influence between SMA and M1 as revealed by the present fMRI effective connectivity analysis (Fig. 4).

Furthermore, a recent electrophysiological study analyzed the activity of individual neurons in the SMA before and during reaching movements in macaques and demonstrated that the firing rate of SMA neurons positively correlated with the complexity of the dynamics of the upcoming movement (Padoa-Schioppa et al., 2004). Moreover, Tankus and colleagues conducted single-unit recordings in human patients undergoing evaluation for epilepsy surgery requiring implantation of electrodes in the SMA region (Tankus et al., 2009). These data revealed a strongrelation between firing rate in the SMA and speed of hand movement (Tankus et al., 2009). Our DCM analysis suggests that these speed-dependent modulations in SMA activity directly impact on M1 activity. Interestingly, we also observed a release of inhibition exerted by SMA on ipsilateral M1 (Fig. 5). Other studies suggested that increasing difficulty levels in sensorimotor tasks lead to a stronger recruitment of ipsilateral motor areas in order to facilitate motor output (Seidler et al., 2004). However, whether the disinhibition of M1 ipsilateral to the moving hand is *causally* involved in higher motor performance cannot be answered with the present study. This hypothesis could be addressed in future studies, e.g., by interfering with ipsilateral M1 activity, e.g., by means of non-invasive brain stimulation techniques like TMS. Neuroimaging and connectivity analyses similar to those of the present study could then help to disentangle the neural consequences of such an intervention.

A new finding of the present study was that not only SMA but also the ventral portion of the lateral premotor cortex modulates M1 activity

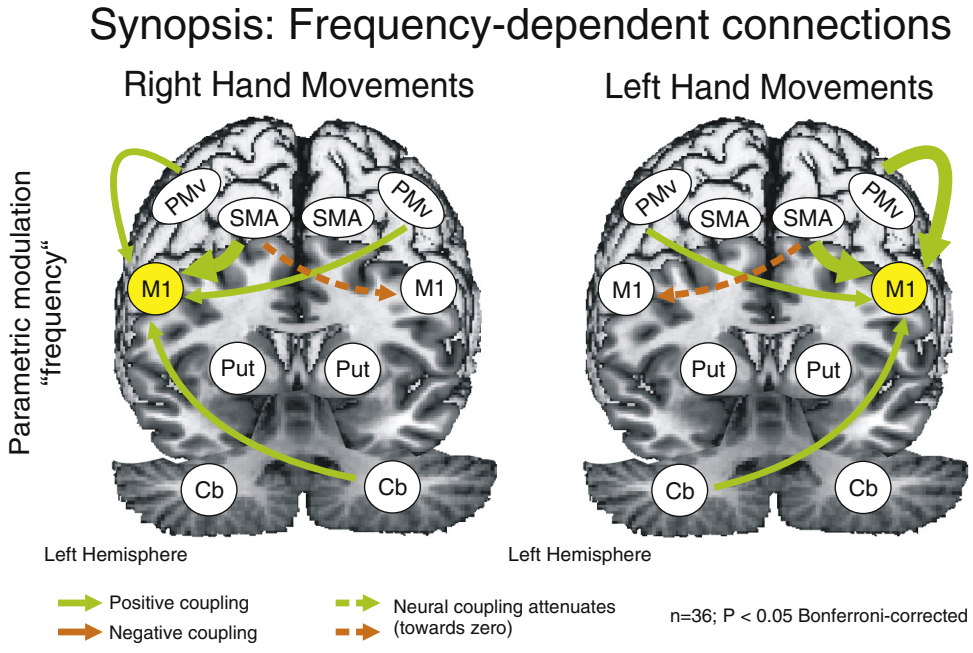

Fig. 5. Parametric modulation of "frequency" during right and left hand fist closures (n = 36; $P < 0.05$, Bonferroni-corrected).

in a frequency-dependent mode. The lateral premotor cortex can be classified into a number of subregions based on anatomical and functional criteria (Rizzolatti et al., 2002; Tokuno and Tanji, 1993). Invasive neurophysiological studies in macaques demonstrated that neurons in ventral portions of the premotor cortex (PMv) are involved in planning and execution of hand and finger movements during grasping (Hoshi and Tanji, 2007; Kubota and Hamada, 1978). Importantly, PMv has the most dominant single corticocortical input into the M1 hand area compared to all other premotor regions (Dum and Strick, 2005). Electrophysiological studies in macaques showed that discharge activity can be detected in PMv (but not in M1) neurons even before a grasping movement is performed (Umilta et al., 2007). Shimazu and colleagues investigated the mechanisms underlying PMv–M1 excitatory interactions by implanting arrays of fine microwires in PMv and M1 and demonstrated that activation of PMv was associated with a facilitation of macaque M1 corticospinal output (Shimazu et al., 2004). This strong PMv–M1 interaction is in line with our connectivity data and supports the pivotal role of PMv for skilled movements of the hands (Rizzolatti et al., 1998). The role of PMv as well as the SMA in hand motor performance has already been suggested by a number of connectivity studies which investigated patients suffering from brain lesions. For example, Rehme et al. demonstrated that higher neural coupling between SMA, PMv, and M1 correlates with better motor performance in stroke patients suffering from hand motor deficits (Rehme et al., 2011). Behavioral improvements of hand motor function following pharmacological stimulation (Wang et al., 2011) or repetitive TMS (Grefkes et al., 2010) also correlated with an increase in neural coupling between SMA, PMv, and M1. The present study adds to these findings by showing that even in healthy subjects a tight relationship exists between premotor-M1 connectivity and modulation of motor performance (as reflected by differences in hand movement frequencies). Therefore, our data are well in line with the hypothesis that reduced motor performance after brain lesions is caused not only by the lesion itself but also from less effective interactions among cortical motor regions remote from the anatomical damage.

Putamen and cerebellum

In addition to cortical areas, anatomical structure like the basal ganglia and the cerebellum constitute critical regions for sustaining and controlling motor performance. We, therefore, also included subcortical areas like the putamen and the cerebellum in the connectivity matrix (Fig. 4). Both the putamen and cerebellum were positively coupled with M1 activity. The putamen receives somatotopic projections from the sensorimotor cortex and is involved in the facilitation and inhibition of actions (Alexander and Crutcher, 1990). Lesion studies further suggested a role of the putamen in the selection and automatic performance of previously learned movements (Griffiths et al., 1994). As the task in the present study is highly overlearned (due to its relative simplicity), we interpret putaminal activity to reflect such automatization processes during the execution of stereotypic fist closures.

The cerebellum receives input from the motor cortex via the pontine nuclei. In contrast, the motor modules in the anterior lobule of the cerebellum project back to M1 via the ventrolateral thalamus (Ramnani, 2006). Several lesion studies in animals and humans demonstrated that the cerebellum is essential for the integration of isolated movements into a skillfully executed and timely coordinated ensemble (Goodkin et al., 1993; Hardiman et al., 1996; Ramnani, 2006). This cerebellar function for motor control might explain its role in the motor task of the present study as here a timing of hand movements in the rhythm of the blinking visual cue is necessary for correct task performance. Our connectivity data identified a frequency-dependent influence from ipsilateral cerebellum on contralateral M1 for both right and left hand movements (Fig. 5). These data nicely fit the findings from invasive electrophysiological studies in macaques which demonstrated that the cerebellar output towards M1 increases with higher task complexity (van Kan et al., 1993). It is well conceivable that increasing movement speed relies on regulatory influences of the cerebellum on motor cortex activity (van Kan et al., 1993), as suggested by the connectivity results of the present study. Moreover, Lin et al. recently investigated functional and effective connectivity of the motor system by combining generalized partial least squares (gPLS) with subsequent structural equation modeling (SEM) and revealed that path weights to and from the cerebellum are associated with changes of movement frequency (Lin et al., 2009). This is in agreement with our results and suggests that the cerebellum plays a pivotal role in sensorimotor integration and temporal organization of movement as outlined above. Interestingly, the coupling of the putamen with M1 was not significantly different at higher hand movement frequencies. This finding indicates that movement automatization for this overlearned simple motor task did not differ between conditions (Poldrack et al., 2005).

Hemispheric differences in frequency dependent modulation of connectivity

Movements of the right or left hand elicited frequency-dependent effects in corresponding connections. However, we found hemispheric differences in the amount by which these connections were modulated. Here, especially the modulation of SMA–M1 and PMv–M1 coupling depended on whether subjects moved their right (dominant) hand or left (non-dominant) hand. Invasive electrophysiological recordings in humans have already demonstrated left–right differences in functional properties of the SMA (Fried et al., 1991). In addition, neuroimaging studies frequently reported a dominant role of the left SMA in right-handed subjects (Babiloni et al., 2003; Jancke et al., 2000). We found a similar effect with respect to frequency-dependent modulations, i.e., a stronger (i.e., "more dominant") effect of the left SMA–M1 coupling compared to PMv–M1 coupling during movements of the right hand, while there was no difference for the corresponding connections during movements of the left hand. This finding raises the interesting hypothesis that hand preference and hemispheric dominance are founded in differences in motor-cortical connectivity. However, an answer to this and other questions related to connectivity and handedness can only be provided when investigating a cohort of left-handed subjects, which was beyond the scope of the present study, but should be performed in future studies.

Limitations and conclusion

One limitation of the present study pertains to the limited number of areas included in the connectivity model. While other areas in prefrontal as well as parietal cortex undoubtedly contributed to the control of even simple hand movements (Cieslik et al., 2012), we restricted the areas to include "key" regions of the motor system. In the present study, we increased the model complexity from the default value of 8 regions to 10 regions. In DCM, model complexity is penalized by more conservative shrinkage priors which make it more difficult for a given connection to become significant. In other words, priors on the connectivity parameters ensure that the system remains stable (Friston et al., 2003). Therefore, that we found significant connections despite a rather more complex model highlights the robustness of the data which is also owing to the fact that we focused on motor system activity which at the single subject level yields high BOLD activation effects in the regions of interest, especially in a block design. The coupling results and their general pattern are, therefore, very similar to what has been published on motor system DCM in previous studies using an 8-region model (Grefkes et al., 2008b; Rehme et al., 2011; Rehme et al., 2013; Wang et al., 2011). However, the situation might be different in other functional systems with more variable BOLD signal changes, e.g., encountered for prefrontal regions in more "cognitive" tasks.

Moreover, a greater spectrum of frequency conditions might have yielded an even more elaborated analysis of frequency-dependent connections, e.g., with respect to non-linear effects. However, we focused on "extreme" frequencies (very slow movements at 0.75 Hz, relatively high frequencies at 3.0 Hz) in order to maximize the behavioral

difference, thereby increasing our chances of finding differences at the neural level.

In conclusion, the present study demonstrates that the influence of movement speed on motor network connectivity is mediated by changes in neural coupling of inter- and intrahemispheric pathways from the premotor areas and cerebellum towards contralateral M1. Our data point to a critical contribution of the premotor cortex and cerebellum in the flexible adaption of the brain to varying motor demands in healthy subjects. Furthermore, the present study yields candidate regions whose causal role in hand motor performance can be tested in future experiments by means of non-invasive brain stimulation techniques like TMS. Finally, furthering our understanding of brain regions that drive motor performance is of particular relevance in a neurorehabilitative setting in order to identify new interaction targets, e.g., by enhancing motor activity in performance-related areas by means of non-invasive brain stimulation.

Supplementary data to this article can be found online at http://dx.doi.org/10.1016/j.neuroimage.2013.05.123.

Acknowledgments

We are grateful to our volunteers, Dr Marc Tittgemeyer and the MR staff for their support. CG was supported by a grant from the German Research Foundation (Deutsche Forschungsgemeinschaft GR 3285/2-1).

Conflict of interests

The authors declare that they have no competing interests.

References

Akkal, D., Dum, R.P., Strick, P.L., 2007. Supplementary motor area and presupplementary motor area: targets of basal ganglia and cerebellar output. J. Neurosci. 27 (40), 10659–10673.
Alexander, G.E., Crutcher, M.D., 1990. Functional architecture of basal ganglia circuits: neural substrates of parallel processing. Trends Neurosci. 13 (7), 266–271.
Arai, N., Lu, M.K., Ugawa, Y., Ziemann, U., 2012. Effective connectivity between human supplementary motor area and primary motor cortex: a paired-coil TMS study. Exp. Brain Res. 220 (1), 79–87.
Ashburner, J., Friston, K.J., 2005. Unified segmentation. NeuroImage 26 (3), 839–851.
Babiloni, C., Carducci, F., Del Gratta, C., Demartin, M., Romani, G.L., Babiloni, F., Rossini, P.M., 2003. Hemispherical asymmetry in human SMA during voluntary simple unilateral movements. An fMRI study. Cortex 39 (2), 293–305.
Boudrias, M.H., Goncalves, C.S., Penny, W.D., Park, C.H., Rossiter, H.E., Talelli, P., Ward, N.S., 2012. Age-related changes in causal interactions between cortical motor regions during hand grip. NeuroImage 59 (4), 3398–3405.
Boussaoud, D., Tanne-Gariepy, J., Wannier, T., Rouiller, E.M., 2005. Callosal connections of dorsal versus ventral premotor areas in the macaque monkey: a multiple retrograde tracing study. BMC Neurosci. 6, 67.
Cieslik, E.C., Zilles, K., Caspers, S., Roski, C., Kellermann, T.S., Jakobs, O., Langner, R., Laird, A.R., Fox, P.T., Eickhoff, S.B., 2012. Is there "one" DLPFC in cognitive action control? Evidence for heterogeneity from co-activation-based parcellation. Cereb. Cortex. http://dx.doi.org/10.1093/cercor/bhs256. (Epub).
Dettmers, C., Fink, G.R., Lemon, R.N., Stephan, K.M., Passingham, R.E., Silbersweig, D., Holmes, A., Ridding, M.C., Brooks, D.J., Frackowiak, R.S., 1995. Relation between cerebral activity and force in the motor areas of the human brain. J. Neurophysiol. 74 (2), 802–815.
Dettmers, C., Lemon, R.N., Stephan, K.M., Fink, G.R., Frackowiak, R.S., 1996. Cerebral activation during the exertion of sustained static force in man. NeuroReport 7 (13), 2103–2110.
Diedrichsen, J., Balsters, J.H., Flavell, J., Cussans, E., Ramnani, N., 2009. A probabilistic MR atlas of the human cerebellum. NeuroImage 46 (1), 39–46.
Dum, R.P., Strick, P.L., 2002. Motor areas in the frontal lobe of the primate. Physiol. Behav. 77 (4–5), 677–682.
Dum, R.P., Strick, P.L., 2005. Frontal lobe inputs to the digit representations of the motor areas on the lateral surface of the hemisphere. J. Neurosci. 25 (6), 1375–1386.
Eickhoff, S.B., Grefkes, C., 2011. Approaches for the integrated analysis of structure, function and connectivity of the human brain. Clin. EEG Neurosci. 42 (2), 107–121.
Eickhoff, S.B., Dafotakis, M., Grefkes, C., Shah, N.J., Zilles, K., Piza-Katzer, H., 2008. Central adaptation following heterotopic hand replantation probed by fMRI and effective connectivity analysis. Exp. Neurol. 212 (1), 132–144.
Eickhoff, S.B., Heim, S., Zilles, K., Amunts, K., 2009. A systems perspective on the effective connectivity of overt speech production. Philos. Trans. A Math. Phys. Eng. Sci. 367 (1896), 2399–2421.
Fridman, E.A., Hanakawa, T., Chung, M., Hummel, F., Leiguarda, R.C., Cohen, L.G., 2004. Reorganization of the human ipsilesional premotor cortex after stroke. Brain 127 (Pt 4), 747–758.
Fried, I., Katz, A., McCarthy, G., Sass, K.J., Williamson, P., Spencer, S.S., Spencer, D.D., 1991. Functional organization of human supplementary motor cortex studied by electrical stimulation. J. Neurosci. 11 (11), 3656–3666.
Friston, K.J., 1994. Functional and effective connectivity in neuroimaging: a synthesis. Hum. Brain Mapp. 2, 56–78.
Friston, K.J., Harrison, L., Penny, W., 2003. Dynamic causal modelling. NeuroImage 19 (4), 1273–1302.
Geyer, S., Matelli, M., Luppino, G., Zilles, K., 2000. Functional neuroanatomy of the primate isocortical motor system. Anat. Embryol. (Berl) 202 (6), 443–474.
Goldman-Rakic, P.S., Bates, J.F., Chafee, M.V., 1992. The prefrontal cortex and internally generated motor acts. Curr. Opin. Neurobiol. 2 (6), 830–835.
Goodkin, H.P., Keating, J.G., Martin, T.A., Thach, W.T., 1993. Preserved simple and impaired compound movement after infarction in the territory of the superior cerebellar artery. Can. J. Neurol. Sci. 20 (Suppl. 3), S93–S104.
Grefkes, C., Fink, G.R., 2005. The functional organization of the intraparietal sulcus in humans and monkeys. J. Anat. 207 (1), 3–17.
Grefkes, C., Fink, G.R., 2012. Disruption of motor network connectivity post-stroke and its noninvasive neuromodulation. Curr. Opin. Neurol. 25 (6), 670–675.
Grefkes, C., Geyer, S., Schormann, T., Roland, P., Zilles, K., 2001. Human somatosensory area 2: observer-independent cytoarchitectonic mapping, interindividual variability, and population map. NeuroImage 14 (3), 617–631.
Grefkes, C., Eickhoff, S.B., Nowak, D.A., Dafotakis, M., Fink, G.R., 2008a. Dynamic intra- and interhemispheric interactions during unilateral and bilateral hand movements assessed with fMRI and DCM. NeuroImage 41 (4), 1382–1394.
Grefkes, C., Nowak, D.A., Eickhoff, S.B., Dafotakis, M., Kust, J., Karbe, H., Fink, G.R., 2008b. Cortical connectivity after subcortical stroke assessed with functional magnetic resonance imaging. Ann. Neurol. 63 (2), 236–246.
Grefkes, C., Nowak, D.A., Wang, L.E., Dafotakis, M., Eickhoff, S.B., Fink, G.R., 2010. Modulating cortical connectivity in stroke patients by rTMS assessed with fMRI and dynamic causal modeling. NeuroImage 50 (1), 233–242.
Griffiths, P.D., Perry, R.H., Crossman, A.R., 1994. A detailed anatomical analysis of neurotransmitter receptors in the putamen and caudate in Parkinson's disease and Alzheimer's disease. Neurosci. Lett. 169 (1–2), 68–72.
Hardiman, M.J., Ramnani, N., Yeo, C.H., 1996. Reversible inactivations of the cerebellum with muscimol prevent the acquisition and extinction of conditioned nictitating membrane responses in the rabbit. Exp. Brain Res. 110 (2), 235–247.
Herz, D.M., Christensen, M.S., Reck, C., Florin, E., Barbe, M.T., Stahlhut, C., Pauls, K.A., Tittgemeyer, M., Siebner, H.R., Timmermann, L., 2012. Task-specific modulation of effective connectivity during two simple unimanual motor tasks: a 122-channel EEG study. NeuroImage 59 (4), 3187–3193.
Hoshi, E., Tanji, J., 2004. Differential roles of neuronal activity in the supplementary and presupplementary motor areas: from information retrieval to motor planning and execution. J. Neurophysiol. 92 (6), 3482–3499.
Hoshi, E., Tanji, J., 2007. Distinctions between dorsal and ventral premotor areas: anatomical connectivity and functional properties. Curr. Opin. Neurobiol. 17 (2), 234–242.
Hoshi, E., Tremblay, L., Feger, J., Carras, P.L., Strick, P.L., 2005. The cerebellum communicates with the basal ganglia. Nat. Neurosci. 8 (11), 1491–1493.
Jakobs, O., Wang, L.E., Dafotakis, M., Grefkes, C., Zilles, K., Eickhoff, S.B., 2009. Effects of timing and movement uncertainty implicate the temporo-parietal junction in the prediction of forthcoming motor actions. NeuroImage 47 (2), 667–677.
Jancke, L., Specht, K., Mirzazade, S., Loose, R., Himmelbach, M., Lutz, K., Shah, N.J., 1998a. A parametric analysis of the 'rate effect' in the sensorimotor cortex: a functional magnetic resonance imaging analysis in human subjects. Neurosci. Lett. 252 (1), 37–40.
Jancke, L., Peters, M., Schlaug, G., Posse, S., Steinmetz, H., Muller-Gartner, H., 1998b. Differential magnetic resonance signal change in human sensorimotor cortex to finger movements of different rate of the dominant and subdominant hand. Brain Res. Cogn. Brain Res. 6 (4), 279–284.
Jancke, L., Specht, K., Mirzazade, S., Peters, M., 1999. The effect of finger-movement speed of the dominant and the subdominant hand on cerebellar activation: a functional magnetic resonance imaging study. NeuroImage 9 (5), 497–507.
Jancke, L., Peters, M., Himmelbach, M., Nosselt, T., Shah, J., Steinmetz, H., 2000. fMRI study of bimanual coordination. Neuropsychologia 38 (2), 164–174.
Jenkins, I.H., Jahanshahi, M., Jueptner, M., Passingham, R.E., Brooks, D.J., 2000. Self-initiated versus externally triggered movements. II. The effect of movement predictability on regional cerebral blood flow. Brain 123 (Pt 6), 1216–1228.
Johansen-Berg, H., Rushworth, M.F., Bogdanovic, M.D., Kischka, U., Wimalaratna, S., Matthews, P.M., 2002. The role of ipsilateral premotor cortex in hand movement after stroke. Proc. Natl. Acad. Sci. U. S. A. 99 (22), 14518–14523.
Kazennikov, O., Hyland, B., Corboz, M., Babalian, A., Rouiller, E.M., Wiesendanger, M., 1999. Neural activity of supplementary and primary motor areas in monkeys and its relation to bimanual and unimanual movement sequences. Neuroscience 89 (3), 661–674.
Kelly, R.M., Strick, P.L., 2003. Cerebellar loops with motor cortex and prefrontal cortex of a nonhuman primate. J. Neurosci. 23 (23), 8432–8444.
Kubota, K., Hamada, I., 1978. Visual tracking and neuron activity in the post-arcuate area in monkeys. J. Physiol. Paris 74 (3), 297–312.
Lin, F.H., Agnew, J.A., Belliveau, J.W., Zeffiro, T.A., 2009. Functional and effective connectivity of visuomotor control systems demonstrated using generalized partial least squares and structural equation modeling. Hum. Brain Mapp. 30 (7), 2232–2251.
Luppino, G., Matelli, M., Camarda, R., Rizzolatti, G., 1993. Corticocortical connections of area F3 (SMA-proper) and area F6 (pre-SMA) in the macaque monkey. J. Comp. Neurol. 338 (1), 114–140.
Lutz, K., Koeneke, S., Wustenberg, T., Jancke, L., 2005. Asymmetry of cortical activation during maximum and convenient tapping speed. Neurosci. Lett. 373 (1), 61–66.

Middleton, F.A., Strick, P.L., 2000. Basal ganglia and cerebellar loops: motor and cognitive circuits. Brain Res. Brain Res. Rev. 31 (2–3), 236–250.
Nakai, T., Kato, C., Glover, G.H., Toma, K., Moriya, T., Matsuo, K., 2003. A functional magnetic resonance imaging study of internal modulation of an external visual cue for motor execution. Brain Res. 968 (2), 238–247.
Nambu, A., Kaneda, K., Tokuno, H., Takada, M., 2002. Organization of corticostriatal motor inputs in monkey putamen. J. Neurophysiol. 88 (4), 1830–1842.
Oldfield, R.C., 1971. The assessment and analysis of handedness: the Edinburgh inventory. Neuropsychologia 9 (1), 97–113.
Padoa-Schioppa, C., Li, C.S., Bizzi, E., 2004. Neuronal activity in the supplementary motor area of monkeys adapting to a new dynamic environment. J. Neurophysiol. 91 (1), 449–473.
Passingham, R.E., 1989. Premotor cortex and the retrieval of movement. Brain Behav. Evol. 33 (2–3), 189–192.
Picard, N., Strick, P.L., 2001. Imaging the premotor areas. Curr. Opin. Neurobiol. 11 (6), 663–672.
Poldrack, R.A., Sabb, F.W., Foerde, K., Tom, S.M., Asarnow, R.F., Bookheimer, S.Y., Knowlton, B.J., 2005. The neural correlates of motor skill automaticity. J. Neurosci. 25 (22), 5356–5364.
Ramnani, N., 2006. The primate cortico-cerebellar system: anatomy and function. Nat. Rev. Neurosci. 7 (7), 511–522.
Rao, S.M., Bandettini, P.A., Binder, J.R., Bobholz, J.A., Hammeke, T.A., Stein, E.A., Hyde, J.S., 1996. Relationship between finger movement rate and functional magnetic resonance signal change in human primary motor cortex. J. Cereb. Blood Flow Metab. 16 (6), 1250–1254.
Rehme, A.K., Eickhoff, S.B., Wang, L.E., Fink, G.R., Grefkes, C., 2011. Dynamic causal modeling of cortical activity from the acute to the chronic stage after stroke. NeuroImage 55 (3), 1147–1158.
Rehme, A.K., Eickhoff, S.B., Grefkes, C., 2013. State-dependent differences between functional and effective connectivity of the human cortical motor system. NeuroImage 67, 237–246.
Rizzolatti, G., Luppino, G., 2001. The cortical motor system. Neuron 31 (6), 889–901.
Rizzolatti, G., Luppino, G., Matelli, M., 1998. The organization of the cortical motor system: new concepts. Electroencephalogr. Clin. Neurophysiol. 106 (4), 283–296.
Rizzolatti, G., Fogassi, L., Gallese, V., 2002. Motor and cognitive functions of the ventral premotor cortex. Curr. Opin. Neurobiol. 12 (2), 149–154.
Rottschy, C., Langner, R., Dogan, I., Reetz, K., Laird, A.R., Schulz, J.B., Fox, P.T., Eickhoff, S.B., 2012. Modelling neural correlates of working memory: a coordinate-based meta-analysis. NeuroImage 60 (1), 830–846.
Rouiller, E.M., Babalian, A., Kazennikov, O., Moret, V., Yu, X.H., Wiesendanger, M., 1994. Transcallosal connections of the distal forelimb representations of the primary and supplementary motor cortical areas in macaque monkeys. Exp. Brain Res. 102 (2), 227–243.
Sadato, N., Ibanez, V., Deiber, M.P., Campbell, G., Leonardo, M., Hallett, M., 1996. Frequency-dependent changes of regional cerebral blood flow during finger movements. J. Cereb. Blood Flow Metab. 16 (1), 23–33.
Sadato, N., Ibanez, V., Campbell, G., Deiber, M.P., Le Bihan, D., Hallett, M., 1997. Frequency-dependent changes of regional cerebral blood flow during finger movements: functional MRI compared to PET. J. Cereb. Blood Flow Metab. 17 (6), 670–679.
Schlaug, G., Sanes, J.N., Thangaraj, V., Darby, D.G., Jancke, L., Edelman, R.R., Warach, S., 1996. Cerebral activation covaries with movement rate. NeuroReport 7 (4), 879–883.
Seidler, R.D., Noll, D.C., Thiers, G., 2004. Feedforward and feedback processes in motor control. NeuroImage 22 (4), 1775–1783.
Shimazu, H., Maier, M.A., Cerri, G., Kirkwood, P.A., Lemon, R.N., 2004. Macaque ventral premotor cortex exerts powerful facilitation of motor cortex outputs to upper limb motoneurons. J. Neurosci. 24 (5), 1200–1211.
Stephan, K.E., Penny, W.D., Daunizeau, J., Moran, R.J., Friston, K.J., 2009. Bayesian model selection for group studies. NeuroImage 46 (4), 1004–1017.
Tankus, A., Yeshurun, Y., Flash, T., Fried, I., 2009. Encoding of speed and direction of movement in the human supplementary motor area. J. Neurosurg. 110 (6), 1304–1316.
Tokuno, H., Tanji, J., 1993. Input organization of distal and proximal forelimb areas in the monkey primary motor cortex: a retrograde double labeling study. J. Comp. Neurol. 333 (2), 199–209.
Umilta, M.A., Brochier, T., Spinks, R.L., Lemon, R.N., 2007. Simultaneous recording of macaque premotor and primary motor cortex neuronal populations reveals different functional contributions to visuomotor grasp. J. Neurophysiol. 98 (1), 488–501.
van Kan, P.L., Houk, J.C., Gibson, A.R., 1993. Output organization of intermediate cerebellum of the monkey. J. Neurophysiol. 69 (1), 57–73.
Wang, L.E., Fink, G.R., Diekhoff, S., Rehme, A.K., Eickhoff, S.B., Grefkes, C., 2011. Noradrenergic enhancement improves motor network connectivity in stroke patients. Ann. Neurol. 69 (2), 375–388.
Witt, S.T., Laird, A.R., Meyerand, M.E., 2008. Functional neuroimaging correlates of finger-tapping task variations: an ALE meta-analysis. NeuroImage 42 (1), 343–356.
Yousry, T.A., Schmid, U.D., Alkadhi, H., Schmidt, D., Peraud, A., Buettner, A., Winkler, P., 1997. Localization of the motor hand area to a knob on the precentral gyrus. A new landmark. Brain 120 (Pt 1), 141–157.

Supplemental Information

	left SMA	right SMA	left PMv	right PMv	left M1	right M1	left Put	right Put	left Cb	right Cb
Subject 1	-8 -8 56	4 -6 54	-46 0 34	54 12 36	-40 -20 56	36 -18 48	-28 4 -6	28 2 0	-34 -58 -26	36 -54 -24
Subject 2	-4 -4 58	4 -4 60	-56 4 32	54 -6 32	-36 -26 62	32 -24 52	-32 -6 6	32 2 -2	-40 -54 -22	30 -52 -26
Subject 3	-4 -4 50	4 -4 50	-54 0 40	52 6 42	-40 -24 62	36 -26 66	-24 0 4	30 0 -4	-32 -54 -28	32 -56 -28
Subject 4	-10 -4 60	4 -6 52	-40 2 52	52 -18 34	-42 -28 62	46 -16 56	-24 2 2	24 6 0	-36 -62 -20	36 -52 -22
Subject 5	-4 -4 58	4 -2 58	-50 -4 42	56 2 46	-38 -24 50	36 -16 50	-24 0 2	28 4 -2	-30 -56 -24	30 -52 -26
Subject 6	-6 -6 56	8 -8 52	-56 4 32	48 -4 52	-38 -18 54	38 -22 54	-26 0 0	28 0 -4	-34 -54 -24	34 -56 -22
Subject 7	-4 -4 56	4 -2 50	-50 -8 50	50 -18 42	-36 -28 58	42 -22 58	-26 0 2	28 4 0	-36 -60 -28	38 -62 -24
Subject 8	-4 -16 56	8 -4 56	-54 2 36	56 2 28	-44 -24 60	42 -24 56	-26 0 0	30 4 0	-36 -58 -24	32 -56 -24
Subject 9	-4 -6 64	12 8 52	-54 -10 44	52 6 26	-38 -24 62	38 -20 54	-28 0 0	24 0 4	-32 -60 -28	34 -56 -22
Subject 10	-4 -28 52	4 4 62	-58 10 30	54 14 40	-32 -24 70	30 -22 58	-26 0 2	28 0 2	-26 -52 -22	28 -50 -26
Subject 11	-4 -6 52	8 -10 52	-50 -10 52	50 2 26	-34 -24 46	30 -24 64	-28 0 0	26 2 0	-30 -62 -22	32 -56 -24
Subject 12	-4 -8 50	10 -8 54	-50 2 44	58 12 30	-30 -20 54	36 -22 50	-24 0 6	28 0 0	-34 -60 -24	40 -54 -26
Subject 13	-6 -6 56	8 8 62	-54 6 34	50 4 38	-38 -24 58	38 -20 58	-26 0 0	28 2 -4	-30 -60 -24	38 -54 -28
Subject 14	-6 -4 54	4 -2 58	-58 4 34	58 4 34	-36 -20 54	38 -22 54	-28 0 2	28 2 -4	-34 -56 -26	34 -58 -26
Subject 15	-6 -4 56	4 6 50	-54 -20 30	58 -4 30	-36 -16 56	30 -24 60	-28 0 0	30 0 0	-22 -58 -24	30 -42 -22
Subject 16	-6 -4 56	6 -4 58	-54 8 34	60 10 34	-38 -22 52	38 -18 48	-26 0 2	26 0 2	-34 -54 -22	34 -54 -28
Subject 17	-4 -4 54	4 4 56	-56 12 34	56 12 40	-42 -12 58	42 -18 52	-26 0 2	28 4 -2	-34 -58 -26	38 -54 -26
Subject 18	-8 -4 48	8 -8 52	-62 4 26	66 6 30	-34 -28 62	34 -26 56	-28 0 0	30 0 -4	-32 -60 -22	34 -54 -22
Subject 19	-4 -2 56	4 0 56	-56 2 38	56 4 42	-40 -22 54	44 -20 58	-28 -4 -4	28 0 -6	-32 -60 -24	34 -60 -24
Subject 20	-4 4 62	4 -4 60	-54 2 38	58 0 44	-30 -24 60	32 -22 58	-26 -2 0	26 4 2	-30 -64 -20	28 -62 -20
Subject 21	-4 -4 56	4 -4 44	-56 8 34	54 6 32	-38 -26 56	36 -24 56	-26 -4 2	26 4 2	-30 -52 -22	42 -56 -20
Subject 22	-6 -10 52	6 -6 54	-58 10 30	62 8 30	-36 -26 58	36 -22 56	-30 6 8	32 -2 -2	-38 -60 -24	38 -54 -28
Subject 23	-4 0 64	4 10 54	-58 8 24	52 8 20	-40 -24 54	40 -16 54	-26 -4 -4	26 0 0	-32 -60 -24	30 -60 -26
Subject 24	-6 -10 60	6 -6 54	-52 -2 44	52 4 48	-38 -26 54	38 -22 58	-28 0 0	28 0 0	-34 -60 -24	34 -58 -22
Subject 25	-6 -6 50	4 0 52	-54 8 42	54 6 38	-32 -24 68	40 -20 54	-26 2 0	26 2 2	-36 -60 -24	34 -58 -22
Subject 26	-10 8 76	8 -16 78	-48 -6 46	52 -2 44	-40 -26 62	42 -22 60	-26 -4 -2	26 0 0	-32 -58 -24	42 -54 -28
Subject 27	-4 -6 64	6 2 52	-56 2 40	40 12 42	-40 -26 66	38 -18 50	-30 0 -2	28 0 -4	-32 -68 -22	38 -60 -20
Subject 28	-4 -8 48	6 -6 50	-52 0 40	50 6 40	-36 -26 66	42 -24 62	-28 4 4	28 0 0	-32 -60 -24	32 -60 -22
Subject 29	-4 10 62	12 10 56	-44 2 32	46 4 30	-38 -28 62	34 -24 64	-28 0 2	22 -6 -6	-32 -60 -20	40 -54 -28
Subject 30	-4 -4 58	6 -4 54	-58 -4 44	56 8 34	-40 -24 58	44 -18 60	-26 -2 0	28 -2 0	-34 -58 -28	36 -54 -28
Subject 31	-6 -4 56	6 -4 56	-52 0 38	58 -8 48	-36 -24 64	42 -22 66	-24 0 4	28 -2 -4	-34 -62 -24	30 -60 -26
Subject 32	-4 -4 58	6 -4 54	-58 -4 44	56 8 34	-40 -24 58	44 -18 60	-28 0 2	28 4 4	-34 -60 -26	34 -66 -24
Subject 33	-6 -10 50	8 0 54	-48 -2 50	54 4 46	-38 -26 64	32 -22 66	-26 -2 -2	26 -2 -4	-38 -60 -20	32 -64 -24
Subject 34	-4 4 56	10 -4 56	-50 -8 40	54 4 48	-38 -24 64	38 -22 66	-26 -4 0	28 -2 -4	-30 -54 -28	30 -48 -26
Subject 35	-6 -16 50	6 0 56	-50 -8 32	56 4 44	-44 -18 62	32 -12 48	-28 0 0	26 2 0	-30 -64 -22	38 -50 -30
Subject 36	-6 -10 50	8 0 54	-48 -2 50	54 0 44	-38 -26 64	36 -20 50	-26 -2 -2	26 -2 -4	-34 -60 -30	32 -64 -24
Mean	-5 -5 56	6 -2 55	-53 0 39	54 3 37	-38 -24 59	38 -21 57	-27 0 1	28 1 -1	-33 -59 -24	34 -56 -25
SD	1,7,6	2,6,5	5,7,7	5,7,8	3,4,5	4,3,5	2,2,3	2,2,3	3,3,3	4,5,3

Supplemental Table I. Individual local fMRI maxima used as ROIs for DCM.

Endogenous connectivity (DCM A-matrix)

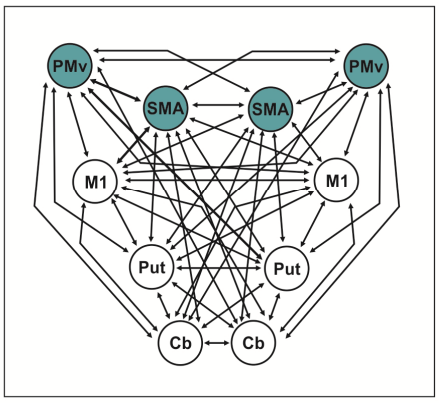

Models of task-dependent connectivity (DCM B-matrix)

model 1

fully connected model

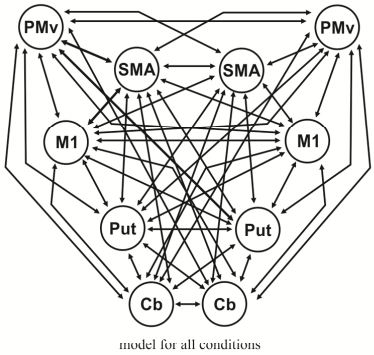

model for all conditions

model 2

as model 1, no interhemispheric SMA-M1 connection

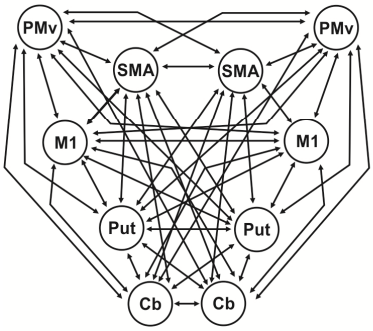

model 3

as model 2, no interhemispheric PMv-M1 connection

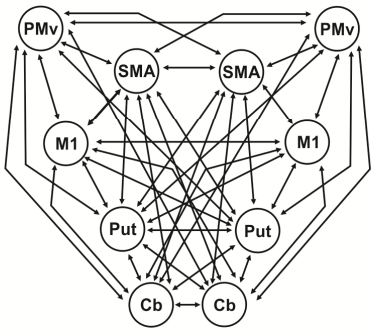

model 4

as model 3, no interhemispheric Put-M1 connection

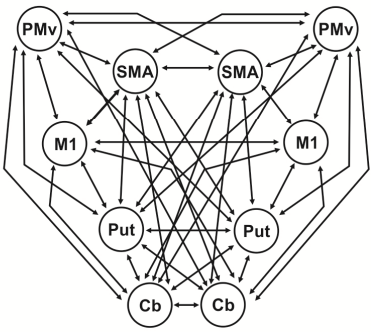

model 5

as model 4, no interhemispheric Cb-M1 connection

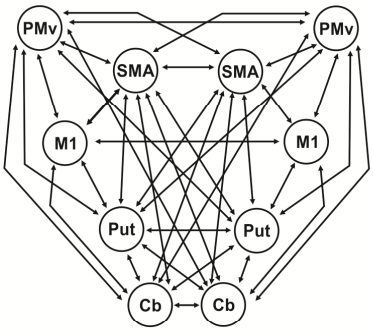

model 6

as model 5, no interhemispheric SMA-PMv connection

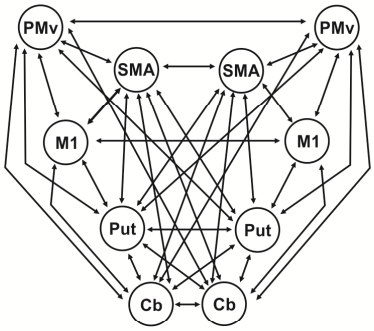

model 7

as model 6, no interhemispheric SMA-Put connection

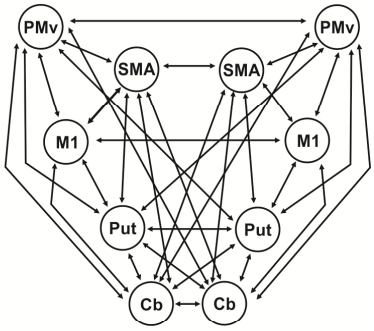

model 8

as model 7, no interhemispheric SMA-Cb connection

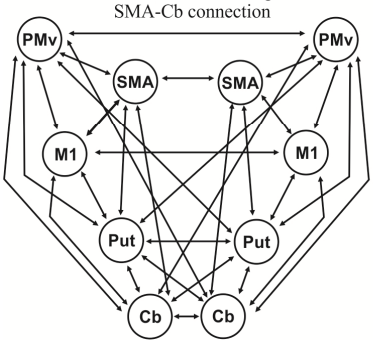

model 9

as model 8, no interhemispheric PMv-Put connection

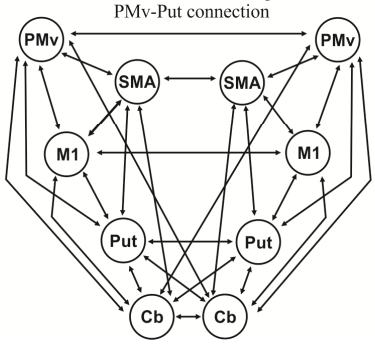

model 10

as model 9, no interhemispheric PMv-Cb connection

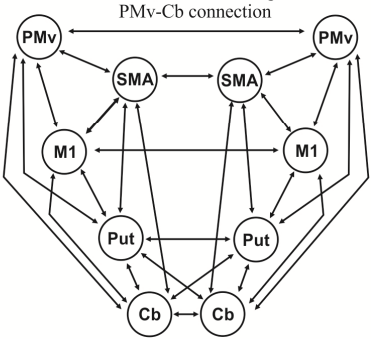

model 11

as model 10, no interhemispheric Put-Cb connection

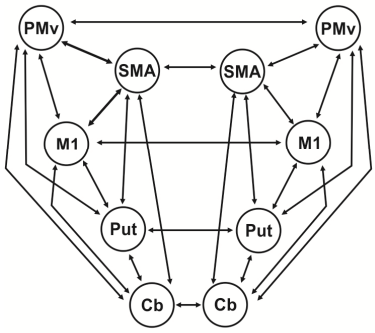

model 12

as model 11, no interhemispheric SMA-SMA connection

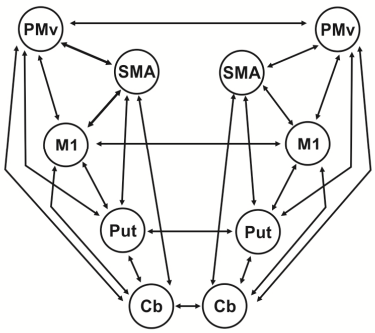

model 13

as model 12, no interhemispheric PMv-PMv connection

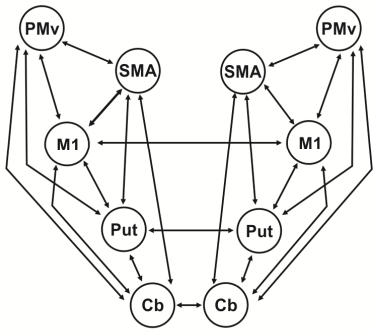

model 14

as model 13, no interhemispheric Put-Put connection

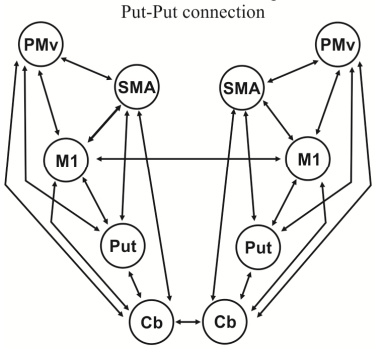

model 15

as model 14, no interhemispheric Cb-Cb connection

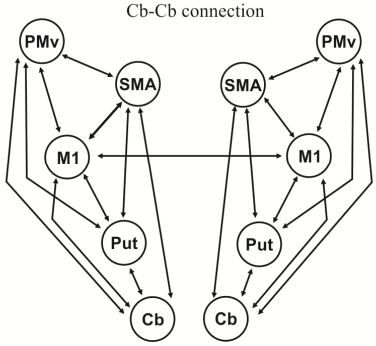

model 16

as model 14, no interhemispheric M1-M1 connection

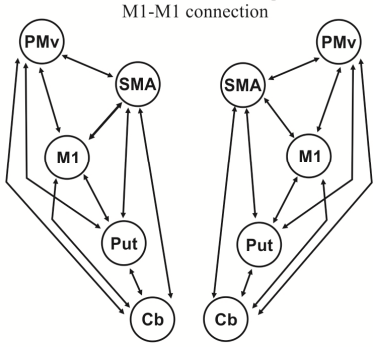

model 17

as model 2, lateralized

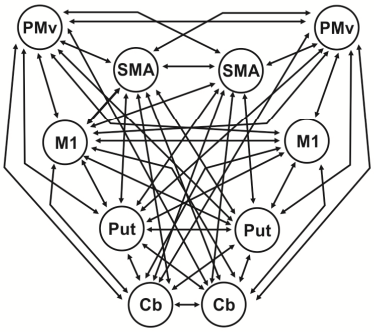

right hand

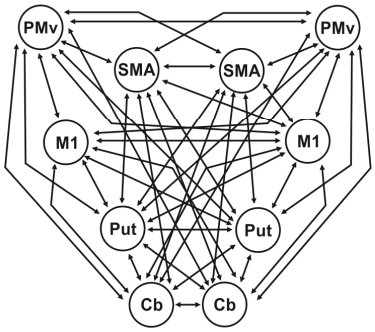

left hand

model 18

as model 3, lateralized

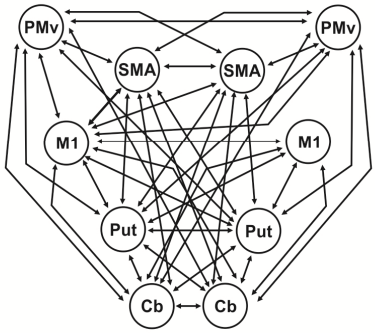

right hand

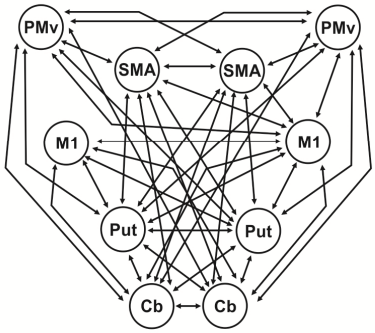

left hand

model 19

as model 4, lateralized

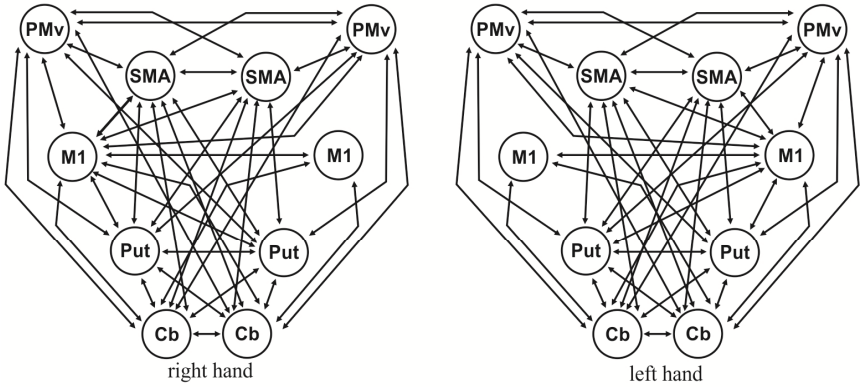

model 20

as model 5, lateralized

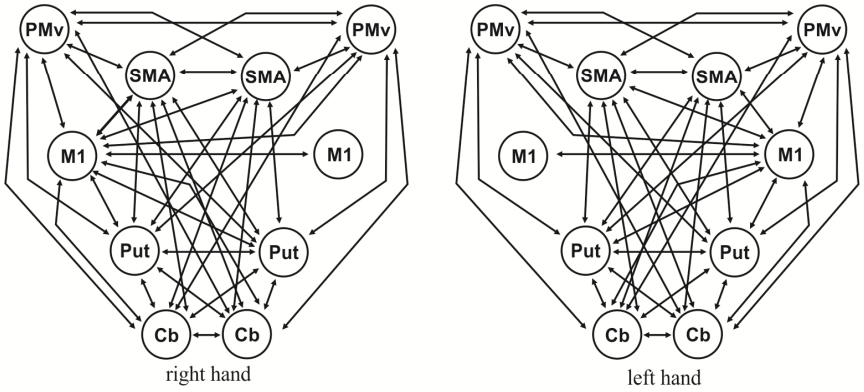

model 21

as model 6, lateralized

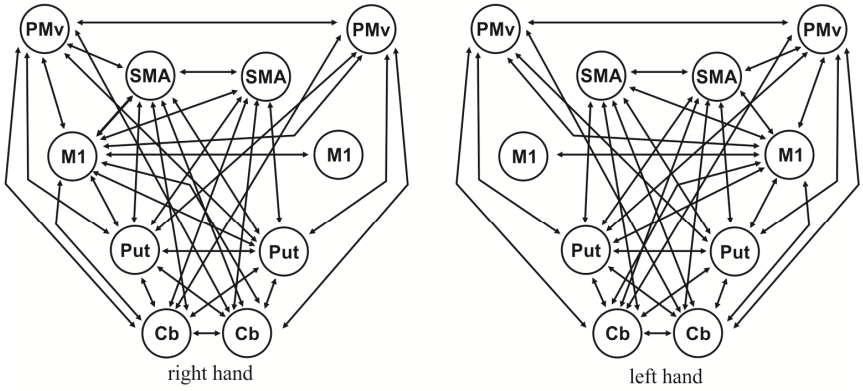

model 22

as model 7, lateralized

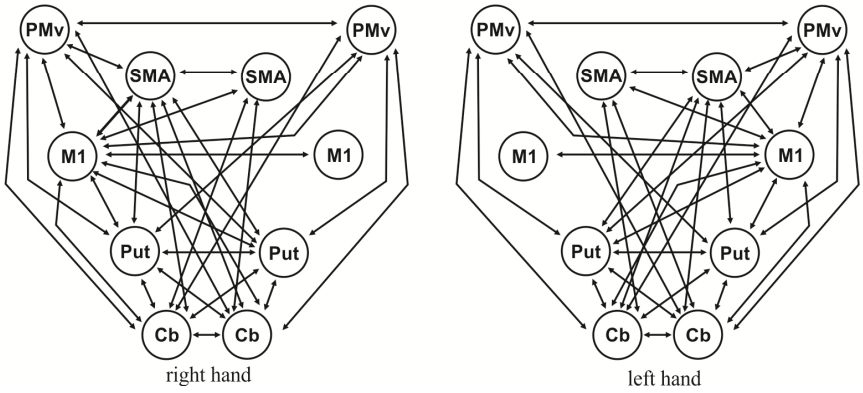

model 23

as model 8, lateralized

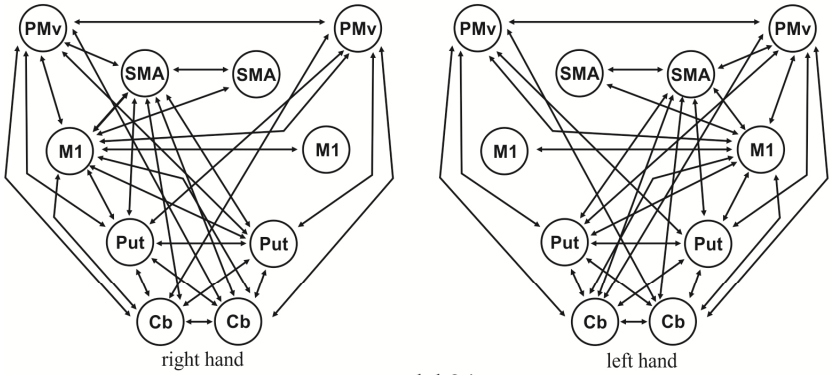

model 24

as model 9, lateralized

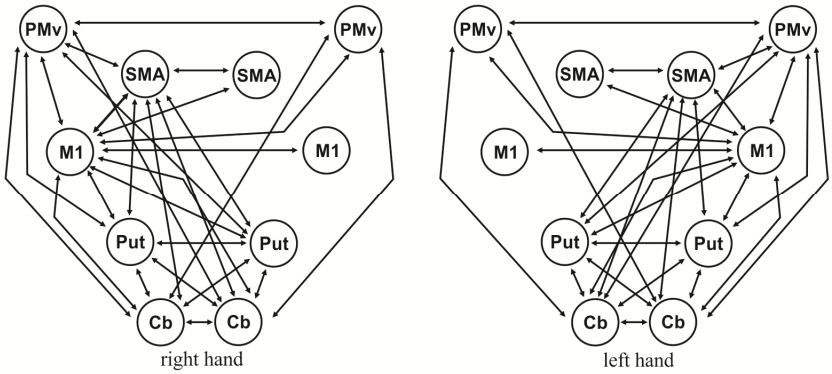

model 25

as model 10, lateralized

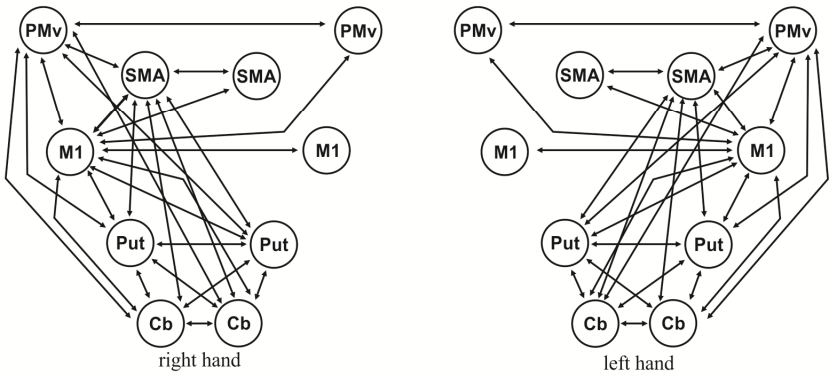

model 26

as model 11, lateralized

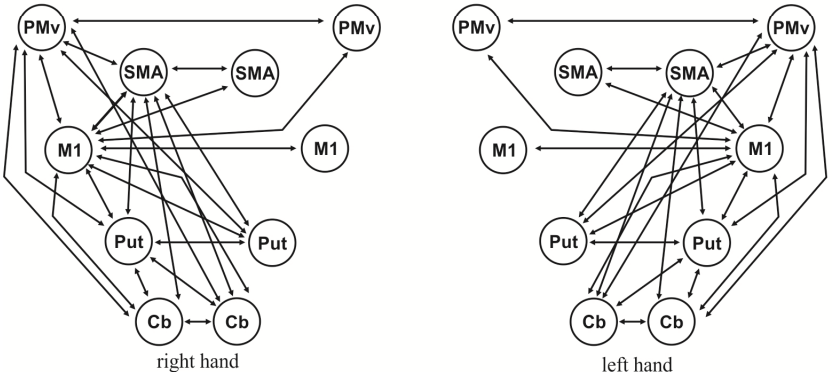

model 27

as model 12, lateralized

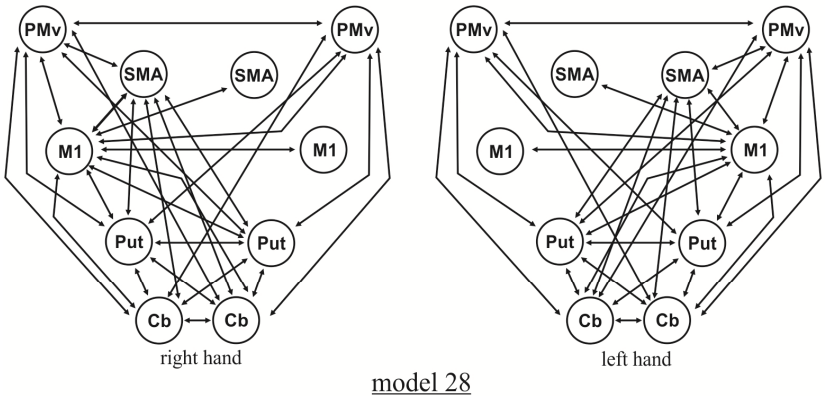

model 28

as model 13, lateralized

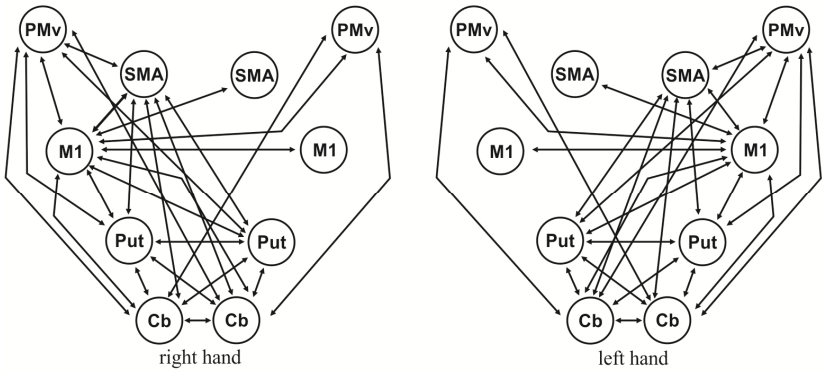

model 29

as model 14, lateralized

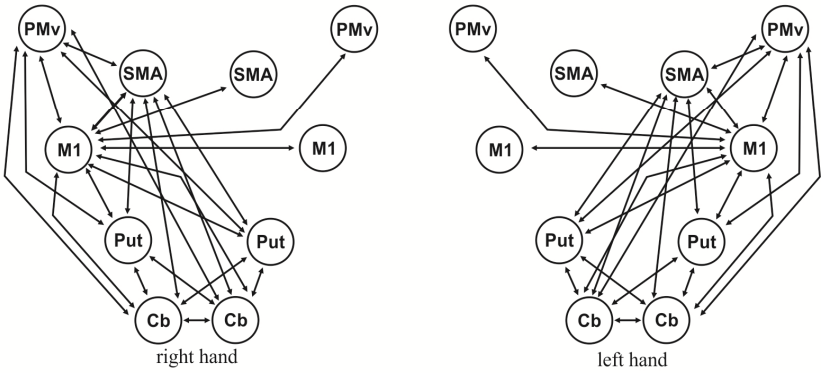

model 30

as model 15, lateralized

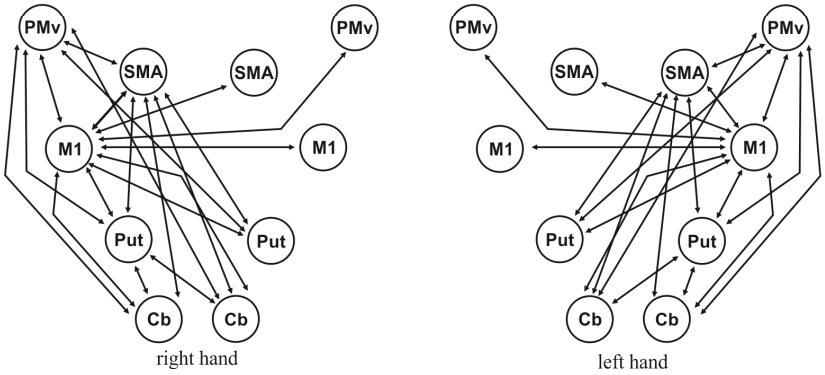

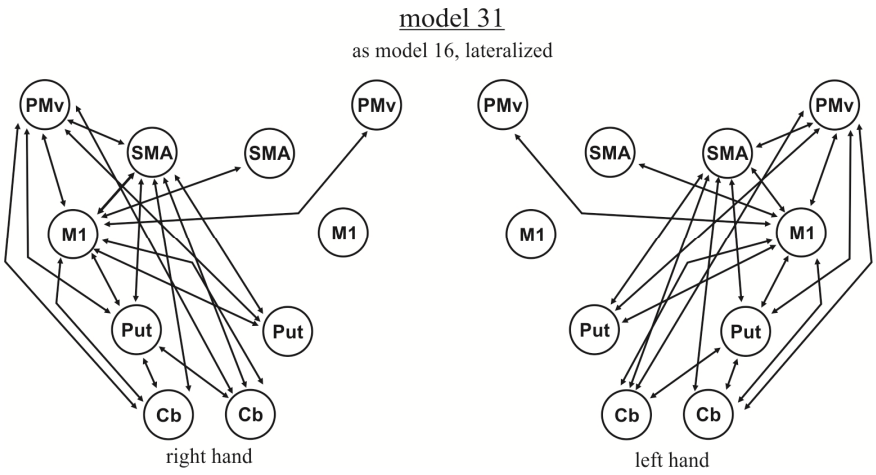

Supplemental Figure 1. 31 models tested in the Bayesian model selection procedure.

Endogenous connectivity					
Connection	Average	p-Value	Connection	Average	p-Value
SMA left -SMA right	0.029	<0.001	SMA right - SMA left	0.033	<0.001
SMA left -PMv left	0.028	<0.001	SMA right - PMv left	0.025	<0.001
SMA left -PMv right	0.020	<0.001	SMA right - PMv right	0.028	<0.001
SMA left -M1 left	0.162	<0.001	SMA right - M1 left	-0.037	0.019 (n.s.)
SMA left -M1 right	-0.032	0.029 (n.s.)	SMA right - M1 right	0.158	<0.001
SMA left -Put left	0.038	<0.001	SMA right - Put left	0.017	0.003 (n.s.)
SMA left -Put right	0.007	0.182 (n.s.)	SMA right - Put right	0.050	<0.001
SMA left -Cb left	0.059	<0.001	SMA right - Cb left	0.094	<0.001
SMA left -Cb right	0.095	<0.001	SMA right - Cb right	0.045	<0.001
PMv left -SMA left	0.025	<0.001	PMv right - SMA left	0.023	<0.001
PMv left -SMA right	0.023	<0.001	PMv right - SMA right	0.028	<0.001
PMv left -PMv right	0.017	<0.001	PMv right - PMv left	0.019	<0.001
PMv left -M1 left	0.060	<0.001	PMv right - M1 left	0.025	0.007 (n.s.)
PMv left -M1 right	0.027	0.022 (n.s.)	PMv right - M1 right	0.046	<0.001
PMv left -Put left	0.025	<0.001	PMv right - Put left	0.019	<0.001
PMv left -Put right	0.019	<0.001	PMv right - Put right	0.023	<0.001
PMv left -Cb left	0.051	<0.001	PMv right - Cb left	0.060	<0.001
PMv left -Cb right	0.056	<0.001	PMv right - Cb right	0.052	<0.001
M1 left -SMA left	0.037	<0.001	M1 right - SMA left	0.020	<0.001
M1 left -SMA right	0.017	<0.001	M1 right - SMA right	0.039	<0.001
M1 left -PMv left	0.022	<0.001	M1 right - PMv left	0.024	<0.001
M1 left -PMv right	0.016	<0.001	M1 right - PMv right	0.024	<0.001
M1 left -M1 right	-0.095	<0.001	M1 right - M1 left	-0.094	<0.001
M1 left -Put left	0.035	<0.001	M1 right - Put left	0.000	0.978 (n.s.)
M1 left -Put right	-0.011	0.009 (n.s.)	M1 right - Put right	0.046	<0.001
M1 left -Cb left	0.017	0.021 (n.s.)	M1 right - Cb left	0.078	<0.001
M1 left -Cb right	0.084	<0.001	M1 right - Cb right	0.007	0.268 (n.s.)
Put left -SMA left	0.021	<0.001	Put right - SMA left	0.018	<0.001
Put left -SMA right	0.021	<0.001	Put right - SMA right	0.025	<0.001
Put left -PMv left	0.016	<0.001	Put right - PMv left	0.015	<0.001
Put left -PMv right	0.015	<0.001	Put right - PMv right	0.018	<0.001
Put left -M1 left	0.039	<0.001	Put right - M1 left	-0.012	0.008 (n.s.)
Put left -M1 right	-0.004	0.301	Put right - M1 right	0.047	<0.001
Put left -Put right	0.019	<0.001	Put right - Put left	0.019	<0.001
Put left -Cb left	0.029	<0.001	Put right - Cb left	0.041	<0.001
Put left -Cb right	0.037	<0.001	Put right - Cb right	0.022	<0.001
Cb left -SMA left	0.040	<0.001	Cb right - SMA left	0.040	<0.001
Cb left -SMA right	0.051	<0.001	Cb right - SMA right	0.040	<0.001
Cb left -PMv left	0.034	<0.001	Cb right - PMv left	0.030	<0.001
Cb left -PMv right	0.035	<0.001	Cb right - PMv right	0.029	<0.001
Cb left -M1 left	0.010	0.135 (n.s.)	Cb right - M1 left	0.077	<0.001
Cb left -M1 right	0.075	<0.001	Cb right - M1 right	0.005	0.332 (n.s.)
Cb left -Put left	0.026	<0.001	Cb right - Put left	0.032	<0.001
Cb left -Put right	0.037	<0.001	Cb right - Put right	0.020	<0.001
Cb left -Cb right	0.065	<0.001	Cb right - Cb left	0.067	<0.001

Supplemental Table II. Significant coupling parameter estimates and their *P*-values ($P < 0.05$, Bonferroni-corrected).

Right Hand Movements					
Main effect "hand"			Parametric modulation "frequency"		
Connection	Average	p-Value	Connection	Average	p-Value
SMA left - SMA right	0.02	<0.001	SMA left - M1 left	0.03	<0.001
SMA left - M1 left	0.17	<0.001	SMA left - M1 right	0.01	<0.001
SMA left - M1 right	-0.06	<0.001	PMv left - M1 left	0.01	<0.001
SMA left - Put left	0.03	<0.001	PMv right - M1 left	0.02	<0.001
SMA left - Cb left	0.03	<0.001	Cb right - M1 left	0.02	<0.001
SMA left - Cb right	0.07	<0.001			
SMA right - SMA left	0.01	<0.001			
SMA right - Put left	0.02	<0.001			
PMv left - SMA right	0.01	<0.001			
PMv left - PMv right	0.01	<0.001			
PMv left - M1 left	0.07	<0.001			
PMv left - M1 right	-0.02	<0.001			
PMv left - Put left	0.01	<0.001			
PMv left - Cb left	0.02	<0.001			
PMv left - Cb right	0.04	<0.001			
PMv right - SMA right	0.01	<0.001			
PMv right - PMv left	0.01	<0.001			
PMv right - M1 left	0.06	<0.001			
PMv right - Put left	0.02	<0.001			
PMv right - Cb left	0.02	<0.001			
PMv right - Cb right	0.03	<0.001			
M1 left - SMA left	0.03	<0.001			
M1 left - SMA right	0.03	<0.001			
M1 left - PMv left	0.02	<0.001			
M1 left - PMv right	0.02	<0.001			
M1 left - M1 right	-0.02	<0.001			
M1 left - Put left	0.03	<0.001			
M1 left - Cb left	0.04	<0.001			
M1 left - Cb right	0.07	<0.001			
M1 right - M1 left	-0.03	<0.001			
Put left - SMA left	0.01	<0.001			
Put left - SMA right	0.01	<0.001			
Put left - PMv left	0.01	<0.001			
Put left - PMv right	0.01	<0.001			
Put left - M1 left	0.04	<0.001			
Put left - Put right	0.01	<0.001			
Put left - Cb left	0.02	<0.001			
Put left - Cb right	0.03	<0.001			
Put right - SMA left	0.01	<0.001			
Put right - Put left	0.01	<0.001			
Put right - Cb right	0.01	<0.001			
Cb left - SMA left	0.01	<0.001			
Cb left - SMA right	0.02	<0.001			
Cb left - PMv left	0.01	<0.001			
Cb left - PMv right	0.01	<0.001			
Cb left - M1 left	0.06	<0.001			
Cb left - Put left	0.02	<0.001			
Cb left - Cb right	0.04	<0.001			
Cb right - SMA left	0.02	<0.001			
Cb right - SMA right	0.02	<0.001			
Cb right - PMv left	0.01	<0.001			
Cb right - PMv right	0.01	<0.001			
Cb right - M1 left	0.09	<0.001			
Cb right - Put left	0.03	<0.001			
Cb right - Cb left	0.03	<0.001			

Supplemental Table IIIa. Coupling parameter estimates and their *P*-values ($P < 0.05$, Bonferroni-corrected).

Left Hand Movements					
Main effect "hand"			Parametric modulation "frequency"		
Connection	Average	p-Value	Connection	Average	p-Value
SMA left - SMA right	0.01	<0.001	SMA right - M1 left	0.01	<0.001
SMA left - PMv left	0.02	<0.001	SMA right - M1 right	0.03	<0.001
SMA left - PMv right	0.01	<0.001	PMv left - M1 right	0.01	<0.001
SMA left - M1 right	0.06	<0.001	PMv right - M1 right	0.03	<0.001
SMA right - SMA left	0.02	<0.001	Cb left - M1 right	0.02	<0.001
SMA right - PMv left	0.02	<0.001			
SMA right - PMv right	0.01	<0.001			
SMA right - M1 left	-0.05	<0.001			
SMA right - M1 right	0.16	<0.001			
SMA right - Put right	0.04	<0.001			
SMA right - Cb left	0.08	<0.001			
SMA right - Cb right	0.03	<0.001			
PMv left - SMA left	0.01	<0.001			
PMv left - M1 right	0.06	<0.001			
PMv left - Put right	0.02	<0.001			
PMv left - Cb left	0.04	<0.001			
PMv left - Cb right	0.02	<0.001			
PMv right - SMA left	0.01	<0.001			
PMv right - SMA right	0.01	<0.001			
PMv right - PMv left	0.01	<0.001			
PMv right - M1 right	0.06	<0.001			
PMv right - Put right	0.02	<0.001			
PMv right - Cb left	0.04	<0.001			
PMv right - Cb right	0.02	<0.001			
M1 left - M1 right	-0.02	<0.001			
M1 right - SMA left	0.03	<0.001			
M1 right - SMA right	0.03	<0.001			
M1 right - PMv left	0.03	<0.001			
M1 right - PMv right	0.02	<0.001			
M1 right - M1 left	-0.02	<0.001			
M1 right - Put right	0.03	<0.001			
M1 right - Cb left	0.08	<0.001			
M1 right - Cb right	0.03	<0.001			
Put left - SMA left	0.01	<0.001			
Put left - SMA right	0.01	<0.001			
Put left - PMv left	0.01	<0.001			
Put left - Put right	0.01	<0.001			
Put left - Cb left	0.01	<0.001			
Put left - Cb right	0.01	<0.001			
Put right - SMA left	0.01	<0.001			
Put right - SMA right	0.01	<0.001			
Put right - PMv left	0.01	<0.001			
Put right - PMv right	0.01	<0.001			
Put right - M1 right	0.04	<0.001			
Put right - Put left	0.01	<0.001			
Put right - Cb left	0.03	<0.001			
Put right - Cb right	0.02	<0.001			
Cb left - SMA left	0.03	<0.001			
Cb left - SMA right	0.03	<0.001			
Cb left - PMv left	0.03	<0.001			
Cb left - PMv right	0.02	<0.001			
Cb left - M1 right	0.09	<0.001			
Cb left - Put left	0.01	<0.001			
Cb left - Put right	0.03	<0.001			
Cb left - Cb right	0.04	<0.001			
Cb right - SMA left	0.02	<0.001			
Cb right - SMA right	0.02	<0.001			
Cb right - PMv left	0.02	<0.001			
Cb right - PMv right	0.01	<0.001			
Cb right - M1 right	0.05	<0.001			
Cb right - Put right	0.02	<0.001			
Cb right - Cb left	0.04	<0.001			

Supplemental Table IIIb. Significant coupling parameter estimates and their *P*-values ($P < 0.05$, Bonferroni-corrected).

3.2

Handedness and effective connectivity of the motor system.

Eva-Maria Pool, Anne K. Rehme, Gereon R. Fink, Simon B. Eickhoff, Christian Grefkes

Neuroimage (2014). 99, 451-460.

NeuroImage 99 (2014) 451–460

Contents lists available at ScienceDirect

NeuroImage

journal homepage: www.elsevier.com/locate/ynimg

Handedness and effective connectivity of the motor system

Eva-Maria Pool [a], Anne K. Rehme [a], Gereon R. Fink [b,c], Simon B. Eickhoff [c,d], Christian Grefkes [a,b,c,*]

[a] Neuromodulation & Neurorehabilitation, Max Planck Institute for Neurological Research, 50931 Cologne, Germany
[b] Department of Neurology, University of Cologne, 50924 Cologne, Germany
[c] Institute of Neuroscience and Medicine (INM-1, INM-3), Jülich Research Centre, 52428 Jülich, Germany
[d] Institute of Clinical Neuroscience and Medical Psychology, Heinrich Heine University, 40225 Düsseldorf, Germany

ARTICLE INFO

Article history:
Accepted 16 May 2014
Available online 23 May 2014

Keywords:
Dynamic causal modeling
Premotor cortex
Motor putamen
Right-handers
Left-handers

ABSTRACT

Handedness denotes the individual predisposition to consistently use the left or right hand for most types of skilled movements. A putative neurobiological mechanism for handedness consists in hemisphere-specific differences in network dynamics that govern unimanual movements.

We, therefore, used functional magnetic resonance imaging and dynamic causal modeling to investigate effective connectivity between key motor areas during fist closures of the dominant or non-dominant hand performed by 18 right- and 18 left-handers. Handedness was assessed employing the Edinburgh-Handedness-Inventory (EHI). The network of interest consisted of key motor regions in both hemispheres including the primary motor cortex (M1), supplementary motor area (SMA), ventral premotor cortex (PMv), motor putamen (Put) and motor cerebellum (Cb).

The connectivity analysis revealed that in right-handed subjects movements of the dominant hand were associated with significantly stronger coupling of contralateral (left, i.e., dominant) SMA with ipsilateral SMA, ipsilateral PMv, contralateral motor putamen and contralateral M1 compared to equivalent connections in left-handers. The degree of handedness as indexed by the individual EHI scores also correlated with coupling parameters of these connections. In contrast, we found no differences between right- and left-handers when testing for the effect of movement speed on effective connectivity.

In conclusion, the data show that handedness is associated with differences in effective connectivity within the human motor network with a prominent role of SMA in right-handers. Left-handers featured less asymmetry in effective connectivity implying different hemispheric mechanisms underlying hand motor control compared to right-handers.

Introduction

Handedness is a fundamental, behavioral characteristic of the motor system that evolves even before birth and stabilizes during early childhood (Fagard, 2013). While to date a formal definition of handedness is missing, it is widely accepted that handedness includes that (i) one hand is consistently preferred for carrying out a particular task, (ii) the same hand is chosen for the majority of tasks to be performed, and (iii) this hand is more proficient than the other in task performance (Hammond, 2002; Serrien et al., 2006). Experimental evidence suggests that this intrinsic behavioral phenomenon is associated with asymmetries in the structural and functional organization of the cerebral cortex (Amunts et al., 1996; Eickhoff et al., 2008; Hammond, 2002). For example, anatomical studies revealed a deeper central sulcus in the dominant compared to the non-dominant hemisphere in both right- and left-handers (Amunts et al., 1996). Furthermore, neuroimaging studies demonstrated an influence of hand dominance on neural activity (Dassonville et al., 1997; Kim et al., 1993; Solodkin et al., 2001; Volkmann et al., 1998). In both right- and left-handers, dominant hand movements were shown to be associated with a greater volume of the hand representation in the contralateral primary motor cortex (M1) (Dassonville et al., 1997; Volkmann et al., 1998). Solodkin and colleagues mapped brain activation patterns in right- and left-handers during single and sequential finger movements and found larger volumes of activation and less hemispheric lateralization in left-handers (Solodkin et al., 2001). The latter finding is compatible with behavioral data demonstrating that hand preference in left-handers is often expressed to a lesser degree than in right-handers (Borod et al., 1984). Finally, transcranial magnetic stimulation (TMS) paradigms provided evidence for handedness-related asymmetries in cortical excitability (Brouwer et al., 2001; Ziemann and Hallett, 2001). Ziemann and Hallett (2001) demonstrated that performing a complex motor task with one hand increases the excitability of the motor cortex contralateral to the inactive hand. This increase was significantly smaller when the task was performed with the dominant (right) as opposed to the non-dominant (left) hand (Ziemann and Hallett, 2001). The authors

* Corresponding author at: Department of Neurology, University Hospital Cologne, Kerpener Straße 62, 50924 Cologne, Germany. Fax: +49 221 478 7005.
E-mail address: christian.grefkes@uk-koeln.de (C. Grefkes).

http://dx.doi.org/10.1016/j.neuroimage.2014.05.048
1053-8119/

hypothesized that the dominant (left) motor cortex exerts more inhibitory control upon the contralateral motor cortex controlling the non-dominant left hand than vice versa. Taken together, the neural mechanisms for hand dominance might rest in hemispheric-specific differences of network dynamics that govern unimanual movements.

Accordingly, we here investigated whether the preference to use the right or left hand in everyday life is reflected by systematic differences in network interactions during unimanual movements. As outlined above, structural and functional neuroimaging studies have already addressed the neural correlates of handedness (Amunts et al., 1996; Dassonville et al., 1997; Kloppel et al., 2007; Solodkin et al., 2001; Volkmann et al., 1998). However, to date little is known about hand preference and the dynamics of the motor network. To this end, we addressed in a functional magnetic resonance imaging (fMRI) study the question whether there are differences in neural activity and interregional interaction of key motor regions between right- ($n = 18$) and left-handers ($n = 18$). Dynamic causal modeling (DCM) was used to assess effective connectivity, i.e., the causal influence that one area exerts upon activity of another (Friston et al., 2003), during unimanual movements of the dominant and non-dominant hands at different frequencies for a bihemispheric network consisting of key motor areas like M1, supplementary motor area (SMA), ventrolateral premotor cortex (PMv), motor putamen (Put) and motor cerebellum (Cb) (Grefkes et al., 2008; Passingham, 1997; Witt et al., 2008). We hypothesized that higher movement speed evokes a stronger BOLD signal especially in the contralateral primary sensorimotor cortex (Jancke et al., 1998; Sadato et al., 1996). Moreover, we hypothesized that movement-related connections are differentially modulated depending on whether subjects are right-handed or left-handed (Kloppel et al., 2007; Solodkin et al., 2001).

Materials and methods

Subjects

The study was approved by the local ethics committee and performed in accordance with the Declaration of Helsinki. Thirty-six subjects (18 right-handers [mean age 25.7 ± 3.0 SD; range: 22–34 years] and 18 left-handers [mean age 24.6 ± 2.6 SD; range: 19–30 years]) with no history of neurological or psychiatric disease gave written informed consent. The two groups were carefully matched for age, sex, and laterality of handedness. The fMRI and connectivity data of the right-handers were included in a previous publication (Pool et al., 2013).

Handedness measurements

Handedness was assessed by asking the subjects to complete the 10-item version of the Edinburgh-Handedness-Inventory (EHI) (Oldfield, 1971). The EHI assesses hand dominance in daily activities (e.g., writing, striking a match, holding a broom). The laterality quotient (LQ) of hand dominance ranges from −100 to 100: an LQ > 25 indicates right-handedness, and an LQ < −25 indicates left-handedness (Pujol et al., 1999). In the present study, the median LQ of the right-handers group was 83 (range: 53 to 100) and the median LQ of the left-handers group was −73 (range: −30 to −100). We computed a Kruskal–Wallis H-test for non-parametric independent group comparisons which showed no significant difference in the degree of handedness between right- and left-handers ($P = 0.188$).

fMRI design

In order to probe neural activity in the motor system, we used a block-design task, where subjects were asked to perform fist closures with their right or left hand at three different frequencies: (i) 0.75 Hz, (ii) 1.5 Hz, and (iii) 3.0 Hz (Pool et al., 2013). The task to be performed was announced on a shielded thin-film transistor (TFT) screen at the rear end of the scanner, which was visible via a mirror mounted to the MR head coil. Written instructions were displayed for 2 s indicating the hand to be moved in the upcoming block of trials. Then, the instructions were replaced by a white circle, which started to blink in red at the respective frequency. Blocks of fist closures (15 s) were separated by resting baselines (15 s plus a temporal jitter of 1–2.5 s) during which a black screen instructed the subjects to rest until the next instruction appeared. Each condition was repeated five times throughout the experiment. Block sequence was pseudo-randomized for each subject. The whole experiment consisted of 30 blocks and lasted ~18 min. Subjects were familiarized with the task twice, first outside the scanner, then inside the scanner. Each subject was able to perform the task without difficulties after a few practise trials due to the relative simplicity of the motor task.

Image acquisition and processing

Functional MR images were acquired on a Siemens Trio 3.0 T scanner using a gradient single-shot echo planar imaging (EPI) sequence with the following parameters: time of repetition (TR) = 2000 ms, time of echo (TE) = 3.0 ms, field of view (FOV) = 220 × 220 mm, flip angle = 90°, voxel size = 3.4 × 3.4 × 3.4 mm^3, volumes = 550 (3 dummy images), and slices = 32, interslice gap = 1 mm. Image slices were acquired in ascending order covering the whole brain from the cerebellum to the vertex. In addition, high-resolution T1-weighted structural images were acquired (TR = 2250 ms, TE = 3.93 ms, FOV = 256 mm, voxel size = 1.0 × 1.0 × 1.0 mm^3, slices = 176).

All analyses (fMRI, dynamic causal modeling) were carried out using Statistical Parametric Mapping (SPM8) (http://www.fil.ion.ucl.ac.uk; release 2009). We defined the "motor dominant hemisphere" as the hemisphere contralateral to the dominant hand (according to the EHI). To investigate the effect of hand dominance, the images of the left-handers were flipped at the midsagittal plane. Thus, for all subjects, after flipping the left hemisphere was defined to be the "motor dominant hemisphere", while the right hemisphere corresponded to the "motor non-dominant hemisphere" contralateral to the non-dominant hand. After realignment of the EPI volumes and co-registration with the anatomical T1-weighted image, all volumes were spatially normalized to the standard template of the Montreal Neurological Institute employing the unified segmentation approach (Ashburner and Friston, 2005). Finally, data were smoothed using an isotropic Gaussian kernel of 8 mm full-width-at-half-maximum.

For statistical analyses, box-car vectors for each condition were convolved with a canonical hemodynamic response function as implemented in SPM8 to create the regressors of interest in the framework of the general linear model (GLM). We used a parametric analysis to identify neural activity that was modulated by different levels of movement frequency. SPMs were computed on a single subject level with onset regressors for each hand (dominant, non-dominant) and respective parametric regressors (1st order polynomial expansion) coding the frequency of a given condition (0.75 Hz, 1.5 Hz, and 3.0 Hz). The time series in each voxel were high-pass filtered at 1/128 Hz to remove low frequency drifts. Movement parameters as assessed by the realignment algorithm were treated as covariates to exclude movement-related variance from the image time series. Furthermore, the temporally jittered instruction period was separately modeled as an additional regressor, i.e., separated from the resting and the movement conditions, to capture BOLD variations related to it but not analyzed further in the group analysis.

The parameter estimates for all four conditions (main effect "dominant hand movements", parametric modulation "dominant hand movements", main effect "non-dominant hand movements", parametric modulation "non-dominant hand movements") were subsequently compared between the groups of left- and right-handers in a 2 (hand) × 2 (main effect/modulation by movement frequency) × 2 (group) full

factorial analysis of variance (ANOVA). Voxels were considered significant when passing a height threshold of $T > 4.2$ ($P < 0.05$, family wise error (FWE)-corrected at the voxel level).

Dynamic causal modeling

We used deterministic bilinear DCM (Friston et al., 2003) to assess effective connectivity between regions activated by the motor task. DCM is a hypothesis-driven approach to model effective connectivity between distinct brain regions. DCM provides three sets of parameters: (i) the endogenous coupling irrespective of the actual experimental condition (DCM A-matrix), (ii) the parameters for context-dependent changes in coupling evoked by the four experimental conditions (i.e., two main effects of hand movements (dominant hand, non-dominant hand)) and two parametric conditions, i.e., the frequency-dependent modulation (dominant hand, non-dominant hand) (DCM B-matrix), and (iii) the direct experimental input to the system that drives regional activity (DCM C-matrix).

As DCMs are computed at the single subject level, we extracted the first eigenvariate of the BOLD time-series, adjusted for effects of interest, from 8 regions-of-interest (ROIs) at subject specific coordinates. ROIs were defined as spheres (radius: 4 mm) centered upon individual activation maxima based on individually normalized SPMs. ROIs in the motor dominant hemisphere were identified using a conjunction analysis across all three movement frequencies of the dominant hand, while ROIs in the non-dominant hemisphere were identified in a conjunction analysis of the corresponding non-dominant hand conditions. The ROIs consisted of M1, SMA, PMv, motor putamen and motor cerebellum, i.e., core regions of the motor system engaged in isolated hand movements (Grefkes et al., 2008; Witt et al., 2008). We chose PMv as ROI rather than PMd as PMv neurons are especially engaged in grasping movements, while PMd neurons are predominantly engaged in arm/reaching movements (Grefkes and Fink, 2005; Rizzolatti and Luppino, 2001; Rottschy et al., 2013). The preference of PMv for hand motor function was also reflected by the BOLD fMRI data of the present study which clearly showed a separable PMv cluster while PMd was only weakly activated and the area of activation extended typically into the M1 activation cluster (Fig. 1).

As individual activation maxima may vary substantially across subjects (Eickhoff et al., 2009), we ensured comparability by selecting coordinates according to the following anatomical constraints: M1 on the rostral wall of the central sulcus at the “hand knob” formation (Yousry et al., 1997), SMA on the mesial wall within the interhemispheric fissure between the paracentral lobule (posterior landmark) and the anterior commissure (Picard and Strick, 2001), PMv situated in the precentral sulcus close to the inferior precentral gyrus and pars opercularis (Rizzolatti et al., 2002), the mediolateral central part of the putamen (Put) (Nambu et al., 2002) and the superior part of the anterior lobe of the cerebellum (Cb) (Diedrichsen et al., 2009). All ROIs were extracted in each subject from both hemispheres using a threshold of $P < 0.001$ (uncorrected). The coordinates of all individual ROIs are given in Supplemental Table I.

Based on structural connectivity data derived from invasive studies in macaque monkeys (Akkal et al., 2007; Boussaoud et al., 2005; Hoshi et al., 2005; Kelly and Strick, 2003; Luppino et al., 1993; Middleton and Strick, 2000; Rouiller et al., 1994), we assumed endogenous connections (DCM A-matrix) as specified in Table 1. Note that connections between the cerebellum and cortical areas are relayed via the thalamus, and hence the coupling parameters from and to the cerebellum reflect the ‘net effect’ of this disynaptic connection. This notion also applies for any other indirect connection captured by the coupling parameters. We furthermore assumed a direct effect of the motor task (DCM C-matrix, input regions) on the activity of all premotor regions (dominant/non-dominant SMA, dominant/non-dominant PMv) (Goldman-Rakic et al., 1992; Wang et al., 2011).

Bayesian model selection

Based on the DCM A-matrix, we set up alternative models of varying complexity representing biologically plausible hypotheses on interregional coupling among ROIs during movements of the right or left hand at different frequencies (DCM B-matrix). Starting from a fully connected DCM B-matrix with 90 connections, we constructed 31 models according to (i) the presence of modulatory effects on interhemispheric connections, and (ii) the lateralization of coupling towards M1 contralateral to the moving hand (Supplemental Fig. 1; cf. Pool et al., 2013). At first, we omitted heterotopic interhemispheric connections between the premotor areas, putamen, cerebellum and M1 (models 2–5). Then we successively removed heterotopic interhemispheric connections between cortical and subcortical motor areas (models 6–11) as well as homotopic connections between motor areas (models 12–16). Finally, all interhemispheric connections were removed (model 16), resulting in very simple models with only a few connections. Afterwards, the same strategy was applied to lateralized models which contained connections only towards M1 contralateral to the moving hand (models 17–31). We then used random effects Bayesian model selection (BMS) to identify the model with the highest posterior evidence, that is, the model which is the most likely generative model given the data (Stephan et al., 2009). To compute the total mean variance explained by this model we used a spm_dcm_fmri_check.m script by Karl Friston (2012; https://www.jiscmail.ac.uk/cgi-bin/webadmin?A2=spm;bebd494.1203).

Statistical analysis of DCM coupling parameters

The coupling parameters of the most likely generative model were tested for statistical significance using a one sample *t*-test ($P < 0.05$, false discovery rate (FDR)-corrected for multiple comparisons). Connections that were linearly modulated by different hand movement frequencies were separately identified from the DCM B-matrix by parametric modulation effects for the dominant or non-dominant hand.

To test for differences in endogenous or task-dependent neural coupling between right- and left-handers, coupling strengths of corresponding connections were compared using independent 2-sample t-tests.

We additionally computed correlation analyses between EHI scores and (i) BOLD activity, and (ii) effective connectivity during movements of the dominant or non-dominant hand.

Results

Neural activity during unilateral fist closures

Visually paced fist closures of the dominant or the non-dominant hand were associated with enhanced BOLD activity in a network of cortical and subcortical areas comprising contralateral primary motor cortex (M1), bilateral supplementary motor area (SMA), and bilateral ventral premotor cortex (PMv), bilateral motor putamen (Put), bilateral anterior lobe of the cerebellum (Cb), and bilateral primary visual (V1) and extrastriate cortex ($P < 0.05$, FWE-corrected, Fig. 1A). Please note that hemispheres were flipped along the x-axis for the left-handers. There was no significant difference in BOLD activity when comparing right-handers with left-handers, neither for movements of the dominant hand, nor for movements of the non-dominant hand.

When testing for the effect of the parametric regressor reflecting different movement frequencies at 0.75 Hz, 1.5 Hz, or 3.0 Hz for dominant and non-dominant hand movements in left-handers and right-handers separately, we found significant clusters of voxels situated in contralateral M1 ($P < 0.05$, FWE-corrected, Fig. 1B):

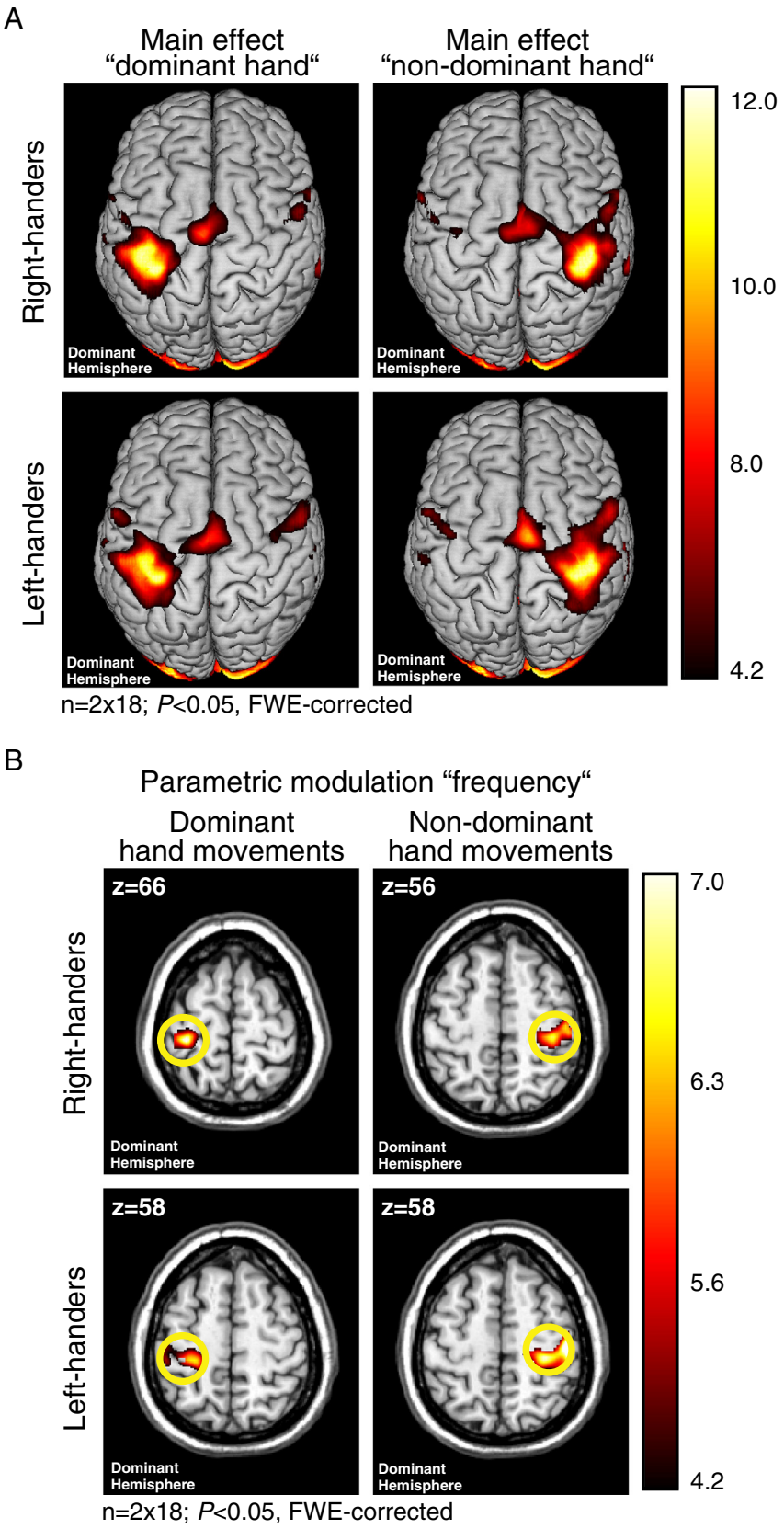

Fig. 1. Neural activity for A visually paced fist closures (main effect “hand”) and B the parametric modulation of “frequency” ($n = 2 \times 18$; $P < 0.05$, FWE-corrected).

BOLD activity in contralateral M1 positively correlated with higher movement frequencies. However, there were no significant group differences in frequency-dependent changes in BOLD activity between right- and left-handers, neither for movements of the dominant hand, nor for movements of the non-dominant hand.

Table 1
Anatomical references for endogenous connectivity (DCM A-matrix).

Connection	Reference
SMA → PMv	Luppino et al. (1993)
SMA → M1	Rouiller et al. (1994)
SMA → Put	Akkal et al. (2007)
SMA → Cb	Akkal et al. (2007)
PMv → SMA	Boussaoud et al. (2005)
PMv → M1	Rouiller et al. (1994)
PMv → Put	Middleton and Strick (2000)
PMv → Cb	Middleton and Strick (2000)
M1 → SMA	Rouiller et al. (1994)
M1 → PMv	Rouiller et al. (1994)
M1 → Put	Middleton and Strick (2000)
M1 → Cb	Middleton and Strick (2000)
Put → SMA	Kelly and Strick (2003)
Put → PMv	Middleton and Strick (2000)
Put → M1	Middleton and Strick (2000)
Put → Cb	Hoshi et al. (2005)
Cb → SMA	Akkal et al. (2007)
Cb → PMv	Middleton and Strick (2000)
Cb → M1	Middleton and Strick (2000)
Cb → Put	Hoshi et al. (2005)

SMA = supplementary motor area, PMv = ventral premotor cortex, M1 = primary motor cortex, Put = motor putamen, Cb = motor cerebellum.

Connectivity analysis

Bayesian model selection

We used dynamic causal modeling (DCM) to estimate effective connectivity in a bilateral network of key motor areas. We evaluated 31 different network models (Supplemental Fig. 1) reflecting biologically plausible hypotheses about the context-specific modulations of interregional coupling. According to random-effects Bayesian model selection, the "fully connected" model (assuming connectivity between all ROIs) showed the highest exceedance probability of all tested models for the entire group as well as for right- and left-handers separately. It was hence considered the most likely generative model of our data (Fig. 2). With respect to the divergence between prior and posterior parameter distributions, we computed total mean variance explained and its standard-deviation. On average 39% ± 11% of variance (range: 14–63%, Supplemental Fig. 2) was explained by the winner model.

Endogenous coupling (DCM A)

Fig. 3 displays the coupling parameters reflecting endogenous connectivity among the motor areas of interest independent of the conditional context (task/rest) ($P < 0.05$, FDR-corrected for multiple comparisons; see also Supplemental Table II for coupling strengths and P-values). The coupling parameters represent connection strengths, describing how fast and strong a response occurs in the target region (Friston et al., 2003). Positive coupling parameters (green arrows) suggest a facilitation of neural activity, whereas negative coupling parameters (red arrows) can be interpreted as inhibition of neural activity. The term "dominant hemisphere" was defined to refer to the hemisphere contralateral to the dominant hand.

In both right- and left-handers, endogenous coupling of neural activity between the motor areas of interest was symmetrically organized across hemispheres (left: dominant hemisphere). The most prominent positive influence on intrinsic M1 activity was exerted by ipsilateral SMA and PMv in both right- and left-handers. In contrast, endogenous coupling

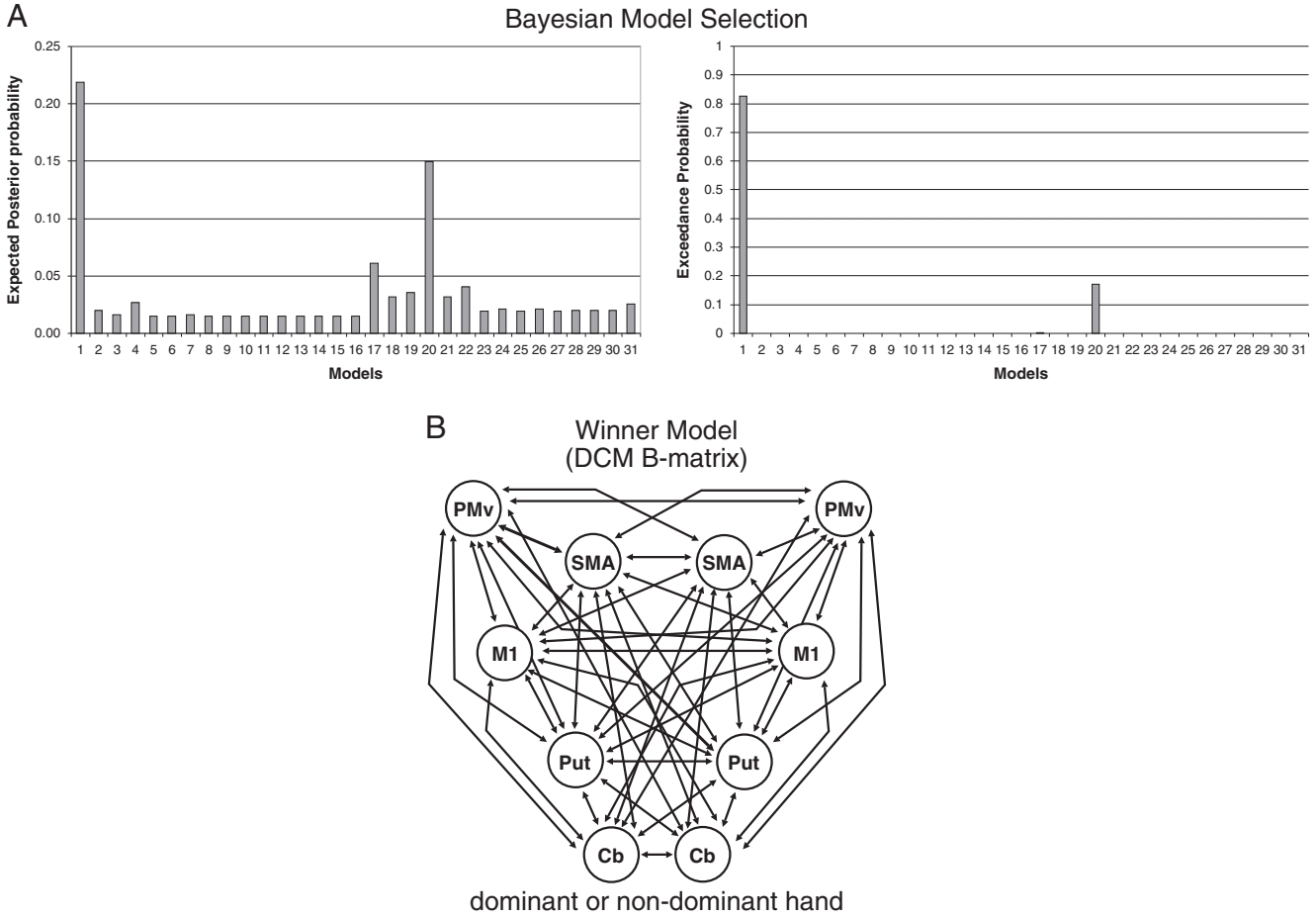

Fig. 2. A Bayesian model selection and B the winner model.

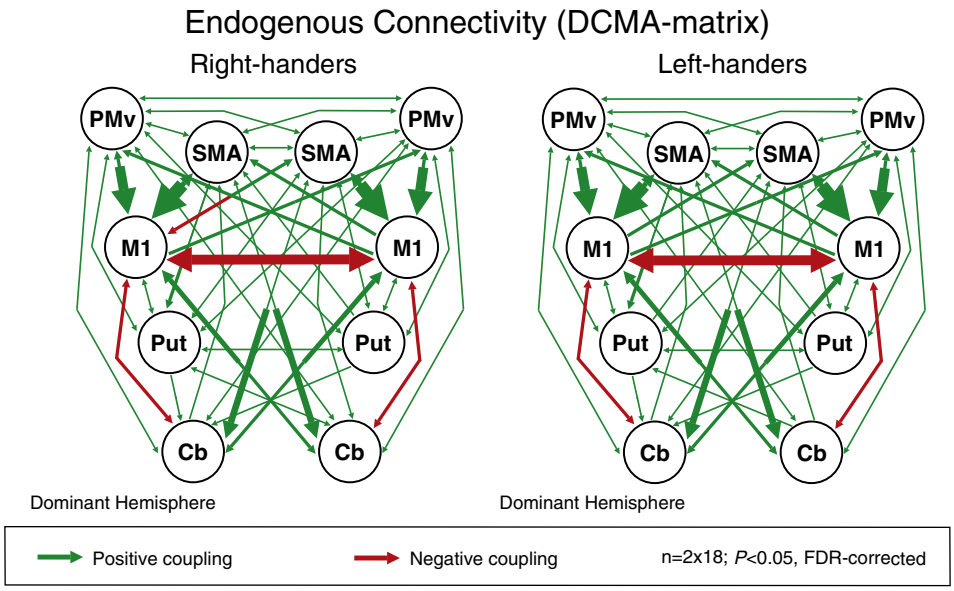

Fig. 3. Endogenous connectivity (DCM A-matrix; n = 2 × 18; $P < 0.05$, FDR-corrected). Green arrows = positive coupling rates, red arrows = negative coupling rates. The width of each arrow corresponds to the coupling strength. In left-handers, the inhibitory connection ndSMA ➔ dM1 is significant at an uncorrected threshold ($P < 0.05$). For mean coupling parameters and *P*-values (one-sample *t*-test against zero) see Supplemental Table II.

between the putamen, cerebellum, and ipsilateral M1 was less pronounced. Intrahemispheric interactions between M1–Put as well as interhemispheric interactions between SMA–M1 and M1–M1 were inhibitory.

Differences between right- and left-handers (DCM A)

When testing for differences between right- and left-handers, we found no significant handedness-dependent effects.

Task-induced changes in neural coupling (DCM B, main effect of hand)

Fig. 4 depicts the effect of unilateral fist closures on the interregional coupling between the motor areas of interest (DCM B-matrix) ($P < 0.05$, FDR-corrected; see also Supplemental Tables IIIa and IIIb for coupling strengths and *P*-values). When right-handers (n = 18) or left-handers (n = 18) moved their dominant hand, neural activity in the contralateral M1 was driven by stronger bilateral coupling with the SMA, PMv, putamen, and cerebellum. In contrast, the influence of premotor regions on M1 ipsilateral to the moving hand was negative suggesting that activity of this region was inhibited. Movements of the non-dominant hand evoked a mirror-reversed pattern of motor network modulations in both groups.

When comparing coupling parameters of the dominant hand with corresponding parameters of the non-dominant hand, we found a stronger excitatory influence on SMA exerted by contralateral M1, contralateral putamen, ipsilateral PMv, ipsilateral cerebellum and ipsilateral SMA ($P < 0.05$, FDR-corrected). In addition, there was a stronger influence from ipsilateral SMA onto ipsilateral cerebellum and both ipsi- and contralateral M1 ($P < 0.05$, FDR-corrected). Our data further revealed a significant stronger inhibitory influence from ipsilateral SMA towards ipsilateral M1 in right-handers while performing movements with the dominant (right) hand ($P < 0.05$, FDR-corrected). In left-handers, we did not find such differences between the dominant and non-dominant hand.

Differences between right- and left-handers (DCM B, main effect of hand)

When testing for differences between right- and left-handers, we found significant effects only for the dominant but not for the non-dominant hand. For dominant hand movements, neural coupling strength exerted from contralateral (dominant) SMA upon contralateral (dominant) M1 was significantly stronger in right-handers as compared to left-handers ($P < 0.05$, FDR-corrected; Fig. 5). Similarly, right-handers featured significantly stronger influences exerted by contralateral M1, contralateral putamen, ipsilateral SMA as well as ipsilateral PMv onto contralateral SMA, and vice versa, during dominant hand movements. This means that particularly connections from and to contralateral (dominant) SMA showed stronger couplings when right-handers moved their dominant, right hand as compared to left-handers moving their dominant hand.

Spearman rank correlations between EHI scores and DCM parameters (Table 2, FDR-corrected for multiple comparisons) revealed significant correlations between EHI scores and coupling parameters for the same connections as reported above for the t-tests comparing neural coupling between right- and left-handers. This finding indicates that also the individual predisposition to preferentially use the right hand was linked to higher coupling parameters of contralateral SMA with other motor areas. In contrast, we found no significant correlations between EHI scores and DCM coupling parameters during movements of the non-dominant hand.

Frequency-dependent changes of neural coupling (DCM B-matrix, parametric modulation)

In a previous publication with a larger sample of subjects (n = 36) (Pool et al., 2013), we demonstrated that in right-handers movements at higher frequencies were associated with a linear increase in neural coupling strengths from contralateral premotor areas (SMA, PMv) towards contralateral M1. When testing for this frequency effect in the present data with a sub-sample of this group (n = 18), the DCM analysis confirmed that right-handers showed increasing excitatory influences from contralateral SMA and ipsilateral PMv onto contralateral M1 associated with higher frequencies during dominant hand movements ($P < 0.05$, FDR-corrected). During non-dominant hand movements, this effect was only significant from contralateral SMA onto contralateral M1 ($P < 0.05$, FDR-corrected). This constitutes a replication of our previous analysis with 36 right-handers (Pool et al., 2013). When testing for frequency-dependent coupling changes during movements of the dominant hand in left-handers, we found no significant effect after FDR correction ($P > 0.05$). At an uncorrected threshold ($P < 0.05$), the DCM analysis showed that increasing movement rate was associated with a stronger excitatory influence from contralateral PMv onto contralateral M1 as well as a stronger inhibitory influence from contralateral SMA onto ipsilateral M1. During movements of the non-dominant hand,

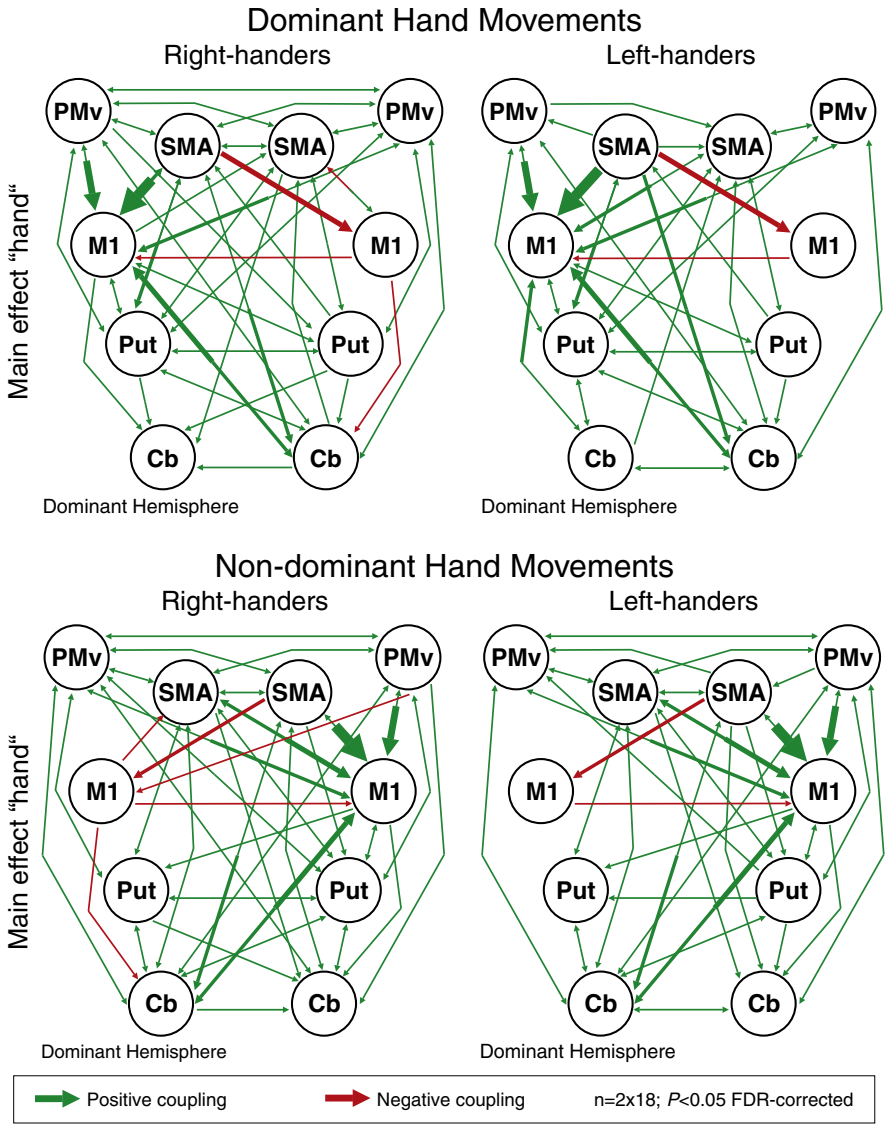

Fig. 4. Modulatory effects on effective connectivity (main effect "hand") during right and left hand fist closures (DCM B-matrix; n = 2 × 18; $P < 0.05$, FDR-corrected). Green arrows = positive coupling rate, red arrows = negative coupling rates. The width of each arrow corresponds to the coupling strength. For mean coupling parameters and *P*-values (one-sample *t*-test against zero) see Supplemental Tables IIIa and IIIb.

again no connection survived FDR correction. At uncorrected thresholds, a frequency-dependent effect could also be observed from contralateral SMA onto ipsilateral M1.

Differences between right- and left-handers (parametric modulation)

When testing for frequency-dependent differences between right- and left-handers, we found no significant effect after FDR correction ($P > 0.05$).

Discussion

We found that during dominant hand movements, neural coupling of contralateral (dominant) SMA with premotor areas, motor putamen and M1 was significantly higher in right-handers as compared to left-handers. Moreover, our results revealed a positive correlation between neural coupling strengths and the Edinburgh Handedness Inventory (EHI) scores during movements of the dominant hand. Together, our findings indicate that a stronger preference to use the right hand corresponds to stronger neural coupling of contralateral SMA when performing dominant hand movements.

Neural activity and handedness

Although several neuroimaging studies have already addressed the issue of handedness (Dassonville et al., 1997; Kim et al., 1993; Kloppel et al., 2007; Siebner et al., 2002; Solodkin et al., 2001; Volkmann et al., 1998), to date our understanding of the relationship between handedness and brain activation remains incomplete. For example, Kim and colleagues observed that right-handers relative to left-handers had larger ipsilateral activation volumes in M1 when performing a repetitive finger–thumb opposition task (Kim et al., 1993). In contrast, Solodkin et al. (2001) reported that right- and left-handers only showed differences in complex motor tasks, while simple hand movements – comparable to those implemented in the present study – did not evoke significant differences in neural activity (Solodkin et al., 2001). In line with the latter finding, we did not find any statistically significant differences in activation clusters between right- and left-handers. The relative simplicity of the task used in the present study also implies that any differences between right- and left-handers were not due to differences in task complexity, but rather reflect "true" differences in neural coupling.

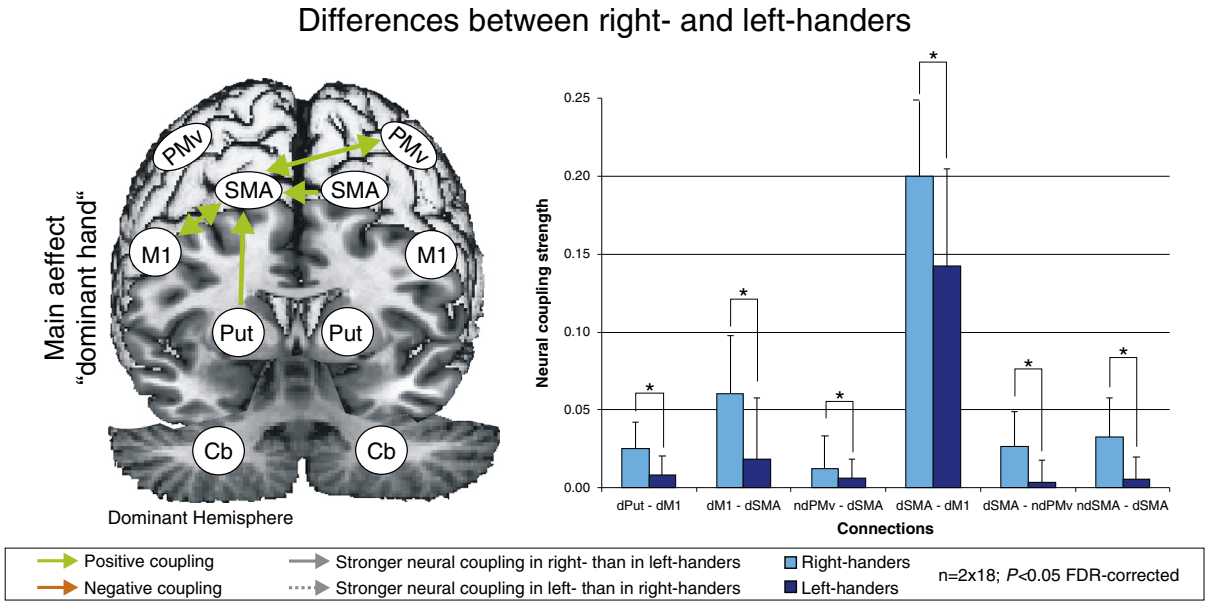

Fig. 5. Differences between right- and left-handers when performing dominant hand movements (* $P < 0.05$, FDR-corrected).

Effective connectivity and handedness

Neural coupling between SMA and M1

At the connectivity level, contralateral SMA exerted a stronger excitatory influence upon contralateral M1 in right-handers as compared to left-handers, when performing dominant hand movements (Fig. 5). The SMA is strongly engaged in movement sequencing and pacing (Jakobs et al., 2009; Jenkins et al., 2000; Passingham, 1989). A number of studies have shown that especially neurons in SMA have hemispheric-specific functional properties (Dum and Strick, 2002; Fried et al., 1991; Hoshi and Tanji, 2004). For example, tract-tracing studies in monkeys revealed that SMA neurons exhibit dense axonal projections to M1 neurons, especially between the respective hand representations of the two areas (Dum and Strick, 2002). Moreover, Hoshi and Tanji (2004) investigated neuronal activity in monkeys performing a target-reach task by following two sets of instructions (the target location and the hand to use to reach the target). These data revealed a selective activity of SMA neurons for either the ipsilateral or the contralateral arm, indicating that the SMA participates in selecting which hand has to be used (Hoshi and Tanji, 2004).

Furthermore, several fMRI studies reported a dominant role of left SMA in right-handers (Babiloni et al., 2003; Jancke et al., 2000; Rogers et al., 2004). Rogers et al. (2004) investigated effective connectivity between SMA and sensorimotor cortex in right-handers using structural equation modeling (Rogers et al., 2004). The authors observed that the positive influence of contralateral SMA on contralateral sensorimotor cortex was stronger during movements of the dominant right hand compared to corresponding connections during movements of the non-dominant left hand. Similar effects were also found in the present study for right-handers. Our data furthermore revealed a stronger inhibitory influence from ipsilateral SMA towards ipsilateral M1 during dominant hand movements as compared to non-dominant hand movements.

In contrast to right-handers, left-handers showed no significant changes in effective connectivity between movements of their dominant or non-dominant hand suggesting that left-handers featured a lack of lateralization to the dominant hand-hemisphere system. This functional finding fits with structural data reported in anatomical studies showing that left-handers compared to right-handers featured less asymmetry with respect to the volume of intracortical connections in the hemisphere contralateral to the preferred hand (Amunts et al., 1996).

Neural coupling between premotor areas and SMA

Interestingly, we found that effective connectivity among the premotor areas of interest was significantly stronger in subjects who preferred their right hand for manual skills, especially with respect to the SMA contralateral to the dominant hand. Several studies already demonstrated that premotor areas, in general, are richly interconnected (Dum and Strick, 2005). The SMA, of all premotor regions, has the densest and most balanced reciprocal connections with the contralateral SMA, premotor cortex as well as with M1 (Boussaoud et al., 2005; Dum and Strick, 2005; Luppino et al., 1993; Rouiller et al., 1994). Major connections between the SMA and PMv have been reported in macaques (Johnson and Ferraina, 1996; Kurata, 1991) and galagos (Fang et al., 2005). These findings correspond well to our connectivity results suggesting a general principle of brain organization with a prominent role of contralateral (dominant) SMA that is stronger interconnected with ipsilateral PMv and ipsilateral SMA in right-handers when performing dominant hand movements as compared to left-handers (Fig. 5). Hence, the degree of effective connectivity of contralateral SMA corresponds to right-handedness and might, therefore, be important for hemispheric-specific control of dominant hand movements in right-handers. In contrast, this effect could not be observed in the opposite direction. Our results thus indicate a differential recruitment profile for left-handers reflected by a weaker effective connectivity network of contralateral SMA when performing dominant hand movements. Corresponding to this, Buckingham and colleagues investigated motor attention in right- and left-handers by combining a discontinuous double-step reaching task

Table 2
Spearman rank correlations between EHI scores and effective connectivity.

Dominant hand movements			Non-dominant hand movements
dM1 – dSMA	Spearman–Rho	.562	**No significant correlations with EHI**
	p-value	.012*	
ndSMA – dSMA	Spearman–Rho	.572	
	p-value	.019*	
ndPMv – dSMA	Spearman–Rho	.487	
	p-value	.045*	
dPut – dSMA	Spearman–Rho	.537	
	p-value	.017*	

(d = dominant hemisphere, contralateral to the dominant hand; nd = non-dominant hemisphere, contralateral to the non-dominant hand).
* $P < 0.05$, FDR-corrected for multiple comparisons; n = 28.

with a Posner-style hand cueing paradigm (Buckingham et al., 2011). The authors demonstrated that right-handers needed more time to inhibit their dominant hand, indicating that their dominant hand was more readily primed to move than their non-dominant hand while left-handers showed neither of these asymmetries, indicating that they lack an equivalent attentional bias for the dominant hand (Buckingham et al., 2011). This finding nicely fits our observation of generally stronger intra- and interhemispheric effective connectivity in right-handers during movements of the dominant hand.

Neural coupling between putamen and SMA

In addition to cortical areas, we found that effective connectivity from contralateral putamen on contralateral SMA was also significantly stronger in subjects who preferred their right hand. The putamen receives somatotopic projections from the sensorimotor cortex and is involved in the facilitation and inhibition of actions (Alexander and Crutcher, 1990). Studies further suggested a role of the putamen in the automation of previously learned movements (Griffiths et al., 1994) as well as in timing mechanisms (Macar et al., 2004; Rao et al., 2001). For example, Macar and collegues used event-related fMRI to investigate healthy right-handed subjects when performing a timing task and a force task (Macar et al., 2004). As expected, the authors revealed an important role of the putamen in timing mechanisms, but also observed prominent activation of SMA during the timing task (Macar et al., 2004). The authors concluded that timing processes could be subserved by a striato-thalamo-cortical pathway including the SMA. Similar effects might also underlie the stronger influence exerted by the putamen onto SMA in right-handers for the dominant hand, as observed in the present study. Moreover, de la Fuente-Fernandez et al. (2000) investigated healthy right-handed subjects by using [^{18}F]fluorodopa positron emission tomography and showed that the degree of right hand preference correlated with fluorodopa uptake in the left putamen. This finding is well in line with our results and suggests a role of the putamen in motor lateralization (de la Fuente-Fernandez et al., 2000).

Limitations and conclusion

One limitation of our study pertains to the limited number of areas included in the connectivity model. Areas known to be involved in the motor control of even simple hand movements, e.g. prefrontal and parietal cortices (Filimon, 2010; Goldman-Rakic, 1987), had to be excluded from the analysis because of the technical and computational limitations of DCM in its current implementation. In DCM, model complexity is penalized by more conservative shrinkage priors which make it more difficult for a given connection to become significant. The reason for this is that the priors on the connectivity parameters ensure that the system remains stable (Friston et al., 2003). Hence, the number of included regions in DCM is always a trade-off between model fit and generalizability. Therefore, that we found significant connections despite a rather complex model (10 regions, 90 connections) highlights the robustness of the data. Moreover, left-handers featured less asymmetry in effective connectivity, despite clear preference to use their left hand for everyday life tasks. We cannot disentangle whether this effect arises from the fact that left-handers live in an environment that is rather made for right-handers (and hence they are more often forced to use their non-dominant right hand which might also affect cortical connectivity). However, the relative simplicity of the motor task used in the present study makes it rather unlikely that relevant use-dependent effects in every-day life may have influenced the differences found between right- and left-handed subjects. It is interesting to note that differences between right- and left-handers were only evident in the connectivity data but not in the "classical" BOLD activation analysis. That connectivity analyses of motor system activity can have higher sensitivity compared to activation analyses has also been shown by Sharma et al. (2009). A reason for that might rest in the region of interest approach used in DCM which corrects for residual interindividual variability in the precise anatomical location of premotor areas in individual subjects. Likewise, in DCM, the hemodynamic response function (HRF) is computed for each and every ROI separately (Friston et al., 2003) in contrast to the "classical" activation analysis, which uses a canonical HRF for all voxels. Hence, DCM better accounts for variability of the HRF between regions, which might further increase its sensitivity for detecting differences between groups of subjects.

In conclusion, the present study suggests that handedness is associated with differences in effective connectivity within the human motor network. Our results reveal a general principle of brain organization with a prominent role of dominant SMA in right-handers. Moreover, our data indicate a strong lateralization in the dominant hand-hemisphere system when performing dominant hand movements. Left-handers showed a weaker asymmetry in motor network connectivity implying different hemispheric mechanism of hand motor control as compared to right-handers.

Supplementary data to this article can be found online at http://dx.doi.org/10.1016/j.neuroimage.2014.05.048.

Acknowledgments

We thank our volunteers and are grateful to Dr Marc Tittgemeyer and the MR staff for the support. CG was supported by a grant from the German Research Foundation (Deutsche Forschungsgemeinschaft GR 3285/2-1). SBE was supported by the Deutsche Forschungsgemeinschaft (DFG, EI 816/4-1; S.B.E. and LA 3071/3-1), the National Institute of Mental Health (R01-MH074457) and the Helmholtz Initiative on Systems Biology. GRF gratefully acknowledges support from the Marga and Walter Boll Stiftung.

Declaration of conflict of interests

The authors declare that they have no competing interests.

References

Akkal, D., Dum, R.P., Strick, P.L., 2007. Supplementary motor area and presupplementary motor area: targets of basal ganglia and cerebellar output. J. Neurosci. 27 (40), 10659–10673.
Alexander, G.E., Crutcher, M.D., 1990. Functional architecture of basal ganglia circuits: neural substrates of parallel processing. Trends Neurosci. 13 (7), 266–271.
Amunts, K., Schlaug, G., Schleicher, A., Steinmetz, H., Dabringhaus, A., Roland, P.E., Zilles, K., 1996. Asymmetry in the human motor cortex and handedness. Neuroimage 4 (3 Pt 1), 216–222.
Ashburner, J., Friston, K.J., 2005. Unified segmentation. Neuroimage 26 (3), 839–851.
Babiloni, C., Carducci, F., Del Gratta, C., Demartin, M., Romani, G.L., Babiloni, F., Rossini, P.M., 2003. Hemispherical asymmetry in human SMA during voluntary simple unilateral movements. An fMRI study. Cortex 39 (2), 293–305.
Borod, J.C., Caron, H.S., Koff, E., 1984. Left-handers and right-handers compared on performance and preference measures of lateral dominance. Br. J. Psychol. 75 (Pt 2), 177–186.
Boussaoud, D., Tanne-Gariepy, J., Wannier, T., Rouiller, E.M., 2005. Callosal connections of dorsal versus ventral premotor areas in the macaque monkey: a multiple retrograde tracing study. BMC Neurosci. 6, 67.
Brouwer, B., Sale, M.V., Nordstrom, M.A., 2001. Asymmetry of motor cortex excitability during a simple motor task: relationships with handedness and manual performance. Exp. Brain Res. 138 (4), 467–476.
Buckingham, G., Main, J.C., Carey, D.P., 2011. Asymmetries in motor attention during a cued bimanual reaching task: left and right handers compared. Cortex 47 (4), 432–440.
Dassonville, P., Zhu, X.H., Uurbil, K., Kim, S.G., Ashe, J., 1997. Functional activation in motor cortex reflects the direction and the degree of handedness. Proc. Natl. Acad. Sci. U. S. A. 94 (25), 14015–14018.
de la Fuente-Fernandez, R., Kishore, A., Calne, D.B., Ruth, T.J., Stoessl, A.J., 2000. Nigrostriatal dopamine system and motor lateralization. Behav. Brain Res. 112 (1–2), 63–68.
Diedrichsen, J., Balsters, J.H., Flavell, J., Cussans, E., Ramnani, N., 2009. A probabilistic MR atlas of the human cerebellum. Neuroimage 46 (1), 39–46.
Dum, R.P., Strick, P.L., 2002. Motor areas in the frontal lobe of the primate. Physiol. Behav. 77 (4–5), 677–682.
Dum, R.P., Strick, P.L., 2005. Frontal lobe inputs to the digit representations of the motor areas on the lateral surface of the hemisphere. J. Neurosci. 25 (6), 1375–1386.
Eickhoff, S.B., Grefkes, C., Fink, G.R., Zilles, K., 2008. Functional lateralization of face, hand, and trunk representation in anatomically defined human somatosensory areas. Cereb. Cortex 18 (12), 2820–2830.

Eickhoff, S.B., Heim, S., Zilles, K., Amunts, K., 2009. A systems perspective on the effective connectivity of overt speech production. Philos. Trans. A Math. Phys. Eng. Sci. 367 (1896), 2399–2421.
Fagard, J., 2013. The nature and nurture of human infant hand preference. Ann. N. Y. Acad. Sci. 1288, 114–123.
Fang, P.C., Stepniewska, I., Kaas, J.H., 2005. Ipsilateral cortical connections of motor, premotor, frontal eye, and posterior parietal fields in a prosimian primate, Otolemur garnetti. J. Comp. Neurol. 490 (3), 305–333.
Filimon, F., 2010. Human cortical control of hand movements: parietofrontal networks for reaching, grasping, and pointing. Neuroscientist 16 (4), 388–407.
Fried, I., Katz, A., McCarthy, G., Sass, K.J., Williamson, P., Spencer, S.S., Spencer, D.D., 1991. Functional organization of human supplementary motor cortex studied by electrical stimulation. J. Neurosci. 11 (11), 3656–3666.
Friston, K.J., Harrison, L., Penny, W., 2003. Dynamic causal modelling. Neuroimage 19 (4), 1273–1302.
Goldman-Rakic, P.S., 1987. Motor control function of the prefrontal cortex. Ciba Found. Symp. 132, 187–200.
Goldman-Rakic, P.S., Bates, J.F., Chafee, M.V., 1992. The prefrontal cortex and internally generated motor acts. Curr. Opin. Neurobiol. 2 (6), 830–835.
Grefkes, C., Fink, G.R., 2005. The functional organization of the intraparietal sulcus in humans and monkeys. J. Anat. 207 (1), 3–17.
Grefkes, C., Eickhoff, S.B., Nowak, D.A., Dafotakis, M., Fink, G.R., 2008. Dynamic intra- and interhemispheric interactions during unilateral and bilateral hand movements assessed with fMRI and DCM. Neuroimage 41 (4), 1382–1394.
Griffiths, P.D., Perry, R.H., Crossman, A.R., 1994. A detailed anatomical analysis of neurotransmitter receptors in the putamen and caudate in Parkinson's disease and Alzheimer's disease. Neurosci. Lett. 169 (1–2), 68–72.
Hammond, G., 2002. Correlates of human handedness in primary motor cortex: a review and hypothesis. Neurosci. Biobehav. Rev. 26 (3), 285–292.
Hoshi, E., Tanji, J., 2004. Differential roles of neuronal activity in the supplementary and presupplementary motor areas: from information retrieval to motor planning and execution. J. Neurophysiol. 92 (6), 3482–3499.
Hoshi, E., Tremblay, L., Feger, J., Carras, P.L., Strick, P.L., 2005. The cerebellum communicates with the basal ganglia. Nat. Neurosci. 8 (11), 1491–1493.
Jakobs, O., Wang, L.E., Dafotakis, M., Grefkes, C., Zilles, K., Eickhoff, S.B., 2009. Effects of timing and movement uncertainty implicate the temporo-parietal junction in the prediction of forthcoming motor actions. Neuroimage 47 (2), 667–677.
Jancke, L., Specht, K., Mirzazade, S., Loose, R., Himmelbach, M., Lutz, K., Shah, N.J., 1998. A parametric analysis of the 'rate effect' in the sensorimotor cortex: a functional magnetic resonance imaging analysis in human subjects. Neurosci. Lett. 252 (1), 37–40.
Jancke, L., Peters, M., Himmelbach, M., Nosselt, T., Shah, J., Steinmetz, H., 2000. fMRI study of bimanual coordination. Neuropsychologia 38 (2), 164–174.
Jenkins, I.H., Jahanshahi, M., Jueptner, M., Passingham, R.E., Brooks, D.J., 2000. Self-initiated versus externally triggered movements. II. The effect of movement predictability on regional cerebral blood flow. Brain 123 (Pt 6), 1216–1228.
Johnson, P.B., Ferraina, S., 1996. Cortical networks for visual reaching: intrinsic frontal lobe connectivity. Eur. J. Neurosci. 8 (7), 1358–1362.
Kelly, R.M., Strick, P.L., 2003. Cerebellar loops with motor cortex and prefrontal cortex of a nonhuman primate. J. Neurosci. 23 (23), 8432–8444.
Kim, S.G., Ashe, J., Hendrich, K., Ellermann, J.M., Merkle, H., Ugurbil, K., Georgopoulos, A.P., 1993. Functional magnetic resonance imaging of motor cortex: hemispheric asymmetry and handedness. Science 261 (5121), 615–617.
Kloppel, S., van Eimeren, T., Glauche, V., Vongerichten, A., Munchau, A., Frackowiak, R.S., Buchel, C., Weiller, C., Siebner, H.R., 2007. The effect of handedness on cortical motor activation during simple bilateral movements. Neuroimage 34 (1), 274–280.
Kurata, K., 1991. Corticocortical inputs to the dorsal and ventral aspects of the premotor cortex of macaque monkeys. Neurosci. Res. 12 (1), 263–280.
Luppino, G., Matelli, M., Camarda, R., Rizzolatti, G., 1993. Corticocortical connections of area F3 (SMA-proper) and area F6 (pre-SMA) in the macaque monkey. J. Comp. Neurol. 338 (1), 114–140.
Macar, F., Anton, J.L., Bonnet, M., Vidal, F., 2004. Timing functions of the supplementary motor area: an event-related fMRI study. Brain Res. Cogn. Brain Res. 21 (2), 206–215.
Middleton, F.A., Strick, P.L., 2000. Basal ganglia and cerebellar loops: motor and cognitive circuits. Brain Res. Brain Res. Rev. 31 (2–3), 236–250.
Nambu, A., Kaneda, K., Tokuno, H., Takada, M., 2002. Organization of corticostriatal motor inputs in monkey putamen. J. Neurophysiol. 88 (4), 1830–1842.
Oldfield, R.C., 1971. The assessment and analysis of handedness: the Edinburgh inventory. Neuropsychologia 9 (1), 97–113.
Passingham, R.E., 1989. Premotor cortex and the retrieval of movement. Brain Behav. Evol. 33 (2–3), 189–192.
Passingham, R.E., 1997. Functional organisation of the motor system. In: Frackowiak, R.S.J., Friston, K.J., Frith, C.D., Dolan, R.J., Mazziotta, J.C. (Eds.), Human Brain Function. Academic Press, San Diego, pp. 243–274.
Picard, N., Strick, P.L., 2001. Imaging the premotor areas. Curr. Opin. Neurobiol. 11 (6), 663–672.
Pool, E.M., Rehme, A.K., Fink, G.R., Eickhoff, S.B., Grefkes, C., 2013. Network dynamics engaged in the modulation of motor behavior in healthy subjects. Neuroimage 82C, 68–76.
Pujol, J., Deus, J., Losilla, J.M., Capdevila, A., 1999. Cerebral lateralization of language in normal left-handed people studied by functional MRI. Neurology 52 (5), 1038–1043.
Rao, S.M., Mayer, A.R., Harrington, D.L., 2001. The evolution of brain activation during temporal processing. Nat. Neurosci. 4 (3), 317–323.
Rizzolatti, G., Luppino, G., 2001. The cortical motor system. Neuron 31 (6), 889–901.
Rizzolatti, G., Fogassi, L., Gallese, V., 2002. Motor and cognitive functions of the ventral premotor cortex. Curr. Opin. Neurobiol. 12 (2), 149–154.
Rogers, B.P., Carew, J.D., Meyerand, M.E., 2004. Hemispheric asymmetry in supplementary motor area connectivity during unilateral finger movements. Neuroimage 22 (2), 855–859.
Rottschy, C., Caspers, S., Roski, C., Reetz, K., Dogan, I., Schulz, J.B., Zilles, K., Laird, A.R., Fox, P.T., Eickhoff, S.B., 2013. Differentiated parietal connectivity of frontal regions for "what" and "where" memory. Brain Struct. Funct. 218 (6), 1551–1567.
Rouiller, E.M., Babalian, A., Kazennikov, O., Moret, V., Yu, X.H., Wiesendanger, M., 1994. Transcallosal connections of the distal forelimb representations of the primary and supplementary motor cortical areas in macaque monkeys. Exp. Brain Res. 102 (2), 227–243.
Sadato, N., Ibanez, V., Deiber, M.P., Campbell, G., Leonardo, M., Hallett, M., 1996. Frequency-dependent changes of regional cerebral blood flow during finger movements. J. Cereb. Blood Flow Metab. 16 (1), 23–33.
Serrien, D.J., Ivry, R.B., Swinnen, S.P., 2006. Dynamics of hemispheric specialization and integration in the context of motor control. Nat. Rev. Neurosci. 7 (2), 160–166.
Sharma, N., Baron, J.C., Rowe, J.B., 2009. Motor imagery after stroke: relating outcome to motor network connectivity. Ann. Neurol. 66 (5), 604–616.
Siebner, H.R., Limmer, C., Peinemann, A., Drzezga, A., Bloem, B.R., Schwaiger, M., Conrad, B., 2002. Long-term consequences of switching handedness: a positron emission tomography study on handwriting in "converted" left-handers. J. Neurosci. 22 (7), 2816–2825.
Solodkin, A., Hlustik, P., Noll, D.C., Small, S.L., 2001. Lateralization of motor circuits and handedness during finger movements. Eur. J. Neurol. 8 (5), 425–434.
Stephan, K.E., Penny, W.D., Daunizeau, J., Moran, R.J., Friston, K.J., 2009. Bayesian model selection for group studies. Neuroimage 46 (4), 1004–1017.
Volkmann, J., Schnitzler, A., Witte, O.W., Freund, H., 1998. Handedness and asymmetry of hand representation in human motor cortex. J. Neurophysiol. 79 (4), 2149–2154.
Wang, L.E., Fink, G.R., Diekhoff, S., Rehme, A.K., Eickhoff, S.B., Grefkes, C., 2011. Noradrenergic enhancement improves motor network connectivity in stroke patients. Ann. Neurol. 69 (2), 375–388.
Witt, S.T., Laird, A.R., Meyerand, M.E., 2008. Functional neuroimaging correlates of finger-tapping task variations: an ALE meta-analysis. Neuroimage 42 (1), 343–356.
Yousry, T.A., Schmid, U.D., Alkadhi, H., Schmidt, D., Peraud, A., Buettner, A., Winkler, P., 1997. Localization of the motor hand area to a knob on the precentral gyrus. A new landmark. Brain 120 (Pt 1), 141–157.
Ziemann, U., Hallett, M., 2001. Hemispheric asymmetry of ipsilateral motor cortex activation during unimanual motor tasks: further evidence for motor dominance. Clin. Neurophysiol. 112 (1), 107–113.

Supplemental Information

Supplemental TABLE I. Individual local fMRI maxima used as ROIs for DCM

	dSMA	ndSMA	dPMv	ndPMv	dM1	ndM1	dPut	ndPut	dCb	ndCb
Subject 1	-8 -6 54	4 -8 56	-54 -4 48	52 2 42	-34 -28 48	34 -26 50	-26 2 8	28 4 -8	-20 -54 -22	20 -54 -22
Subject 2	-4 -4 54	4 -4 54	-56 0 42	54 -2 46	-34 -28 58	36 -18 52	-26 0 2	26 0 6	-24 -46 -24	28 -44 -26
Subject 3	-8 -8 54	12 -10 50	-60 2 36	58 2 34	-36 -30 54	36 -30 56	-28 -4 -2	26 2 2	-32 -60 -28	30 -56 -26
Subject 4	-4 -4 54	4 -10 50	-56 2 40	58 6 36	-40 -22 56	38 -32 64	-26 -2 2	26 0 -2	-26 -54 -30	36 -62 -30
Subject 5	-6 2 48	4 -4 50	-50 -12 40	58 8 34	-36 -28 56	36 -20 66	-28 0 2	26 2 2	-24 -52 -28	28 -52 -28
Subject 6	-10 -4 52	6 -10 52	-58 -4 44	60 2 22	-34 -30 60	36 -26 56	-28 -6 -2	26 6 0	-28 -54 -24	38 -50 -26
Subject 7	-4 -12 56	4 -10 58	-56 8 30	60 4 32	-44 -24 56	42 -22 50	-26 6 0	30 10 2	-28 -50 -24	28 -54 -24
Subject 8	-8 -4 68	4 4 56	-54 -12 48	54 0 48	-40 -26 54	38 -22 52	-30 -4 -2	28 -6 -4	-34 -64 -24	30 -54 -24
Subject 9	-8 -12 56	10 0 56	-58 2 36	58 2 30	-42 -28 64	42 -28 56	-28 0 0	30 2 -6	-24 -50 -26	26 -50 -24
Subject 10	-6 -10 52	4 -12 54	-54 6 40	52 -16 42	-32 -28 68	38 -24 52	-28 0 -4	26 6 -2	-22 -48 -26	28 -48 -22
Subject 11	-4 -10 60	4 -4 54	-60 2 32	54 0 40	-36 -28 64	38 -26 54	-28 -6 -4	28 -2 -2	-24 -54 -26	26 -52 -24
Subject 12	-10 -8 50	10 -4 52	-58 -2 40	56 -12 48	-42 -28 64	38 -28 56	-28 -2 -8	28 -4 -8	-24 -50 -26	28 -48 -28
Subject 13	-4 -8 50	4 -4 52	-60 0 32	52 4 38	-40 -28 58	40 -26 60	-28 -4 -8	28 -4 2	-38 -60 -22	26 -54 -22
Subject 14	-4 -8 58	4 4 52	-58 -4 42	58 8 32	-40 -26 56	44 -22 56	-26 4 4	26 4 4	-34 -52 -28	34 -48 -30
Subject 15	-6 -8 58	4 4 52	-60 4 22	62 8 26	-40 -20 60	34 -24 56	-26 2 -6	26 0 4	-26 -50 -28	22 -52 -22
Subject 16	-8 -6 54	6 -2 56	-56 0 40	56 4 36	-36 -24 52	36 -26 54	-26 2 -2	26 2 -4	-38 -62 -22	36 -58 -22
Subject 17	-6 -4 54	4 -8 56	-60 12 30	62 4 36	-44 -22 60	42 -24 64	-28 0 -6	28 -8 2	-24 -52 -24	24 -50 -24
Subject 18	-6 -8 56	6 -6 54	-52 -8 38	54 -4 48	-36 -28 66	40 -28 64	-28 -4 -2	28 -4 -4	-26 -50 -26	26 -50 -26
Subject 19	-8 -2 50	8 0 50	-54 4 38	54 6 42	-36 -30 64	38 -30 62	-28 0 0	28 -2 4	-24 -52 -24	22 -54 -20
Subject 20	-4 -6 54	8 -4 52	-50 6 42	56 2 34	-38 -22 52	38 -22 52	-28 -4 0	26 -4 4	-28 -58 -22	36 -48 -26
Subject 21	-4 -8 56	8 -12 56	-54 6 38	58 -16 46	-36 -30 58	34 -28 66	-28 -4 -4	28 -6 -2	-22 -52 -26	26 -50 -26
Subject 22	-10 -12 52	4 -14 48	-56 8 32	52 10 32	-36 -28 62	34 -22 58	-26 6 2	28 -4 0	-32 -56 -24	24 -50 -24
Subject 23	-8 -8 54	6 -16 52	-62 8 30	62 8 36	-30 -30 66	36 -28 58	-28 0 -8	28 -8 -8	-20 -50 -26	24 -48 -26
Subject 24	-4 -6 58	8 0 54	-50 4 34	52 4 40	-36 -22 66	36 -32 64	-28 4 -4	26 4 0	-24 -54 -24	28 -48 -26
Subject 25	4 0 42	4 -8 46	-52 6 42	52 6 34	-40 -28 64	40 -30 58	-28 -6 -6	26 2 2	-24 -50 -26	30 -64 -20
Subject 26	-10 -2 54	6 6 50	-54 -2 44	58 4 30	-40 -22 52	40 -24 50	-28 -6 0	28 0 0	-30 -48 -28	36 -54 -24
Subject 27	-4 0 56	4 -10 52	-52 2 46	58 4 34	-34 -24 68	36 -28 58	-26 0 2	28 0 -2	-22 -54 -22	22 -54 -24
Subject 28	-8 -10 58	6 -4 56	-62 8 28	58 10 38	-38 -20 48	32 -24 48	-28 -4 2	26 0 4	-24 -52 -22	24 -50 -26
Subject 29	-8 -6 50	4 -4 56	-64 0 28	62 -18 28	-32 -28 48	36 -20 46	-28 -8 -2	28 -6 -4	-26 -54 -24	20 -56 -20
Subject 30	-4 -10 56	4 -2 56	-56 4 36	52 10 40	-40 -26 62	40 -28 62	-26 2 6	28 4 -4	-28 -52 -26	22 -52 -24
Subject 31	-8 -6 50	8 -4 50	-54 8 28	58 6 32	-38 -28 62	38 -28 62	-26 0 -8	28 -8 4	-20 -52 -22	22 -52 -24
Subject 32	-6 -14 56	10 -6 56	-60 4 26	56 6 42	-38 -24 64	32 -26 52	-28 -8 -2	28 -8 -2	-22 -54 -20	26 -50 -22
Subject 33	-4 -16 56	4 -14 56	-50 -10 46	56 4 34	-42 -26 60	38 -22 50	-28 -2 -4	28 8 -10	-40 -52 -28	34 -60 -22
Subject 34	-6 -4 54	6 0 56	-58 2 36	58 -18 46	-36 -22 70	42 -22 46	-26 8 -6	26 6 -4	-22 -50 -26	26 -50 -26
Subject 35	-6 -8 58	4 -10 52	-60 4 36	60 4 34	-36 -28 54	36 -26 50	-28 -2 -6	28 4 -8	-20 -56 -22	20 -52 -20
Subject 36	-4 -4 50	4 -4 50	-52 6 42	52 2 44	-38 -24 50	36 -26 56	-26 -2 4	26 4 6	-24 -54 -26	22 -50 -26
Mean	-6 -7 54	6 -5 53	-56 2 37	56 2 37	-38 -26 59	38 -26 56	-27 -1 -2	27 -0 -1	-26 -53 -25	27 -52 -24
SD	3,4,4	2,5,3	4,6,7	3,8,6	3,3,6	3,3,6	1,4,4	1,5,4	5,4,2	5,4,3

d = dominant hemisphere, nd = non-dominant hemisphere

Supplemental Table I. Individual local fMRI maxima used as ROIs for DCM

Endogenous connectivity (DCM A-matrix)

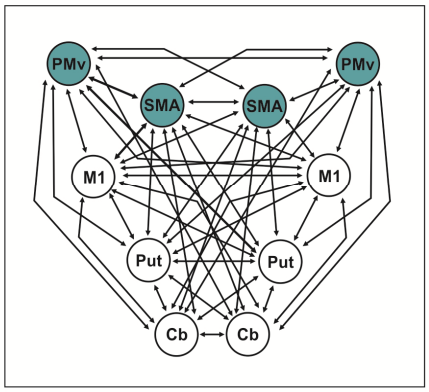

Models of task-dependent connectivity (DCM B-matrix)

model 1

fully connected model

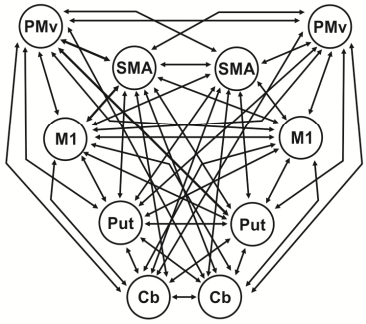

model for all conditions

model 2

as model 1, no interhemispheric SMA-M1 connection

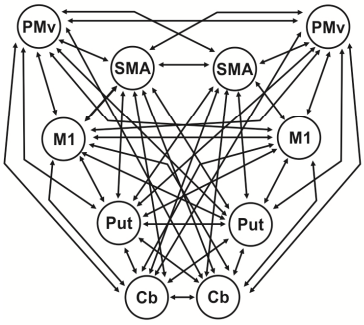

model 3

as model 2, no interhemispheric PMv-M1 connection

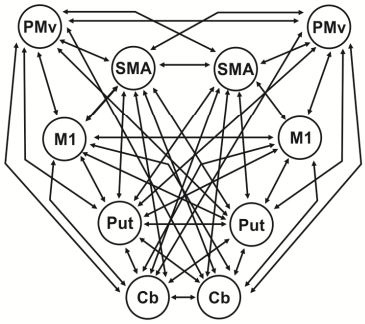

model 4

as model 3, no interhemispheric Put-M1 connection

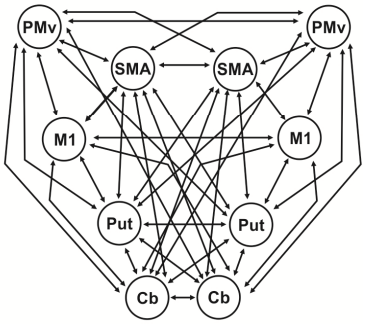

model 5

as model 4, no interhemispheric Cb-M1 connection

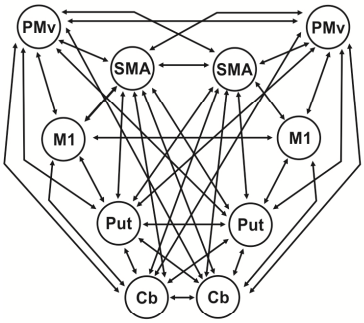

model 6

as model 5, no interhemispheric SMA-PMv connection

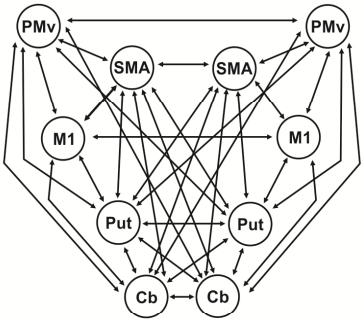

model 7

as model 6, no interhemispheric SMA-Put connection

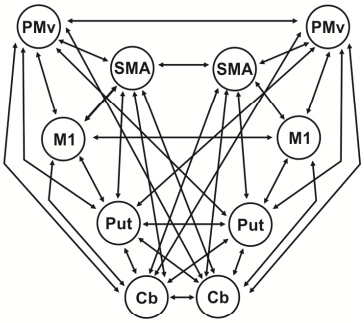

model 8

as model 7, no interhemispheric SMA-Cb connection

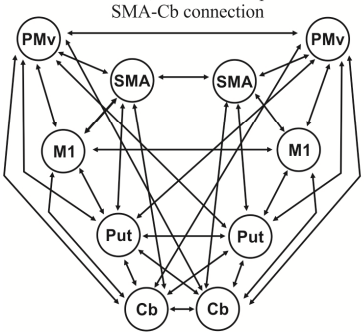

model 9

as model 8, no interhemispheric PMv-Put connection

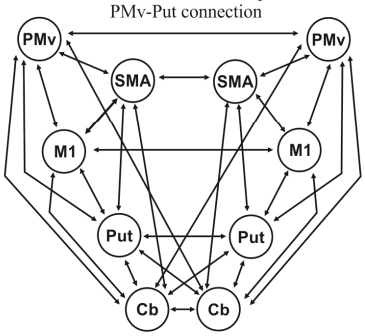

model 10

as model 9, no interhemispheric PMv-Cb connection

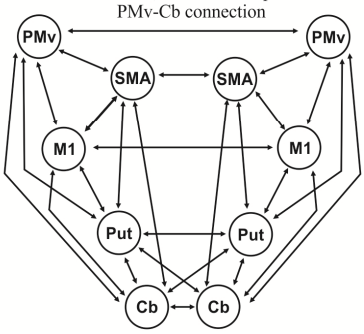

model 11

as model 10, no interhemispheric Put-Cb connection

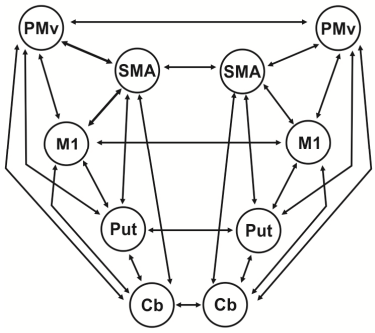

model 12

as model 11, no interhemispheric SMA-SMA connection

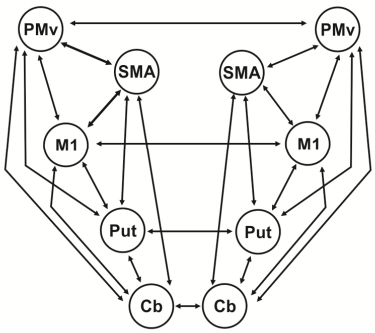

model 13

as model 12, no interhemispheric PMv-PMv connection

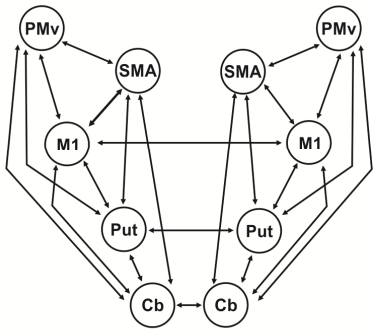

model 14

as model 13, no interhemispheric Put-Put connection

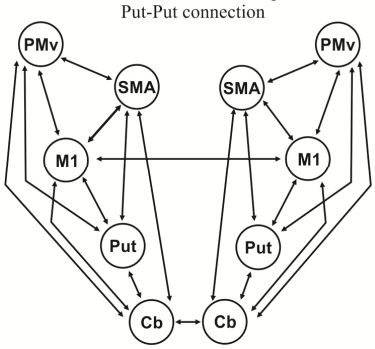

model 15

as model 14, no interhemispheric Cb-Cb connection

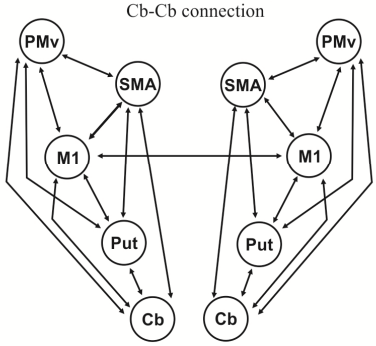

model 16

as model 14, no interhemispheric M1-M1 connection

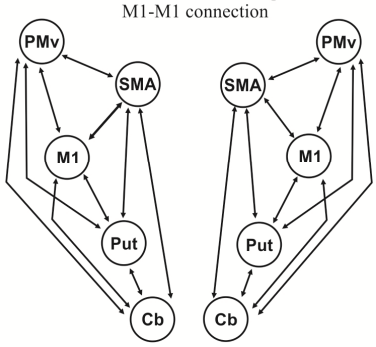

model 17

as model 2, lateralized

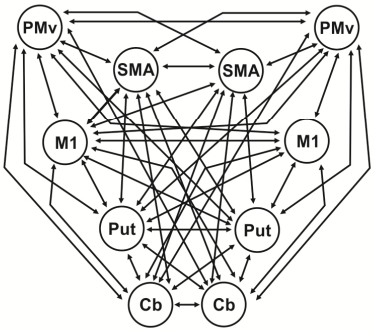

right hand

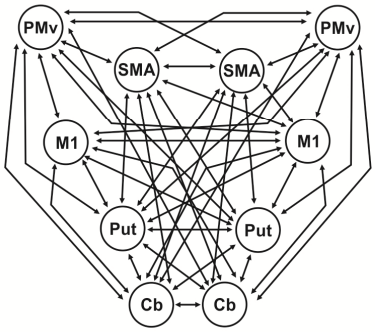

left hand

model 18

as model 3, lateralized

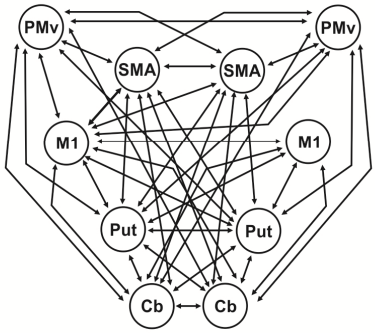

right hand

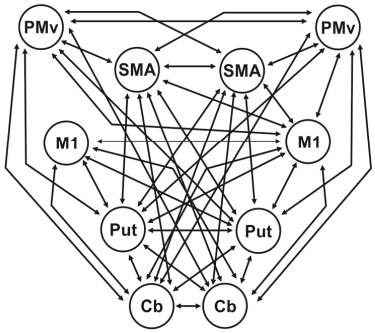

left hand

model 19

as model 4, lateralized

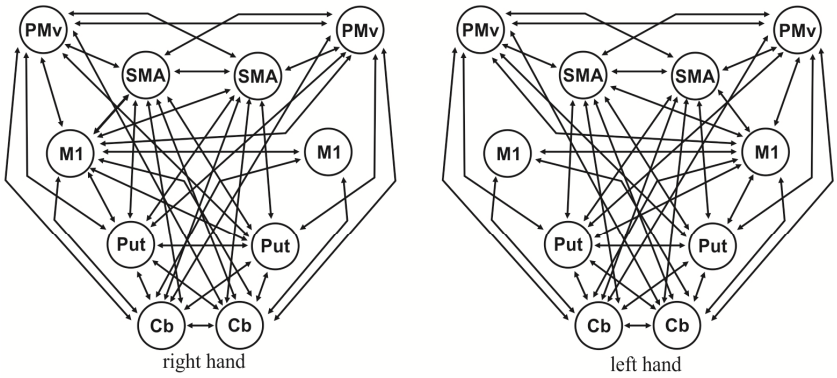

model 20

as model 5, lateralized

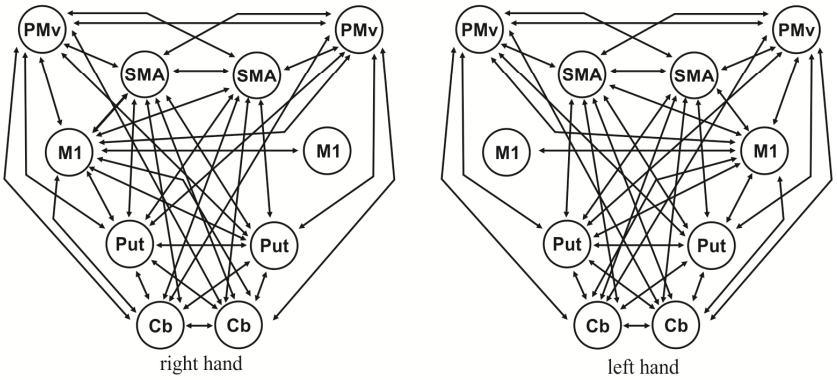

model 21

as model 6, lateralized

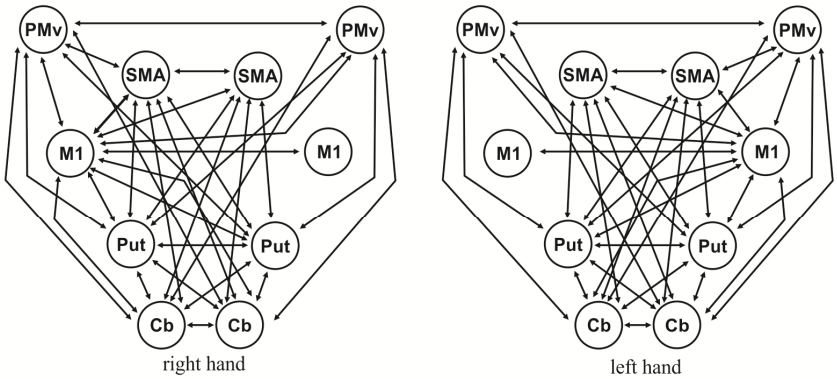

model 22

as model 7, lateralized

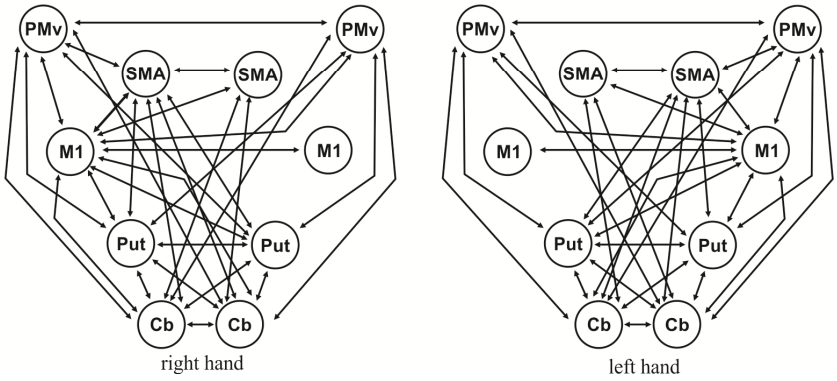

model 23

as model 8, lateralized

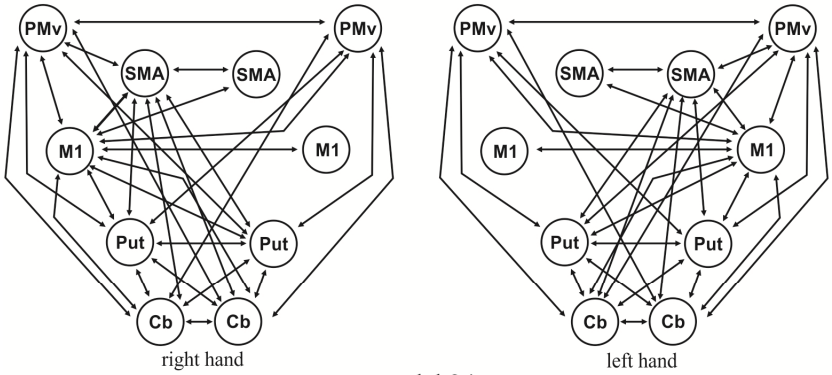

model 24

as model 9, lateralized

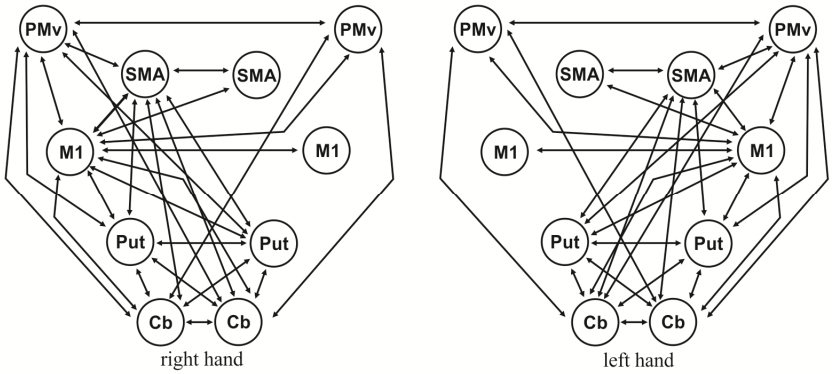

model 25

as model 10, lateralized

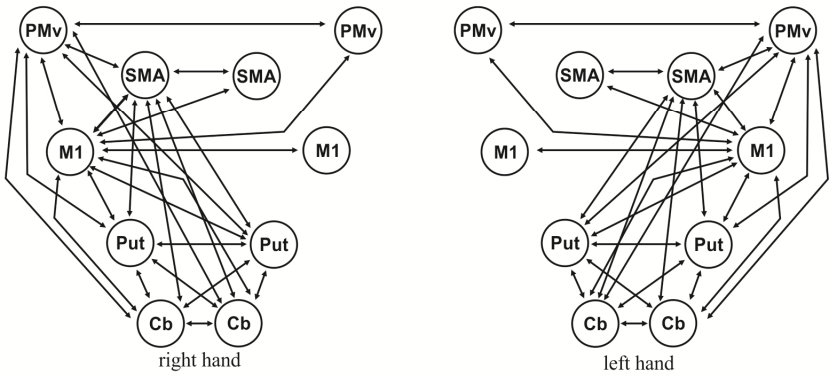

model 26

as model 11, lateralized

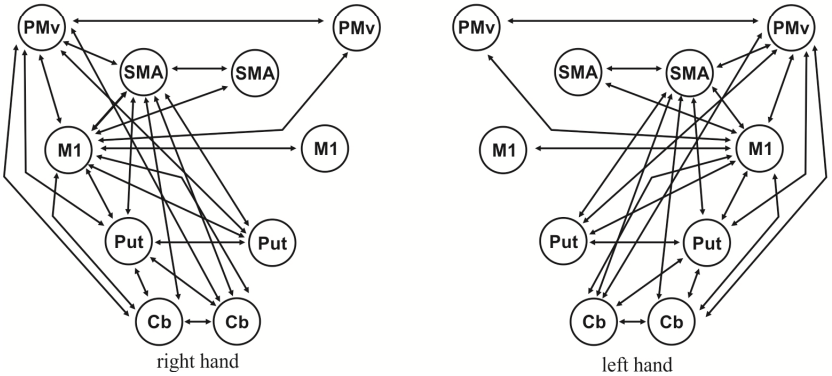

model 27

as model 12, lateralized

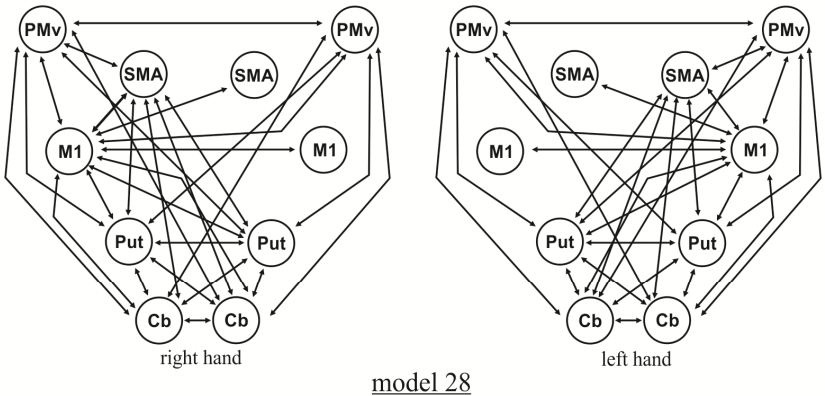

model 28

as model 13, lateralized

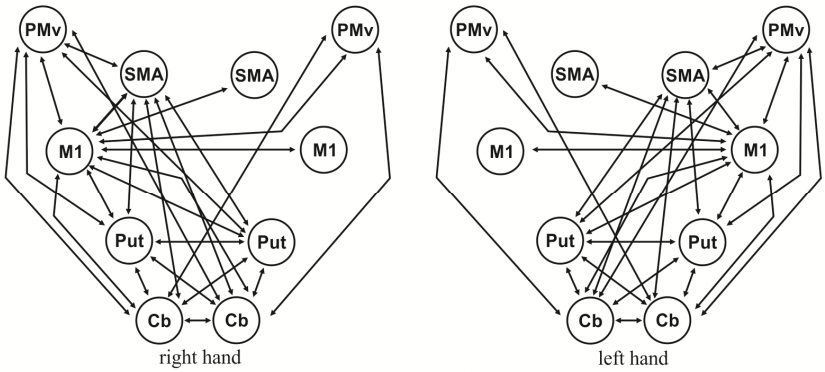

model 29

as model 14, lateralized

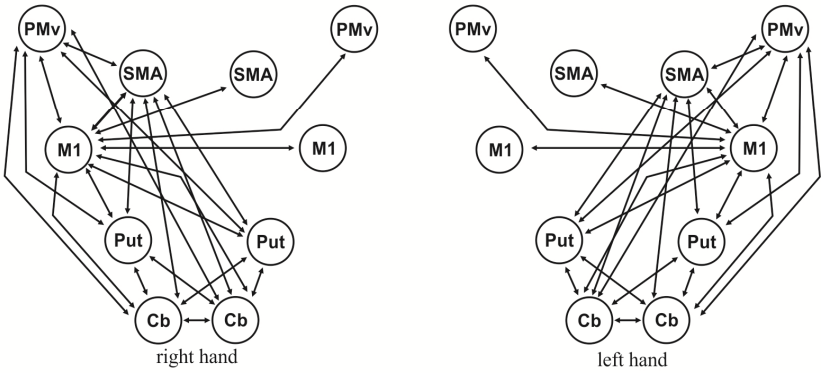

model 30

as model 15, lateralized

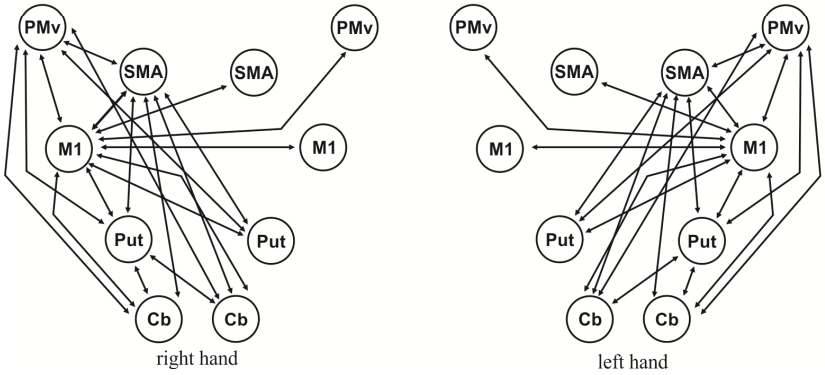

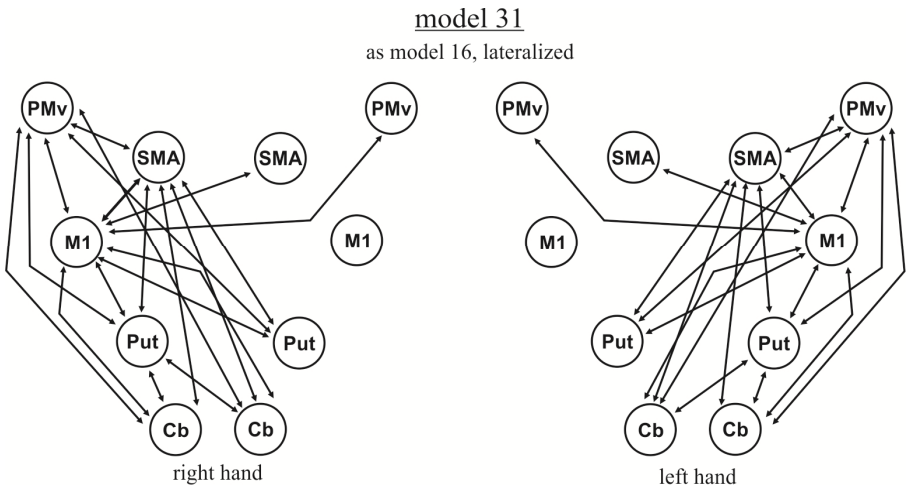

Supplemental Figure 1. 31 models tested in the Bayesian model selection procedure.

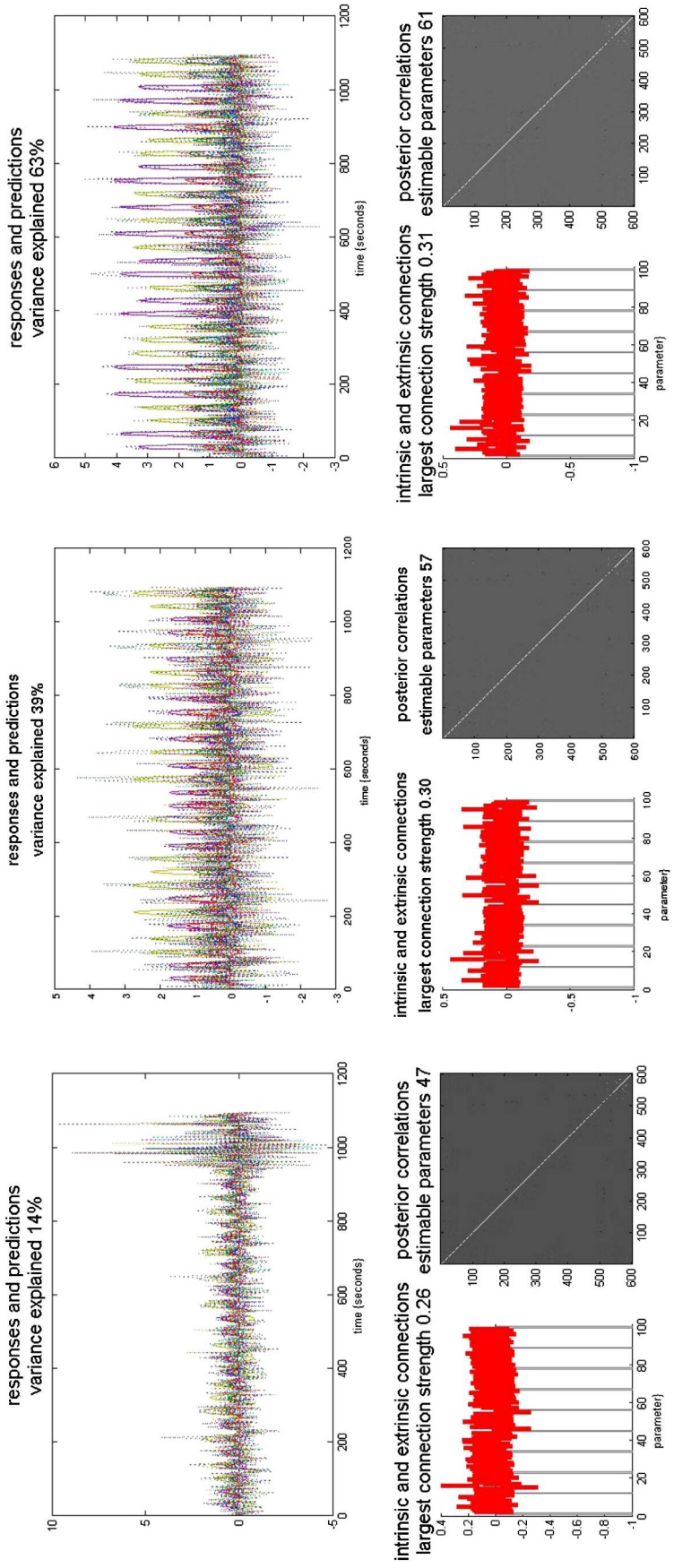

Supplemental Figure 2. Total mean variance explained and its standard-deviation.

Endogenous connectivity											
Right-handers						Left-handers					
Connection	Average	p-Value	Connection	Average	p-Value	Connection	Average	p-Value	Connection	Average	p-Value
dPut - ndPut	0.01	< 0.001	ndPut - dPut	0.01	< 0.001	dPut - ndPut	0.01	0.010	ndPut - dPut	0.01	0.013
dPut - dCb	0.02	0.001	ndPut - dCb	0.04	< 0.001	dPut - dCb	0.01	0.171	ndPut - dCb	0.04	< 0.001
dPut - ndCb	0.05	< 0.001	ndPut - ndM1	0.05	< 0.001	dPut - ndCb	0.05	< 0.001	ndPut - ndCb	0.01	0.066
dPut - dM1	0.05	< 0.001	ndPut - dPMv	0.02	< 0.001	dPut - dM1	0.05	< 0.001	ndPut - dM1	0.00	0.331
dPut - dPMv	0.02	< 0.001	ndPut - ndPMv	0.02	< 0.001	dPut - ndM1	-0.01	0.099	ndPut - ndM1	0.04	< 0.001
dPut - ndPMv	0.02	< 0.001	ndPut - dSMA	0.03	< 0.001	dPut - dPMv	0.02	0.004	ndPut - dPMv	0.01	0.007
dPut - dSMA	0.04	< 0.001	ndPut - ndSMA	0.02	< 0.001	dPut - ndPMv	0.01	< 0.001	ndPut - ndPMv	0.01	< 0.001
dPut - ndSMA	0.02	< 0.001	ndCb - dPut	0.04	< 0.001	dPut - dSMA	0.02	< 0.001	ndPut - dSMA	0.01	0.001
dCb - dPut	0.02	0.003	ndCb - dM1	0.15	< 0.001	dPut - ndSMA	0.01	0.002	ndPut - ndSMA	0.02	< 0.001
dCb - ndPut	0.04	< 0.001	ndCb - ndM1	-0.04	< 0.001	dCb - dPut	0.01	0.026	ndCb - dPut	0.05	< 0.001
dCb - dM1	-0.04	< 0.001	ndCb - dPMv	0.04	< 0.001	dCb - ndPut	0.04	< 0.001	ndCb - ndPut	0.01	0.053
dCb - ndM1	0.15	< 0.001	ndCb - ndPMv	0.03	< 0.001	dCb - ndCb	0.01	0.579	ndCb - dCb	0.00	0.733
dCb - dPMv	0.04	< 0.001	ndCb - dSMA	0.07	< 0.001	dCb - dM1	-0.03	0.008	ndCb - dM1	0.15	< 0.001
dCb - ndPMv	0.05	< 0.001	ndCb - ndSMA	0.03	< 0.001	dCb - ndM1	0.15	< 0.001	ndCb - ndM1	-0.04	< 0.001
dCb - dSMA	0.05	< 0.001	ndM1 - ndPut	0.05	< 0.001	dCb - dPMv	0.03	0.001	ndCb - dPMv	0.04	< 0.001
dCb - ndSMA	0.06	< 0.001	ndM1 - dCb	0.15	< 0.001	dCb - ndPMv	0.03	< 0.001	ndCb - ndPMv	0.03	< 0.001
dM1 - dPut	0.04	< 0.001	ndM1 - ndCb	-0.05	< 0.001	dCb - dSMA	0.03	< 0.001	ndCb - dSMA	0.05	< 0.001
dM1 - dCb	-0.05	0.007	ndM1 - dM1	-0.10	< 0.001	dCb - ndSMA	0.05	< 0.001	ndCb - ndSMA	0.02	0.002
dM1 - ndCb	0.16	< 0.001	ndM1 - dPMv	0.03	< 0.001	dM1 - dPut	0.05	< 0.001	ndM1 - dPut	0.00	0.260
dM1 - ndM1	-0.10	< 0.001	ndM1 - ndPMv	0.04	< 0.001	dM1 - ndPut	0.00	0.727	ndM1 - ndPut	0.04	< 0.001
dM1 - dPMv	0.03	< 0.001	ndM1 - dSMA	0.04	< 0.001	dM1 - dCb	-0.04	0.002	ndM1 - dCb	0.15	< 0.001
dM1 - ndPMv	0.03	< 0.001	ndM1 - ndSMA	0.06	< 0.001	dM1 - ndCb	0.16	< 0.001	ndM1 - ndCb	-0.04	< 0.001
dM1 - dSMA	0.06	< 0.001	ndPMv - dPut	0.02	< 0.001	dM1 - ndM1	-0.10	< 0.001	ndM1 - dM1	-0.09	< 0.001
dM1 - ndSMA	0.02	0.003	ndPMv - ndPut	0.03	< 0.001	dM1 - dPMv	0.04	< 0.001	ndM1 - dPMv	0.02	0.001
dPMv - dPut	0.03	< 0.001	ndPMv - dCb	0.08	< 0.001	dM1 - ndPMv	0.03	< 0.001	ndM1 - ndPMv	0.03	< 0.001
dPMv - ndPut	0.02	0.013	ndPMv - ndCb	0.04	0.001	dM1 - dSMA	0.05	< 0.001	ndM1 - dSMA	0.02	0.003
dPMv - dCb	0.04	0.001	ndPMv - dM1	0.02	0.007	dM1 - ndSMA	0.01	0.017	ndM1 - ndSMA	0.05	< 0.001
dPMv - ndCb	0.06	< 0.001	ndPMv - ndM1	0.08	< 0.001	dPMv - dPut	0.04	< 0.001	ndPMv - dPut	0.02	< 0.001
dPMv - dM1	0.08	< 0.001	ndPMv - dPMv	0.02	< 0.001	dPMv - ndPut	0.02	< 0.001	ndPMv - ndPut	0.02	< 0.001
dPMv - ndPMv	0.03	< 0.001	ndPMv - dSMA	0.05	< 0.001	dPMv - dCb	0.05	0.005	ndPMv - dCb	0.06	< 0.001
dPMv - dSMA	0.04	< 0.001	ndPMv - ndSMA	0.04	< 0.001	dPMv - ndCb	0.10	< 0.001	ndPMv - ndCb	0.05	< 0.001
dPMv - ndSMA	0.03	< 0.001	ndSMA - dPut	0.02	0.019	dPMv - dM1	0.10	< 0.001	ndPMv - dM1	0.04	< 0.001
dSMA - dPut	0.05	0.000	ndSMA - ndPut	0.06	< 0.001	dPMv - ndM1	0.03	0.071	ndPMv - ndM1	0.05	< 0.001
dSMA - ndCb	0.17	< 0.001	ndSMA - dCb	0.16	< 0.001	dPMv - ndPMv	0.03	< 0.001	ndPMv - dPMv	0.02	< 0.001
dSMA - dM1	0.20	< 0.001	ndSMA - ndCb	-0.03	0.031	dPMv - dSMA	0.04	< 0.001	ndPMv - dSMA	0.02	< 0.001
dSMA - dPMv	0.03	< 0.001	ndSMA - dM1	-0.06	0.001	dPMv - ndSMA	0.03	< 0.001	ndPMv - ndSMA	0.03	< 0.001
dSMA - ndPMv	0.04	< 0.001	ndSMA - ndM1	0.20	< 0.001	dSMA - dPut	0.05	< 0.001	ndSMA - dPut	0.01	0.094
dSMA - ndSMA	0.05	< 0.001	ndSMA - dPMv	0.03	< 0.001	dSMA - ndPut	0.01	0.107 (n.s.)	ndSMA - ndPut	0.05	< 0.001
			ndSMA - ndPMv	0.04	< 0.001	dSMA - dCb	0.01	0.304 (n.s.)	ndSMA - dCb	0.15	< 0.001
			ndSMA - dSMA	0.05	< 0.001	dSMA - ndCb	0.14	< 0.001	ndSMA - ndM1	0.18	< 0.001
						dSMA - dM1	0.15	< 0.001	ndSMA - dPMv	0.02	< 0.001
						dSMA - ndM1	-0.03	0.200 (n.s.)	ndSMA - ndPMv	0.02	< 0.001
						dSMA - dPMv	0.03	< 0.001	ndSMA - dSMA	0.02	< 0.001
						dSMA - ndPMv	0.02	< 0.001			
						dSMA - ndSMA	0.02	< 0.001			

d = dominant hemisphere, nd = non-dominant hemisphere

Supplemental Table II. Coupling parameter estimates and their *P*-values ($P < 0.05$, FDR-corrected).

Main effect "dominant hand"					
Right-handers			Left-handers		
Connection	Average	p-Value	Connection	Average	p-Value
dPut - ndPut	0.01	< 0.001	dPut - ndPut	0.01	0.005
dPut - dCb	0.01	0.003	dPut - dCb	0.01	0.001
dPut - ndCb	0.03	< 0.001	dPut - ndCb	0.03	< 0.001
dPut - dM1	0.05	< 0.001	dPut - dM1	0.05	< 0.001
dPut - dPMv	0.01	0.002	dPut - dPMv	0.01	0.003
dPut - ndPMv	0.02	< 0.001	dPut - ndPMv	0.01	< 0.001
dPut - dSMA	0.03	< 0.001	dPut - dSMA	0.01	0.015
dPut - ndSMA	0.02	< 0.001	dPut - ndSMA	0.01	< 0.001
ndPut - dPut	0.01	0.001	ndPut - dPut	0.00	0.013
ndPut - dCb	0.00	0.032	ndPut - ndCb	0.01	0.004
ndPut - ndCb	0.01	0.007	ndPut - dM1	0.01	0.007
ndPut - dM1	0.01	0.006	ndPut - dSMA	0.00	0.006
ndPut - ndPMv	0.01	0.010	ndPut - ndSMA	0.00	0.006
ndPut - dSMA	0.01	0.002	dCb - dPut	0.00	0.004
ndPut - ndSMA	0.01	0.010	dCb - ndCb	0.02	0.008
ndCb - dPut	0.03	< 0.001	dCb - dM1	0.02	0.011
ndCb - ndPut	0.02	< 0.001	dCb - ndSMA	0.01	0.007
ndCb - dCb	0.02	0.017	ndCb - dPut	0.02	< 0.001
ndCb - dM1	0.13	< 0.001	ndCb - ndPut	0.01	0.003
ndCb - dPMv	0.03	0.002	ndCb - dCb	0.03	0.002
ndCb - ndPMv	0.04	< 0.001	ndCb - dM1	0.13	< 0.001
ndCb - dSMA	0.05	< 0.001	ndCb - dPMv	0.03	0.006
ndCb - ndSMA	0.05	< 0.001	ndCb - ndPMv	0.02	< 0.001
dM1 - dPut	0.04	< 0.001	ndCb - ndSMA	0.04	< 0.001
dM1 - ndPut	0.02	< 0.001	dM1 - dPut	0.02	< 0.001
dM1 - dCb	0.02	0.025	dM1 - ndPut	0.01	0.004
dM1 - ndCb	0.11	< 0.001	dM1 - dCb	0.03	0.001
dM1 - dPMv	0.03	0.002	dM1 - ndCb	0.11	< 0.001
dM1 - ndPMv	0.04	< 0.001	dM1 - dPMv	0.03	0.006
dM1 - dSMA	0.06	< 0.001	dM1 - ndPMv	0.03	< 0.001
dM1 - ndSMA	0.06	< 0.001	dM1 - ndSMA	0.04	< 0.001
ndM1 - ndCb	-0.02	< 0.001	ndM1 - dM1	-0.02	0.019
ndM1 - dM1	-0.03	< 0.001	dPMv - dPut	0.02	< 0.001
ndM1 - ndSMA	-0.01	0.008	dPMv - ndCb	0.09	< 0.001
dPMv - dPut	0.02	< 0.001	dPMv - dM1	0.13	< 0.001
dPMv - ndPut	0.01	0.026	dPMv - ndM1	-0.04	0.001
dPMv - ndCb	0.05	< 0.001	dPMv - ndSMA	0.02	0.006
dPMv - dM1	0.08	< 0.001	ndPMv - dPut	0.01	< 0.001
dPMv - ndM1	-0.02	0.010	ndPMv - ndCb	0.05	< 0.001
dPMv - ndPMv	0.02	0.001	ndPMv - dM1	0.06	< 0.001
dPMv - dSMA	0.02	0.001	ndPMv - ndSMA	0.01	< 0.001
dPMv - ndSMA	0.02	< 0.001	dSMA - dPut	0.02	< 0.001
ndPMv - dPut	0.02	< 0.001	dSMA - ndCb	0.11	< 0.001
ndPMv - ndPut	0.01	0.016	dSMA - dM1	0.14	< 0.001
ndPMv - ndCb	0.04	< 0.001	dSMA - ndM1	-0.04	< 0.001
ndPMv - dM1	0.06	< 0.001	dSMA - ndSMA	0.02	0.007
ndPMv - dPMv	0.01	0.006	ndSMA - dPut	0.01	0.022
ndPMv - dSMA	0.02	< 0.001	ndSMA - ndPut	0.00	0.016
ndPMv - ndSMA	0.02	< 0.001	ndSMA - ndCb	0.04	0.011
dSMA - dPut	0.04	< 0.001	ndSMA - dM1	0.06	0.015
dSMA - ndCb	0.14	< 0.001	ndSMA - ndPMv	0.01	0.008
dSMA - dM1	0.20	< 0.001			
dSMA - ndM1	-0.07	< 0.001			
dSMA - ndPMv	0.03	< 0.001			
dSMA - ndSMA	0.05	< 0.001			
ndSMA - dPut	0.02	0.001			
ndSMA - ndPut	0.02	0.001			
ndSMA - dCb	0.02	0.003			
ndSMA - ndM1	0.01	0.021			
ndSMA - dPMv	0.02	0.001			
ndSMA - ndPMv	0.02	0.001			
ndSMA - dSMA	0.03	< 0.001			

d = dominant hemisphere, nd = non-dominant hemisphere

Supplemental Table IIIa. Coupling parameter estimates and their p-values (P<0.05, FDR-corrected).

Main effect "non-dominant hand"					
Right-handers			Left-handers		
Connection	Average	p-Value	Connection	Average	p-Value
dPut - ndPut	0.00	0.001	dPut - dCb	0.01	0.015
dPut - dCb	0.01	< 0.001	dPut - ndM1	0.02	0.004
dPut - ndCb	0.01	< 0.001	dPut - ndPMv	0.01	0.018
dPut - ndM1	0.02	< 0.001	dPut - dSMA	0.01	0.011
dPut - dPMv	0.01	< 0.001	dPut - ndSMA	0.01	0.010
dPut - ndPMv	0.00	0.004	ndPut - dPut	0.01	0.023
dPut - dSMA	0.01	< 0.001	ndPut - dCb	0.03	< 0.001
dPut - ndSMA	0.01	0.003	ndPut - ndCb	0.01	0.022
ndPut - dPut	0.01	< 0.001	ndPut - ndM1	0.04	< 0.001
ndPut - dCb	0.03	< 0.001	ndPut - dPMv	0.01	0.002
ndPut - ndCb	0.01	< 0.001	ndPut - ndPMv	0.01	< 0.001
ndPut - ndM1	0.04	< 0.001	ndPut - dSMA	0.01	< 0.001
ndPut - dPMv	0.01	< 0.001	ndPut - ndSMA	0.01	< 0.001
ndPut - ndPMv	0.01	< 0.001	dCb - dPut	0.01	0.010
ndPut - dSMA	0.02	< 0.001	dCb - ndPut	0.02	< 0.001
ndPut - ndSMA	0.01	0.003	dCb - ndCb	0.02	0.003
dCb - dPut	0.02	< 0.001	dCb - ndM1	0.13	< 0.001
dCb - ndPut	0.01	0.002	dCb - dPMv	0.03	< 0.001
dCb - ndCb	0.02	0.001	dCb - ndPMv	0.02	< 0.001
dCb - ndM1	0.12	< 0.001	dCb - dSMA	0.03	< 0.001
dCb - dPMv	0.03	< 0.001	dCb - ndSMA	0.03	0.002
dCb - ndPMv	0.02	0.001	ndCb - dCb	0.02	0.027
dCb - dSMA	0.06	< 0.001	ndCb - ndPMv	0.01	0.020
dCb - ndSMA	0.02	0.013	ndCb - dSMA	0.01	0.015
ndCb - ndPut	0.00	0.024	dM1 - ndM1	-0.02	0.022
ndCb - dPMv	0.01	0.019	ndM1 - dPut	0.01	0.003
ndCb - ndSMA	0.01	0.014	ndM1 - ndPut	0.02	< 0.001
dM1 - dCb	-0.01	0.006	ndM1 - dCb	0.11	< 0.001
dM1 - ndM1	-0.02	0.003	ndM1 - ndCb	0.02	0.002
dM1 - dSMA	-0.01	0.011	ndM1 - dPMv	0.04	< 0.001
ndM1 - dPut	0.02	< 0.001	ndM1 - ndPMv	0.02	< 0.001
ndM1 - ndPut	0.02	0.001	ndM1 - dSMA	0.04	< 0.001
ndM1 - dCb	0.09	< 0.001	ndM1 - ndSMA	0.04	0.002
ndM1 - ndCb	0.02	0.001	dPMv - ndPut	0.01	0.004
ndM1 - dPMv	0.04	< 0.001	dPMv - dCb	0.06	< 0.001
ndM1 - ndPMv	0.02	< 0.001	dPMv - ndM1	0.09	0.001
ndM1 - dSMA	0.06	< 0.001	dPMv - ndPMv	0.01	0.003
ndM1 - ndSMA	0.02	0.009	dPMv - dSMA	0.02	< 0.001
dPMv - dPut	0.01	0.006	dPMv - ndSMA	0.02	0.016
dPMv - dCb	0.04	0.009	ndPMv - ndPut	0.01	0.001
dPMv - ndCb	0.01	0.006	ndPMv - dCb	0.05	< 0.001
dPMv - ndM1	0.05	0.004	ndPMv - ndM1	0.07	< 0.001
dPMv - ndPMv	0.01	0.014	ndPMv - dPMv	0.01	< 0.001
dPMv - dSMA	0.02	< 0.001	ndPMv - dSMA	0.01	< 0.001
ndPMv - ndPut	0.01	< 0.001	ndPMv - ndSMA	0.01	0.012
ndPMv - dCb	0.06	< 0.001	dSMA - dPut	0.01	0.010
ndPMv - dM1	-0.02	0.002	dSMA - ndPut	0.01	0.025
ndPMv - ndM1	0.09	< 0.001	dSMA - dCb	0.04	0.002
ndPMv - dPMv	0.01	< 0.001	dSMA - ndCb	0.01	0.031
ndPMv - dSMA	0.03	< 0.001	dSMA - ndM1	0.05	0.002
dSMA - dPut	0.01	0.002	dSMA - dPMv	0.02	0.003
dSMA - ndPut	0.02	< 0.001	dSMA - ndPMv	0.01	< 0.001
dSMA - dCb	0.07	< 0.001	dSMA - ndSMA	0.02	0.006
dSMA - ndCb	0.01	0.023	ndSMA - ndPut	0.02	< 0.001
dSMA - ndM1	0.10	< 0.001	ndSMA - dCb	0.12	< 0.001
dSMA - dPMv	0.02	0.001	ndSMA - dM1	-0.05	< 0.001
dSMA - ndPMv	0.01	0.011	ndSMA - ndM1	0.17	< 0.001
dSMA - ndSMA	0.01	0.020	ndSMA - dPMv	0.02	0.001
ndSMA - ndPut	0.02	< 0.001	ndSMA - dSMA	0.02	0.003
ndSMA - dCb	0.11	< 0.001			
ndSMA - dM1	-0.04	< 0.001			
ndSMA - ndM1	0.16	< 0.001			
ndSMA - dPMv	0.01	0.001			
ndSMA - dSMA	0.03	< 0.001			

d = dominant hemisphere, nd = non-dominant hemisphere

Supplemental Table IIIb. Coupling parameter estimates and their p-values (P<0.05, FDR-corrected).

Total Mean Variance	0.39 %
SD	± 11 %

Supplemental Table IV. Total mean variance of the winner model.

3.3

Functional resting-state connectivity of the human motor network: Differences between right- and left-handers.

Eva-Maria Pool, Anne K. Rehme, Gereon R. Fink, Simon B. Eickhoff, Christian Grefkes

(under review)

Functional resting-state connectivity of the human motor network: Differences between right- and left-handers

Eva-Maria Pool[1,2], Anne K. Rehme[1,2], Simon B. Eickhoff[2,3], Gereon R. Fink[1,2], Christian Grefkes[1,2]

[1] Institute of Neuroscience and Medicine (INM-1, INM-3), Jülich Research Centre, 52428 Jülich, Germany
[2] Department of Neurology, University of Cologne, 50931 Cologne, Germany
[3] Institute of Clinical Neuroscience and Medical Psychology, Heinrich Heine University, 40225 Düsseldorf, Germany

Corresponding Author: Dr. Christian Grefkes
Department of Neurology
University Hospital Cologne
Kerpener Straße 62
50937 Cologne, Germany
Tel. +49-221-478-4000, Fax. +49-221-478-7005
E-mail: christian.grefkes@uk-koeln.de

Article Type: Research Article
Word count (summary): 241
Word count (text): 3.904
Number of references: 53

Keywords: handedness, dorsolateral premotor cortex, inferior frontal gyrus, support vector machine

Declaration of conflict of interests:

The authors declare that they have no competing interests.

ABSTRACT

Handedness is associated with differences in activation levels in various motor tasks performed with the dominant or non-dominant hand. Here we tested whether handedness is reflected in the functional architecture of the motor system even in the absence of an overt motor task. Using resting-state functional magnetic resonance imaging we investigated 18 right- and 18 left-handers. Handedness was assessed by the Edinburgh-Handedness-Inventory (EHI). We computed whole-brain functional connectivity maps of the left and right primary motor cortex (M1). To test for the effect of handedness we computed group contrasts and regression analyses including the EHI score as a covariate. We further used a multivariate linear support vector machine (SVM) classifier to reveal the specificity of brain regions for classifying right- and left-handers based on individual resting-state maps. Using left M1 as seed region, functional connectivity analysis revealed stronger interhemispheric functional connectivity between left M1 and right dorsolateral premotor cortex (PMd) in right-handers as compared to left-handers. This connectivity cluster contributed to the individual classification of right- and left-handers with 86.2% accuracy. Control analyses of non-motor resting-state networks including the speech and the visual network revealed no significant differences in functional connectivity related to handedness. In conclusion, our data reveal an intrinsically higher functional connectivity in right-handers. These results may help to explain that hand preference is more lateralised in right-handers than in left-handers. Furthermore, enhanced functional connectivity between left M1 and right PMd may serve as an individual marker of handedness.

1 INTRODUCTION

Handedness, i.e., the preference to use one hand over the other, is associated with differences in activation levels in various motor tasks performed with the dominant or non-dominant hand (Hammond, 2002). One of the earliest observation of lateralized brain function was reported by Pierre-Paul Broca who on the basis of aphasia and left hemisphere damage concluded that the left hemisphere is responsible for language-related behavior in right-handed patients (Broca, 1863). Since then, several studies have confirmed that hemispheric asymmetries of both structural and functional cortical organization are related to handedness (Amunts et al., 1996; Hammond, 2002). Using magnetic resonance morphometry, Amunts et al. demonstrated that the depth of the central sulcus is related to handedness. In right-handers, the left central sulcus was deeper than the right, and vice versa in left-handers. Analysis of macrostructural asymmetry was complemented by converging results of an analysis of microstructure (i.e., tissue compartment containing dendrites, axons, and synapses) in Brodmann's area 4. Based on their findings Amunts et al. suggested that hand preference is associated with increased structural connectivity and an increased intrasulcal surface of the precentral gyrus in the dominant hemisphere (Amunts et al., 1996). Using functional MRI (fMRI), Jäncke and colleagues investigated right-handers performing a sequence task (touching of all four fingers with the thumb) at two different frequencies (1.0 Hz and 3.0 Hz) (Jäncke et al., 1998). In right-handers they observed stronger right hemispheric activation when performing the task with the left hand compared to activity in the left hemisphere when performing the same task with the right hand (Jäncke et al., 1998). Solodkin and colleagues further revealed differences in the fMRI activation patterns between simple and complex digit movements in right- and left-handers: while simple movements did not show differences with respect to handedness, neural activations underlying complex movements were more extended in left-handers compared to right-handers (Solodkin et al., 2001). In addition, we recently showed that effective connectivity, i.e., the causal influence that one area exerts over another area, between motor areas was

differentially modulated in right- and left-handers depending on whether movements were performed with the dominant or non-dominant hand (Pool et al., 2014). More precisely, effective connectivity analysis revealed that in right-handed subjects movements of the dominant hand were associated with significantly stronger coupling of contralateral (left, i.e., dominant) SMA with ipsilateral SMA, ipsilateral ventral premotor cortex (PMv), contralateral motor putamen and contralateral M1 (compared to equivalent connections in left-handers). Individual EHI scores as an index of the expression of handedness also correlated with coupling parameters of these connections. In contrast, we did not observe differences between right- and left-handers when testing for the effect of movement speed on effective connectivity. Based on these observations we concluded that handedness is associated with differences in effective connectivity within the human motor network with a prominent role of left SMA in right-handers. The fact that left-handers featured less asymmetry in effective connectivity strongly suggested differential hemispheric mechanisms underlying hand motor control in left- and right-handers (Pool et al., 2014).

However, differences in task performance (either in absolute performance measures or in hidden parameters like attention and effort) are inherent putative confounds for all task-based fMRI studies (Lowe et al., 1998; Yan et al., 2012). For example, performing a standard motor task might be less demanding when using the dominant hand compared to the non-dominant hand, which may also affect neural activation levels, e.g., in frontoparietal areas. Therefore, resting-state fMRI seems an attractive approach to overcome these putative confounds as it allows to investigate networks independent from performance.

We, accordingly, used resting-state fMRI to investigate handedness-dependent effects on resting-state functional connectivity in 18 right-handed and 18 left-handed healthy volunteers. To test whether effects were specifically related to the motor system, we also investigated resting-state functional connectivity maps of the visual system and the language system using the primary visual cortex (V1) and the pars triangularis of the inferior frontal gyrus (IFG) as seed regions. Consistent with previous studies revealing a hemispheric asymmetry related to handedness during motor performance (Haaland et al., 2004; Jäncke et al., 1998;

Solodkin et al., 2001) and structural investigations reporting handedness-related macroscopic and microscopic asymmetries (Amunts et al., 1996), we hypothesized that differences within the human motor network between right- and left-handers can already be detected in absence of an overt motor task. In addition to this mass-univariate group comparison, we used a multivariate linear support vector machine (SVM) classifier algorithm (Chang and Lin, 2011) to test whether resting-state functional connectivity between brain regions specifically contributes also to the *individual* classification of right- and left-handers.

2 MATERIAL AND METHODS

2.1 Subjects

The study was approved by the local ethics committee and performed in accordance with the Declaration of Helsinki. Thirty-six subjects [18 right-handers (10 males; 22-33 yrs old; mean age 26.1 ± 3.0 SD) and 18 left-handers (7 males; 19-30 yrs old; mean age 24.3 ± 2.6 SD)] with no history of neurological or psychiatric disease gave informed consent. Activation data of frequency-dependent modulation was previously published for this cohort of subjects (Pool et al., 2013, 2014).

To ensure that there were no significant differences in head movement parameters between right- and left-handed subjects we compared framewise displacement (FD) and root-mean-square (RMS) of the realignment parameters of the resting-state data in a two-sample t-test. Both tests showed no significant differences between groups (FD: P=0.302; RMS: P=0.259) (Power et al., 2012; Van Dijk et al., 2012).

2.2 Handedness measurements

Handedness was assessed by asking the subjects to complete the Edinburgh-Handedness-Inventory (EHI) (Oldfield, 1971). The EHI is a test to assess hand dominance in daily activities (e.g., writing, striking a match, holding a broom). The laterality quotient (LQ) of hand dominance ranges from -100 to 100: An LQ > 25 indicates right-handedness, a LQ < -25 left-

handedness (Pujol et al., 1999). The median LQ value of the right-handers was *88* (range: 53 to 100) and the median LQ of the left-handers was *-71* (range: -30 to -100). We computed Mood's median test for non-parametric group comparisons, showing no significant difference between the median degree of handedness of right- and left-handers (*P*=0.176).

2.3 Data acquisition

All subjects underwent resting-state functional magnetic resonance imaging (rs-fMRI). MR images were acquired on a Siemens Trio 3.0 T scanner (Siemens Medical Solutions, Erlangen, Germany). The resting-state paradigm was measured using a gradient echo planar imaging (EPI) sequence with the following parameters: TR = 2000 ms, TE = 30 ms, FOV = 220 mm, 32 slices, 3.4 × 3.4 × 3.4 mm^3 voxel size, 1 mm gap, flip angle = 90°, rs-fMRI: 184 volumes (3 dummy images). The slices covered the whole brain extending from the vertex to lower parts of the cerebellum.

For the resting-state assessment, subjects were instructed to remain motionless and to fixate on a red cross on a black screen for about 6 min. We choose a scanning time around 6 min because longer scanning times do not improve the signal-to-noise of the data, but promote fatigue of the subjects (Van Dijk et al., 2010).

2.4 Image preprocessing

The resting-state fMRI data was conjointly preprocessed using Statistical Parametric Mapping (SPM8, http://www.fil.ion.ucl.ac.uk/spm). After realignment of the EPI volumes and co-registration, all volumes were spatially normalized to the standard template of the Montreal Neurological Institute employing the unified segmentation approach (Ashburner and Friston, 2005). Finally, data were smoothed using an isotropic Gaussian kernel of 8 mm full-width-at-half-maximum.

2.5 Data analyses

2.5.1 fMRI resting-state data

Variance that could be explained by known confounds was removed from each voxel of the fMRI time-series. Confound regressors included the mean-centered global, grey matter, white matter and cerebrospinal fluid signal intensities and their squared values, the six head motion parameters, their squared values as well as their first-order derivatives (Satterthwaite et al., 2013). In the following step, data was band-pass filtered preserving frequencies between 0.01 Hz and 0.08 Hz. Coordinates from an activation likelihood estimation (ALE) meta-analysis (Hardwick et al., 2012) of peak activations in left and right M1 on the rostral wall of the central sulcus at the “hand knob” formation (Yousry et al., 1997) were used as seed regions for the resting-state analysis (see Table I). The time course within a sphere of 8 mm-diameter centered on the seed voxel coordinate was correlated with the time course of every other voxel in the brain by means of linear Pearson´s correlation coefficients (zu Eulenburg et al., 2012).

2.5.2 Control Analyses

To test whether differences in functional connectivity between right- and left-handers were specific for the resting-state motor network, additional analyses were performed for non-motor resting-state networks with seeds in the (i) inferior frontal gyrus (IFG, pars opercularis; BA 44, “speech network”), and the (ii) occipital poles / calcarine sulcus (V1; BA17, “primary visual network”). The seed coordinates for the speech network were defined from ALE meta-analyses of peak activations associated with several core aspects of language including overt and covert speech, semantics, phonology and syntax (Clos et al., 2013). The seed coordinates for the visual network were defined from group activation maxima based on a visually cued sensorimotor task described by Pool et al. (2014) (see Table I).

2.5.3 Statistics

Correlation coefficients of the resting-state functional connectivity maps were converted to Fisher’s Z-scores using the formula $Z = (1/2) \times \ln(1+r)/(1-r) = \operatorname{atanh}(r)$ to yield approximately normally distributed data. For each seed region (left/right M1, left/right IFG, and left/right V1),

the individual maps were entered into flexible factorial general linear models (GLMs) with the factor GROUP (levels: right-handers, left-handers). We used GENDER as a covariate for the different resting-state maps to correct for differences between groups. In addition, we computed regression analyses for significant GLM effects between resting-state maps and the EHI score to investigate whether there was a correlation between the degree of handedness and functional connectivity (P<0.05, FWE-corrected at the cluster level). Differential contrasts were masked with thresholded resting-state maps of right-handers respectively left-handers (P<0.001, uncorrected) to ensure that we only included voxels that were different between right- and left-handers.

2.6 Support Vector Machine (SVM) Classification

We next tested whether regions showing significant group differences in resting-state functional connectivity between right- and left handers also allow classifying handedness at the level of individual maps. Therefore, we used a linear support-vector machine (SVM) (Chang and Lin, 2011) implemented in Matlab. As a linear parameter, voxel-wise connectivity was scaled to range between 0 and 1. Model optimization was embedded in a leave-one-subject-out cross-validation scheme. For training, every subject was left out once and classified based on the model optimized for the rest of the sample constituting the training data set. Voxels were selected for each training set according to a significant t-test (P<0.001) and the left-out subject was classified based on the features selected in the respective training sample. Thus, classification of data was independent from the selection criteria applied in the training step to prevent any feature selection bias (Kriegeskorte et al., 2009). In the training, the misclassification hyperparameter C, ranging from small (C=0.0001) to large (C=30), was optimized using nested cross-validation on the current training set which consisted of an inner loop that is used for model selection and an outer loop that ensures an unbiased model evaluation (please see Rehme et al., 2014, for a more detailed description). We then computed the posterior balanced accuracy of classifications across all outer loops

and reported 95% confidence intervals (CIs) (Brodersen et al., 2010). Chi-squared tests for equal distributions of correct and incorrect classifications were used to test for significance.

To test whether regions showing significant group differences in functional connectivity were specifically related to handedness in individual subjects, we computed a second SVM analysis. Here, individual resting-state maps were masked by the significant group difference in the GLM analysis (P<0.05, cluster-level FWE corrected) and entered into the SVM analysis as described above with a fixed number of voxels. We again report the posterior balanced accuracy with CIs and significance levels.

Finally, we computed the SVM weight image showing areas of regional functional connectivity that contribute to the classification of the two groups.

3 RESULTS

3.1 Left M1 resting-state connectivity

Connectivity of the left M1 seed region comprised a bihemispheric motor network including M1 and premotor areas as well as parts of the somatosensory and superior parietal cortex (P<0.05, FWE-corrected at the cluster level; Figure 1A). When computing group contrasts to test for differences related to handedness, we found stronger functional connectivity between left M1 and right dorsolateral premotor cortex (PMd) [maximum (*x, y, z):* 34 -8 54] in right-handers as compared to left-handers (P<0.05, FWE-corrected at the cluster level; Figure 1B). The reverse contrast showed no significant differences between the two groups. Multiple regression analysis between EHI scores and resting-state functional connectivity of left M1 confirmed a positive correlation with significant voxels in right PMd [*x, y, z:* 32 -8 52], i.e., the same region as found in the group contrasts (P<0.05, FWE-corrected at the cluster level; Figure 2). However, when computing correlations between EHI and resting-state functional connectivity for left- and right-handers separately we did not find significant effects, even at uncorrected thresholds. Therefore, the individual degree of handedness is not correlated with resting-state connectivity.

3.2 Right M1 resting-state connectivity analyses

Computing functional connectivity of the right M1 seed region yielded a similar yet mirror-reversed map as observed for the left M1 seed region (P<0.05, FWE-corrected at the cluster level; Figure 1A). However, when computing group contrasts with right M1 as seed region we found no significant difference between right- and left-handers (P>0.05, uncorrected on the cluster level).

3.3 Multivariate SVM classification

The SVM classifying right- and left-handers based on resting-state functional connectivity of left M1 yielded a posterior classification accuracy of 86.2% (P<0.001, CI=69.8-92.5%; right-handers: 83.3% and left-handers: 88.9%). The SVM weight image reveals that resting-state functional connectivity between left M1 and right PMd contributed to the classification of right-handers as compared to left handers at the level of individual subjects (Figure 3). Hence, a similar region as found for the mass-univariate analyses separated right- from left-handers. In addition, to test for the specifity of the right PMd cluster as revealed by the GLM analysis (see 3.1) for the contrast “Left M1 seed: right-handers vs. left-handers” was specific enough to separate right- and left-handers based on individual resting-state maps. This second SVM analysis showed that resting-state functional connectivity for this particular cluster yielded a posterior classification accuracy of 83.3% (P<0.001, CI=66.7-90.7%; right-handers: 83.3% and left-handers: 83.3%).

When testing for right M1 as seed region, the SVM results showed performance at chance level (classification accuracy = 50%, P=0.499).

3.4 Control analyses

Seeding from the left inferior frontal gyrus (IFG) revealed positive coupling with a bihemispheric speech network comprising IFG (area 44 and 45), bilateral inferior and superior parietal cortex, and postcentral gyrus (P<0.05, FWE-corrected at the cluster level;

Figure 4). A similar yet mirror reversed pattern was observed when seeding from right IFG. However, there was no significant difference between right- and left-handers for any IFG seed region (P>0.05, uncorrected).

For the visual network, we found significant coupling of both the left- and right-hemispheric V1 seed region with a bihemispheric visual network comprising V1 and secondary visual areas (P<0.05, FWE-corrected at the cluster level; Figure 4). Again, differential contrasts with V1 as a seed region did not show a significant difference between right- and left-handers (P>0.05, uncorrected).

Likewise, the SVM approach could not discriminate between right- and left-handers based on resting-state functional connectivity of the language or visual network (feature selection threshold: P<0.001 uncorrected; classification accuracy for both the language network and the visual network <50 %, i.e., chance level; P>0.9).

4 DISCUSSION

We found that right-handedness was associated with stronger interhemispheric functional connectivity between left M1 as seed region and contralateral PMd as compared to left-handedness. In addition to these mass-univariate analyses, the SVM analysis showed that interhemispheric functional connectivity between left M1 and right PMd allows making individual classifications as to whether subjects are left- or right-handed. When investigating the Broca speech network or the visual network as control, we found no differences between right- and left-handers, underlining the specificity of our finding for the resting-state motor network.

4.1 Handedness and Brain Activity

A number of previous studies found differences in brain activity between right- and left-handers in different motor tasks (Dassonville et al., 1997; Kim et al., 1993; Solodkin et al., 2001; Volkmann et al., 1998). For example, Kim and colleagues revealed larger ipsilateral

activation volumes in M1 in right-handers as compared to left-handers when performing a repetitive finger-thumb opposition task (Kim et al., 1993). Dassonville and colleagues observed a stronger lateralization of neural activity within the motor cortex according to increasing degrees of handedness for both right- and left-handers (Dassonville et al., 1997). Solodkin and colleagues mapped brain activation patterns in right- and left-handers during single and sequential finger movements and found larger volumes of activation and less hemispheric lateralization in left-handers (Solodkin et al., 2001). These findings are in line with behavioral data revealing that hand preference in left-handers is often expressed to a lesser degree than in right-handers (Borod et al., 1984). Handedness-related asymmetries have also been demonstrated in cortical excitability using transcranial magnetic stimulation (TMS) paradigms (Brouwer et al., 2001; Ziemann and Hallett, 2001). For example, Ziemann and Hallett (2001) showed a smaller increase of the excitability of the motor cortex contralateral to the inactive hand during right than during left hand movements. This finding indicates that the left motor cortex exerts more inhibitory control upon the contralateral motor cortex (controlling the left hand) than vice versa (Ziemann and Hallett, 2001). Data suggest that the neural mechanisms underlying handedness might rest in hemispheric-specific differences of network dynamics that govern unimanual movements.

4.2 Handedness-dependent effects on connectivity

The new finding of the present study is that we found a strong association between handedness and resting-state functional connectivity of M1 with contralateral PMd. Both M1 and PMd are considered to represent key motor structures for movement preparation and execution (Hoshi and Tanji, 2004; Schluter et al., 1998). Several tract-tracing studies provide evidence that the preparatory activity in PMd neurons facilitates the initiation of arm movements according to predetermined motor parameters (Churchland and Shenoy, 2007; Churchland et al., 2006; Hoshi and Tanji, 2007). PMd projects to the superior part of the parietal cortex, where sensorimotor integration occurs, and the motor cortex, where the movement is executed. Using double pulse TMS, Liuzzi and colleagues revealed that during

movement preparation with the right hand, the right PMd exerted a more pronounced late facilitatory influence on the left M1 in right handers (Liuzzi et al., 2009). This result is in line with the findings of the present study showing a stronger intrinsic connectivity between right PMd and left M1 even in the absence of movement preparation for the right (dominant) hand of right-handers compared to the right (non-dominant) hand of left-handers. As we did not find a similar effect for functional connectivity between left PMd and right M1 – neither in the mass-univariate group analysis nor in the multivariate SVM analysis – data strongly suggest that interhemispheric interactions between premotor areas and M1 are more lateralized in right-handers. Consistent with this suggestion, structural connectivity has also been shown to be more lateralized in right-handers compared to left-handers: Using diffusion tensor imaging and graph theoretical measures to investigate handedness-related differences in white-matter properties, Li and colleagues observed that right-handed subjects had significantly more asymmetries in small-world properties of white matter tracts than left-handed subjects (Li et al., 2014). Other studies confirm lateralization differences in functional connectivity dependent on handedness. For example, Saenger and colleagues found that in right-handers functional connectivity of the default mode network (DMN) shows more hemispheric asymmetries compared to left-handers (Saenger et al., 2012). Interestingly, during childhood development, asymmetries in resting-state functional connectivity of the motor system towards the left hemisphere reflect better motor performance in right-handed children at the age of 10 yrs. Taken together, these findings suggest that an enhanced lateralization of motor network properties is a consistent feature of right-handed subjects. Findings are compatible with developmental studies showing that right hand preference can be already observed before birth; for example, ultrasound studies revealed that about 90% of the fetuses suck the thumb of their right hand (Hepper et al., 2005), suggesting a strong genetic influence for handedness.

Nevertheless, over and above genetic/developmental properties use-dependent effects are likely to impact on asymmetries of the motor system (Haaland et al., 2000; Karni et al., 1995; Kloppel et al., 2007). This needs to be kept in mind particularly when studying left-handers:

left-handers are likely to have learned to live in a world in which many tools and procedures are made for right-handers (Porac, 1996). Consistently, left-handers were demonstrated to be more flexible in using both hands in activities of daily living (Bryden et al., 2011; Vaid et al., 1989). In line with this, Landau and D'Esposito showed that subjects trained to use both hands feature less hemispheric asymmetry of the motor system (Landau and D'Esposito, 2006). Thus, a reduced hemispheric lateralization of functional connectivity in left-handers relative to right-handers as shown by our results might also result from a stronger use of the non-dominant right hand for everyday life tasks (in left-handers).

4.3 Handedness-dependent effects on IFG resting-state connectivity

Our data did not reveal an effect of handedness on functional connectivity of the IFG (Broca speech network, BA 44). It is well established that the left hemisphere is dominant for speech-language functions in over 90% of right-handers (Szaflarski et al., 2006). In contrast, language dominance in left-handers is less lateralised (Goodglass and Quadfasel, 1954; Ratcliff et al., 1980; Satz, 1979; Steinmetz et al., 1991). In healthy subjects, Knecht and colleagues revealed that the incidence of right-hemisphere language dominance increased linearly with the degree of left-handedness. This suggests that handedness and language dominance are determined by multiple factors, e.g., complex genetic or non-genetic factors in the formation of the phenotype (Knecht et al., 2000). However, it must be noted that not only right-handers but also a large fraction of left-handers have a left-hemispheric dominance for language. For example, Pujol and colleagues investigated 100 healthy right- and left-handers using fMRI and a word generation task within the scanner (Pujol et al., 1999). The authors observed that 70% of the left-handers have left cerebral language dominance while 30% show a right dominant or bilateral pattern (Pujol et al., 1999). Assuming similar proportions for the sample of the present study, it is not surprising that functional connectivity of the IFG was insufficient for separating subjects based on handedness. Conversely, it underlines the robustness of handedness-dependent effects on M1 resting-state functional connectivity. Likewise, no effects were observed with respect to the V1 resting-state network.

4.4 Conclusion

In conclusion, the present study revealed that right-handedness is associated with stronger interhemispheric resting-state functional connectivity between primary and premotor cortex. The stronger lateralization of the motor system in right-handers might help to explain the behavioral effect that right-handedness is usually more lateralised than left-handedness who with left-handers tending to be more flexible in the use of both their right and left hand.

ACKNOWLEDGMENTS

We thank our volunteers and are grateful to Dr Marc Tittgemeyer and the MR staff for support. CG was supported by a grant from the Deutsche Forschungsgemeinschaft (GR 3285/2-1). SBE was supported by the Deutsche Forschungsgemeinschaft (DFG, EI 816/4-1; EI 816/6-1 and LA 3071/3-1), the National Institute of Mental Health (R01-MH074457) and the European EFT program (Human Brain Project). GRF gratefully acknowledges additional support from the Marga and Walter Boll Stiftung.

REFERENCES

Amunts, K., Schlaug, G., Schleicher, A., Steinmetz, H., Dabringhaus, A., Roland, P.E., Zilles, K., 1996. Asymmetry in the human motor cortex and handedness. Neuroimage 4, 216-222.

Ashburner, J., Friston, K.J., 2005. Unified segmentation. Neuroimage 26, 839-851.

Borod, J.C., Caron, H.S., Koff, E., 1984. Left-handers and right-handers compared on performance and preference measures of lateral dominance. Br J Psychol 75 (Pt 2), 177-186.

Broca, P., 1863. Localisation des fonctions cérébrales. Siège de la faculté du langage articulé (3 avril). Bulletin de la Société d'Anthropologie de Paris 4, 200-202.

Brodersen, K.H., Ong, C.S., Stephan, K.E., Buhmann, J.M., 2010. The balanced accuracy and its posterior distribution. Proceedings of the 20th International Conference on Pattern Recognition., 3121–3124.

Brouwer, B., Sale, M.V., Nordstrom, M.A., 2001. Asymmetry of motor cortex excitability during a simple motor task: relationships with handedness and manual performance. Exp Brain Res 138, 467-476.

Bryden, P.J., Mayer, M., Roy, E.A., 2011. Influences of task complexity, object location, and object type on hand selection in reaching in left and right-handed children and adults. Dev Psychobiol 53, 47-58.

Chang, C.C., Lin, C.J., 2011. LIBSVM: A library for support vector machines. ACM Trans Intell Syst Technol. 27, 1–39.

Churchland, M.M., Shenoy, K.V., 2007. Delay of movement caused by disruption of cortical preparatory activity. J Neurophysiol 97, 348-359.

Churchland, M.M., Yu, B.M., Ryu, S.I., Santhanam, G., Shenoy, K.V., 2006. Neural variability in premotor cortex provides a signature of motor preparation. J Neurosci 26, 3697-3712.

Clos, M., Amunts, K., Laird, A.R., Fox, P.T., Eickhoff, S.B., 2013. Tackling the multifunctional nature of Broca's region meta-analytically: co-activation-based parcellation of area 44. Neuroimage 83, 174-188.

Dassonville, P., Zhu, X.H., Uurbil, K., Kim, S.G., Ashe, J., 1997. Functional activation in motor cortex reflects the direction and the degree of handedness. Proc Natl Acad Sci U S A 94, 14015-14018.

Goodglass, H., Quadfasel, F.A., 1954. Language laterality in left-handed aphasics. Brain 77, 521-548.

Haaland, K.Y., Elsinger, C.L., Mayer, A.R., Durgerian, S., Rao, S.M., 2004. Motor sequence complexity and performing hand produce differential patterns of hemispheric lateralization. J Cogn Neurosci 16, 621-636.

Haaland, K.Y., Harrington, D.L., Knight, R.T., 2000. Neural representations of skilled movement. Brain 123 (Pt 11), 2306-2313.

Hammond, G., 2002. Correlates of human handedness in primary motor cortex: a review and hypothesis. Neurosci Biobehav Rev 26, 285-292.

Hardwick, R.M., Rottschy, C., Miall, R.C., Eickhoff, S.B., 2012. A quantitative meta-analysis and review of motor learning in the human brain. Neuroimage 67C, 283-297.

Hepper, P.G., Wells, D.L., Lynch, C., 2005. Prenatal thumb sucking is related to postnatal handedness. Neuropsychologia 43, 313-315.

Hoshi, E., Tanji, J., 2004. Differential roles of neuronal activity in the supplementary and presupplementary motor areas: from information retrieval to motor planning and execution. J Neurophysiol 92, 3482-3499.

Hoshi, E., Tanji, J., 2007. Distinctions between dorsal and ventral premotor areas: anatomical connectivity and functional properties. Curr Opin Neurobiol 17, 234-242.

Jäncke, L., Peters, M., Schlaug, G., Posse, S., Steinmetz, H., Muller-Gartner, H., 1998. Differential magnetic resonance signal change in human sensorimotor cortex to finger movements of different rate of the dominant and subdominant hand. Brain Res Cogn Brain Res 6, 279-284.

Karni, A., Meyer, G., Jezzard, P., Adams, M.M., Turner, R., Ungerleider, L.G., 1995. Functional MRI evidence for adult motor cortex plasticity during motor skill learning. Nature 377, 155-158.

Kim, S.G., Ashe, J., Hendrich, K., Ellermann, J.M., Merkle, H., Ugurbil, K., Georgopoulos, A.P., 1993. Functional magnetic resonance imaging of motor cortex: hemispheric asymmetry and handedness. Science 261, 615-617.

Kloppel, S., van Eimeren, T., Glauche, V., Vongerichten, A., Munchau, A., Frackowiak, R.S., Buchel, C., Weiller, C., Siebner, H.R., 2007. The effect of handedness on cortical motor activation during simple bilateral movements. Neuroimage 34, 274-280.

Knecht, S., Drager, B., Deppe, M., Bobe, L., Lohmann, H., Floel, A., Ringelstein, E.B., Henningsen, H., 2000. Handedness and hemispheric language dominance in healthy humans. Brain 123 Pt 12, 2512-2518.

Kriegeskorte, N., Simmons, W.K., Bellgowan, P.S., Baker, C.I., 2009. Circular analysis in systems neuroscience: the dangers of double dipping. Nat Neurosci 12, 535-540.

Landau, S.M., D'Esposito, M., 2006. Sequence learning in pianists and nonpianists: an fMRI study of motor expertise. Cogn Affect Behav Neurosci 6, 246-259.

Li, M., Chen, H., Wang, J., Liu, F., Long, Z., Wang, Y., Iturria-Medina, Y., Zhang, J., Yu, C., Chen, H., 2014. Handedness- and hemisphere-related differences in small-world brain networks: a diffusion tensor imaging tractography study. Brain Connect 4, 145-156.

Liuzzi, G., Horniss, V., Hoppe, J., Heise, K., Zimerman, M., Gerloff, C., Hummel, F.C., 2009. Distinct temporospatial interhemispheric interactions in the human primary and premotor cortex during movement preparation. Cereb Cortex 20, 1323-1331.

Lowe, M.J., Mock, B.J., Sorenson, J.A., 1998. Functional connectivity in single and multislice echoplanar imaging using resting-state fluctuations. Neuroimage 7, 119-132.

Oldfield, R.C., 1971. The assessment and analysis of handedness: the Edinburgh inventory. Neuropsychologia 9, 97-113.

Pool, E.M., Rehme, A.K., Fink, G.R., Eickhoff, S.B., Grefkes, C., 2013. Network dynamics engaged in the modulation of motor behavior in healthy subjects. Neuroimage 82C, 68-76.

Pool, E.M., Rehme, A.K., Fink, G.R., Eickhoff, S.B., Grefkes, C., 2014. Handedness and effective connectivity of the motor system. Neuroimage 99, 451-460.

Porac, C., 1996. Attempts to switch the writing hand: relationships to age and side of hand preference. Laterality 1, 35-44.

Power, J.D., Barnes, K.A., Snyder, A.Z., Schlaggar, B.L., Petersen, S.E., 2012. Spurious but systematic correlations in functional connectivity MRI networks arise from subject motion. Neuroimage 59, 2142-2154.

Pujol, J., Deus, J., Losilla, J.M., Capdevila, A., 1999. Cerebral lateralization of language in normal left-handed people studied by functional MRI. Neurology 52, 1038-1043.

Ratcliff, G., Dila, C., Taylor, L., Milner, B., 1980. The morphological asymmetry of the hemispheres and cerebral dominance for speech: a possible relationship. Brain Lang 11, 87-98.

Rehme, A.K., Volz, L.J., Feis, D.L., Bomilcar-Focke, I., Liebig, T., Eickhoff, S.B., Fink, G.R., Grefkes, C., 2014. Identifying Neuroimaging Markers of Motor Disability in Acute Stroke by Machine Learning Techniques. Cereb Cortex.

Saenger, V.M., Barrios, F.A., Martinez-Gudino, M.L., Alcauter, S., 2012. Hemispheric asymmetries of functional connectivity and grey matter volume in the default mode network. Neuropsychologia 50, 1308-1315.

Satterthwaite, T.D., Elliott, M.A., Gerraty, R.T., Ruparel, K., Loughead, J., Calkins, M.E., Eickhoff, S.B., Hakonarson, H., Gur, R.C., Gur, R.E., Wolf, D.H., 2013. An improved framework for confound regression and filtering for control of motion artifact in the preprocessing of resting-state functional connectivity data. Neuroimage 64, 240-256.

Satz, P., 1979. A test of some models of hemispheric speech organization in the left- and right-handed. Science 203, 1131-1133.

Schluter, N.D., Rushworth, M.F., Passingham, R.E., Mills, K.R., 1998. Temporary interference in human lateral premotor cortex suggests dominance for the selection of movements. A study using transcranial magnetic stimulation. Brain 121 (Pt 5), 785-799.

Solodkin, A., Hlustik, P., Noll, D.C., Small, S.L., 2001. Lateralization of motor circuits and handedness during finger movements. Eur J Neurol 8, 425-434.

Steinmetz, H., Volkmann, J., Jancke, L., Freund, H.J., 1991. Anatomical left-right asymmetry of language-related temporal cortex is different in left- and right-handers. Ann Neurol 29, 315-319.

Szaflarski, J.P., Holland, S.K., Schmithorst, V.J., Byars, A.W., 2006. fMRI study of language lateralization in children and adults. Hum Brain Mapp 27, 202-212.

Vaid, J., Bellugi, U., Poizner, H., 1989. Hand dominance for signing: clues to brain lateralization of language. Neuropsychologia 27, 949-960.

Van Dijk, K.R., Hedden, T., Venkataraman, A., Evans, K.C., Lazar, S.W., Buckner, R.L., 2010. Intrinsic functional connectivity as a tool for human connectomics: theory, properties, and optimization. J Neurophysiol 103, 297-321.

Van Dijk, K.R., Sabuncu, M.R., Buckner, R.L., 2012. The influence of head motion on intrinsic functional connectivity MRI. Neuroimage 59, 431-438.

Volkmann, J., Schnitzler, A., Witte, O.W., Freund, H., 1998. Handedness and asymmetry of hand representation in human motor cortex. J Neurophysiol 79, 2149-2154.

Yan, L.R., Wu, Y.B., Hu, D.W., Qin, S.Z., Xu, G.Z., Zeng, X.H., Song, H., 2012. Network asymmetry of motor areas revealed by resting-state functional magnetic resonance imaging. Behav Brain Res 227, 125-133.

Yousry, T.A., Schmid, U.D., Alkadhi, H., Schmidt, D., Peraud, A., Buettner, A., Winkler, P., 1997. Localization of the motor hand area to a knob on the precentral gyrus. A new landmark. Brain 120 (Pt 1), 141-157.

Ziemann, U., Hallett, M., 2001. Hemispheric asymmetry of ipsilateral motor cortex activation during unimanual motor tasks: further evidence for motor dominance. Clin Neurophysiol 112, 107-113.

zu Eulenburg, P., Caspers, S., Roski, C., Eickhoff, S.B., 2012. Meta-analytical definition and functional connectivity of the human vestibular cortex. Neuroimage 60, 162-169.

FIGURE LEGENDS

Figure 1. A Whole brain group analyses of the motor network (n=36, *P*<0.05, FWE-corrected on the cluster level*;* colour bar represents t-values) **B** Differential contrasts (n=36, *P*<0.05, FWE-corrected on the cluster level, cluster finding threshold *P*<0.001*;* colour bar represents t-values). **X** = seed region.

Figure 2. Whole-brain regression analysis of left M1 including EHI scores as covariate (n=36, *P*<0.05, FWE-corrected on the cluster level; colour bar represents t-values). **X** = seed region M1.

Figure 3. Multivariate SVM classification. Resting-state functional connectivity of left M1 provided 86.2% mean accuracy for the classification of handedness.
Red: Areas of voxelwise resting-state functional connectivity which contribute to the classification of right-handers; Blue: Areas of voxelwise resting-state functional connectivity which contribute to the classification of left-handers; **X** = seed region M1.

Figure 4. Control analyses of the Broca speech network and the visual network (n=36, *P*<0.05, FWE-corrected on the cluster level*;* colour bar represents t-values). **X** = seed region.

8. Table I

TABLES

Table I. Seed Regions.

Seed Region	*x*	*Y*	*z*
Left M1	-38	-24	62
Right M1	34	-22	62
Left IFG	-58	25	8
Right IFG	48	26	6
Left V1	-18	-102	2
Right V1	12	-102	0

M1 = primary motor cortex, IFG = inferior frontal gyrus, V1 = primary visual cortex

9. Figure 1

Click here to download 9. Figure: Fig1.eps

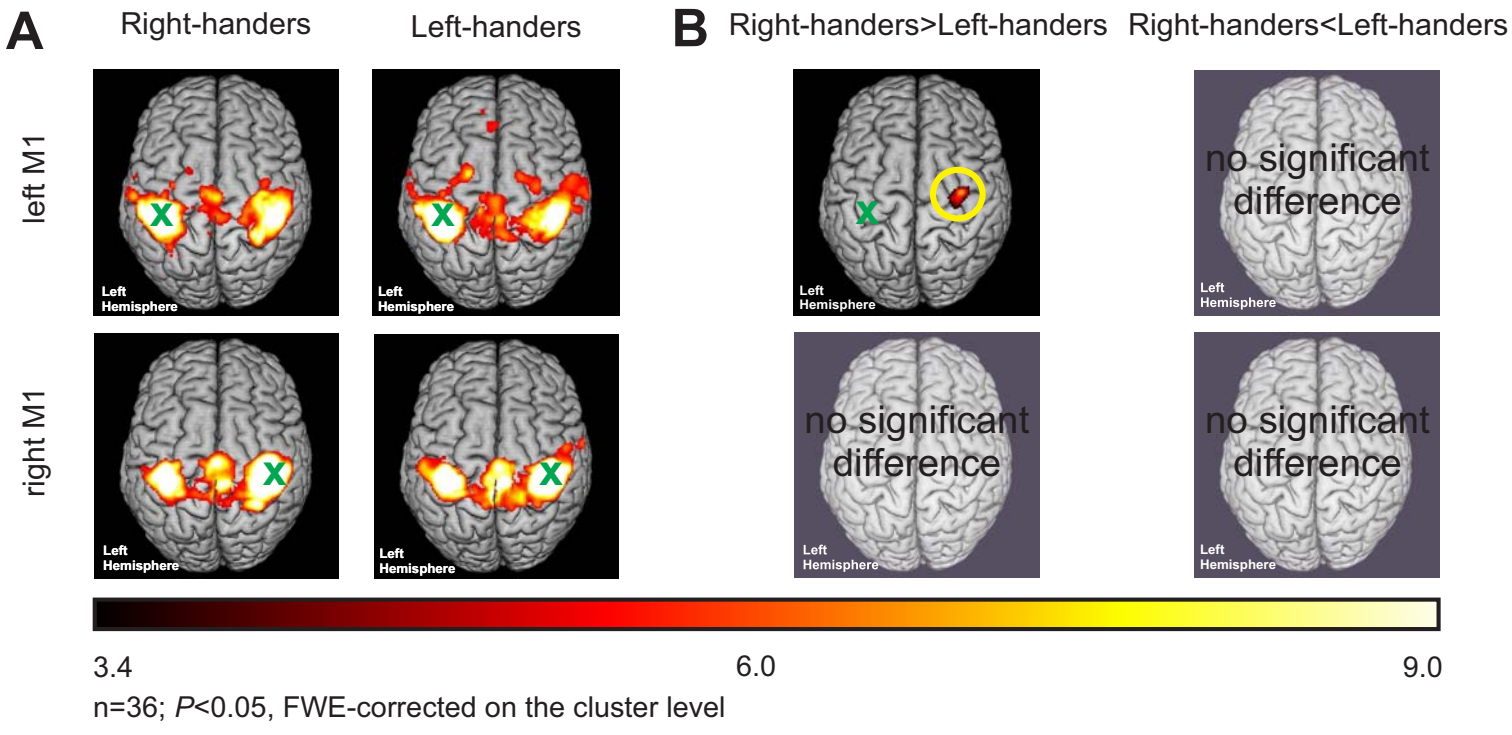

Figure 1

9. Figure 2
Click here to download 9. Figure: Fig2.eps

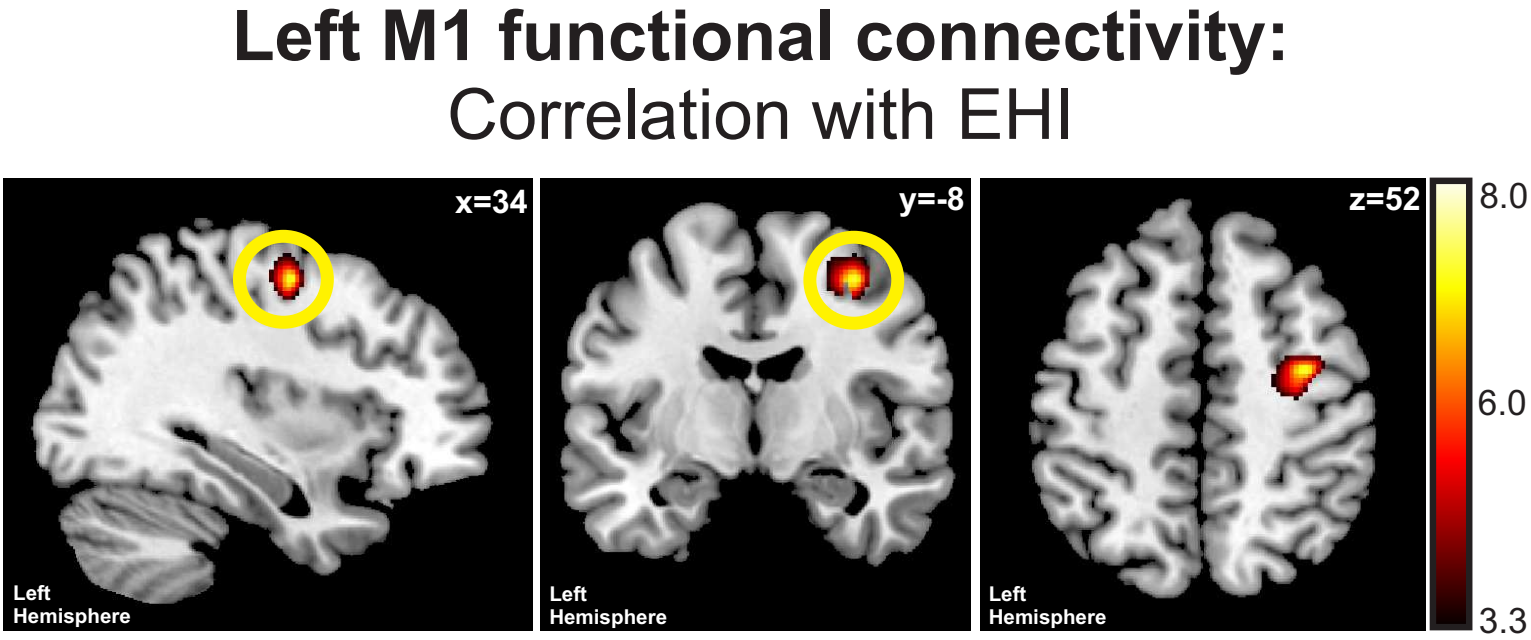

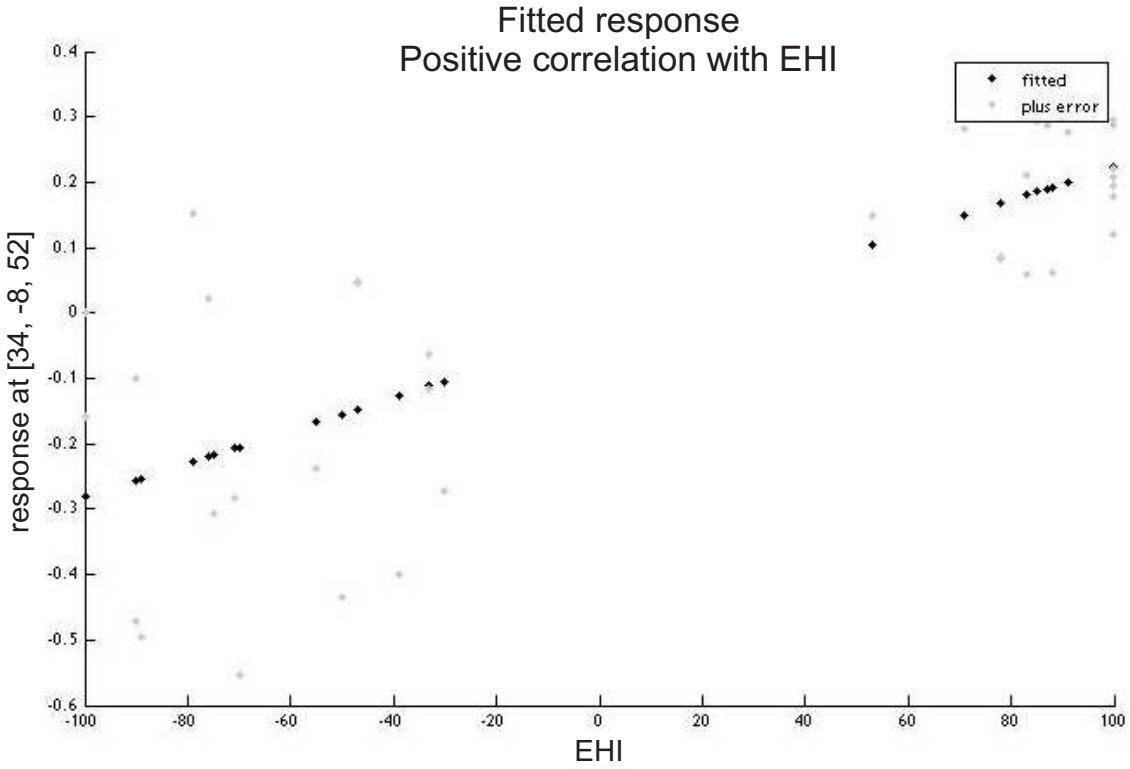

Figure 2

9. Figure 3

Click here to download 9. Figure: Fig3.eps

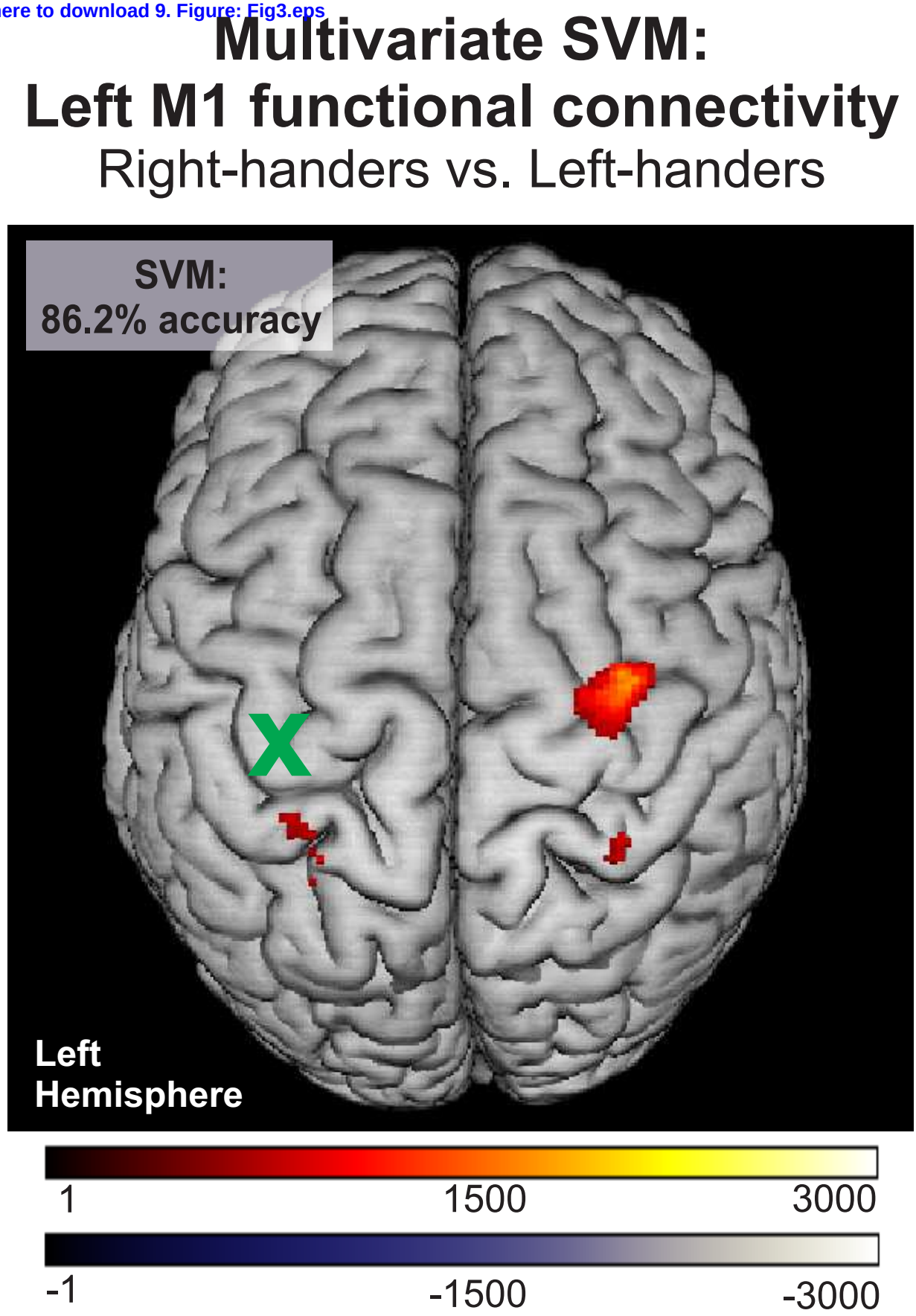

Figure 3

9. Figure 4

Click here to download 9. Figure: Fig4.eps

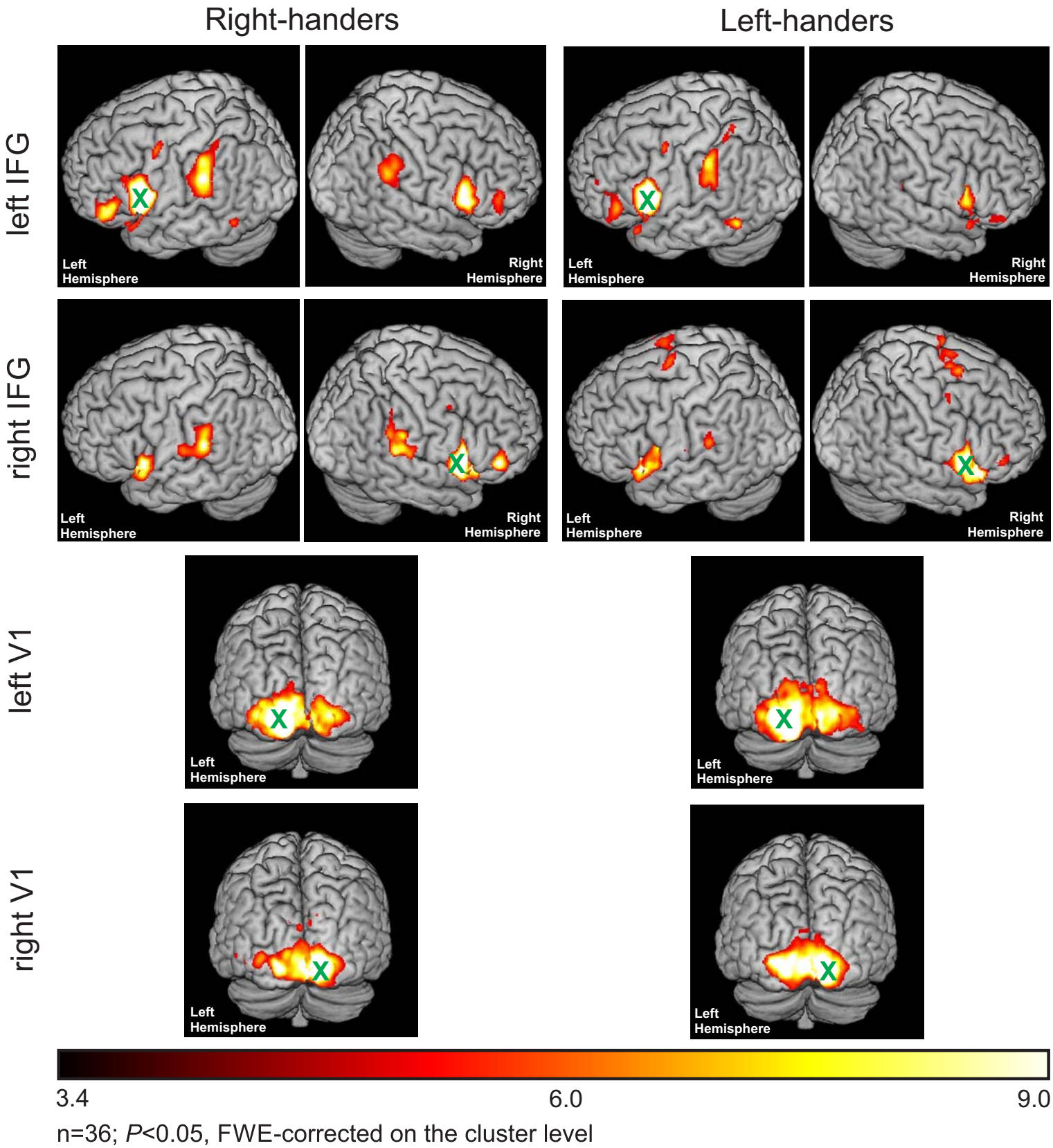

Figure 4

IV Discussion

The aim of the present studies was to investigate the relationship between the functional properties of the cerebral motor network and motor behavior by using functional neuroimaging and models of connectivity.

4.1 Network dynamics engaged in the modulation of motor behavior

We first tested the effect of movement speed on network dynamics. Accordingly, in the first study, 36 right-handed subjects were investigated with fMRI while performing fist closures at different movement frequencies (0.75 Hz, 1.5 Hz and 3.0 Hz). In the second study, we included 18 of these right-handers and additionally 18 left-handers. Subjects had to perform the same task as in the first study. To estimate the dynamic modulation of neural coupling among brain regions of the network models, we investigated the effective connectivity, i.e., the influence that one area exerts over another area (Friston et al., 2003), by using DCM.

The connectivity data of both studies revealed hemispheric differences in the amount by which the coupling of premotor areas and M1 was modulated, depending on which hand was moved. Other connections were not modulated by changes in motor performance. These findings suggest that a stronger coupling, especially between contralateral premotor areas (SMA, PMv) and M1, enables increased motor performance of simple unilateral hand movements. The functional relevance of both SMA and PMv in hand motor performance has already been demonstrated by studies which investigated patients suffering from brain lesions after a stroke (Rehme et al., 2011a; Wang et al., 2011). Thus, behavioral improvements of hand motor function in hemiparetic stroke patients following pharmacological stimulation (Wang et al., 2011) or repetitive transcranial magnetic stimulation (TMS) (Grefkes et al., 2010) were associated with an increase in neural coupling between SMA, PMv, and M1. Furthermore, Rehme and colleagues demonstrated that higher neural coupling strength between premotor areas and M1 correlates with better motor performance in stroke patients suffering from hand motor deficits (Rehme et al., 2011a). Therefore, our data add to the findings from stroke studies showing that premotor-M1 connectivity plays an essential role for recovery and motor performance, and are well in line with the hypothesis that reduced motor performance after brain lesions is caused not only by dysfunction of lesioned areas but also by disrupted effective interactions among cortical motor regions remote from the anatomical damage (Carrera and Tononi, 2014; Grefkes and Fink, 2014). Moreover, our

findings suggest that increasing motor performance results from a dynamic modulation of connectivity between distinct key motor regions that allows the brain to flexible adapt to an increasing motor demand (as reflected by differences in hand movement frequencies). Beside the crucial role of premotor-M1 connectivity, our data further identified a frequency-dependent influence from ipsilateral cerebellum on contralateral M1 for both right and left hand movements. The cerebellum receives input from the motor cortex via the pontine nuclei (Ramnani, 2006). In contrast, the motor modules in the anterior part of the cerebellum project back to M1 via the ventrolateral thalamus (Ramnani, 2006). Lesion studies in animals and humans further demonstrated the functional relevance of the cerebellum for the integration of isolated movements into a skill fully executed and timely coordinated ensemble (Goodkin et al., 1993; Hardiman et al., 1996; Ramnani, 2006). This cerebellar function for motor control might explain its role in the motor task as here a timing of hand movements as instructed by the rhythm of a blinking visual cue is necessary for correct task performance.

In conclusion, our findings indicate that the influence of an increasing motor demand on motor network connectivity is mediated by changes in neural coupling of inter- and intrahemispheric pathways from the premotor areas and cerebellum towards contralateral M1. Our data point to a critical contribution of the premotor cortex and cerebellum in the flexible adaption of the brain to varying motor demands in healthy subjects. Furthermore, the present study provides candidate regions whose causal role in hand motor performance can now be tested in future experiments by means of non-invasive brain stimulation techniques like TMS.

4.2 Effects of handedness on effective connectivity within the motor system

In the second study, we used fMRI to investigate whether handedness has a differential impact on the dynamic modulation of the motor system in 18 right- and 18 left-handers while performing fist closures at different movement frequencies (0.75 Hz, 1.5 Hz and 3.0 Hz).

The effective connectivity analysis revealed that during dominant hand movements, neural coupling of contralateral (dominant) SMA with premotor areas and M1 was significantly higher in right-handers as compared to left-handers. Thus, a generally higher task-dependent coupling of left SMA with a number of premotor regions and M1 suggest a key role of this motor area in subjects preferring their right hand for manuals skills. In line with this conclusion, also other neuroimaging studies demonstrated the functional relevance of the dominant left SMA in right-handers (Babiloni et al., 2003; Jäncke et al., 2000; Rogers et al., 2004). Rogers and colleagues reported stronger positive influence of contralateral SMA on contralateral sensorimotor cortex during movements of the dominant right hand relative to

corresponding connections during movements of the non-dominant left hand when investigating the effective connectivity between SMA and sensorimotor cortex in right-handers using structural equation modelling as a measure of effective connectivity (Rogers et al., 2004). Note that Rogers and colleagues investigated no left-handers in contrast to the study presented in this thesis.

Interestingly, the present data did not find significant differences in effective connectivity between movements of the dominant or non-dominant hand in left-handers. Thus, left-handers might be characterized by a differential recruitment profile that is reflected by a weaker effective connectivity network of contralateral SMA when performing dominant hand movements. The literature on differences in effective connectivity related to handedness is scarce. One study addressing this topic was published by Buckingham and colleagues (2011) who investigated motor attention in right- and left-handers by combining a discontinuous double-step reaching task with a Posner-style hand cueing paradigm (Buckingham et al., 2011). The authors demonstrated that right-handers needed more time to inhibit their dominant hand as compared to left-handers, indicating that their dominant hand was more readily primed to move than their non-dominant hand (Buckingham et al., 2011). In contrast, left-handers showed neither of these asymmetries, indicating that they lack an equivalent attentional bias for the dominant hand (Buckingham et al., 2011). This finding nicely fits our observation of generally stronger intra- and interhemispheric effective connectivity in right-handers during movements of the dominant hand.

In addition to cortical areas, we found that effective connectivity from contralateral putamen onto contralateral SMA was also significantly stronger in subjects who preferred their right hand for manual skills. The putamen is involved in the automation of previously learned movements (Griffiths et al., 1994) as well as in timing mechanisms (Macar et al., 2004; Rao et al., 2001). Macar and colleagues (2004) further observed a prominent neural activation of SMA when subject performed the timing task indicating that timing processes could be subserved by a striato-thalamo-cortical pathway including SMA (Macar et al., 2004). Similar effects might also underlie the stronger influence exerted by motor putamen onto SMA in right-handers for the dominant hand, as suggested by our findings. In line with our results, de la Fuente-Fernandez and colleagues further revealed a correlation between the degree of right hand preference and the uptake of the radiotracer fluorodopa in the left putamen as measured by positron-emission tomography (PET), suggesting that the putamen plays a crucial role in motor lateralization (de la Fuente-Fernandez et al., 2000).

In conclusion, our findings suggest a relation between handedness and differences in effective connectivity within the activated human motor network. Our findings point to a strong lateralization in the dominant hand-hemisphere system when performing dominant hand movements in right-handers. Here, the dominant SMA plays a prominent role in terms of brain organization. In contrast, left-handedness is characterized by a weaker asymmetry in motor network connectivity implying different hemispheric mechanisms of hand motor control as compared to right-handers.

4.3 Effects of handedness on functional resting-state connectivity within the motor system

In the third study we used resting-state fMRI to investigate the effects of handedness on functional connectivity. Right-handers showed a stronger interhemispheric functional connectivity between left M1 as seed region and contralateral PMd as compared to left-handers. Furthermore, the SVM analysis showed that interhemispheric connectivity between left M1 and right PMd allows making individual classifications as to whether subjects are left- or right-handed. In contrast, we found no differences between right- and left-handers for the Broca speech network or the visual network as resting-state control networks. Based on the individual resting-state maps using IFG or V1 as seed regions, the SVM could not classify right- and left-handers, underlining the specificity of our findings for the resting-state motor network.

In summary, the new finding of the third study was that we found a strong association between handedness and connectivity of M1 with contralateral PMd on an intrinsic functional level. Both M1 and PMd are considered key motor structures for movement preparation and execution (Hoshi and Tanji, 2004; Schluter et al., 1998). As our data revealed a stronger resting-state connectivity of right PMd with left M1 at rest but no similar effect for functional connectivity between left PMd and right M1, we conclude that interhemispheric interactions between premotor areas and M1 seem to be more lateralized in right-handers. Several connectivity studies already demonstrated that structural connectivity is more lateralized in right-handers as compared to left-handers. For example, Li and colleagues used diffusion tensor imaging (DTI) and graph theoretical measures to investigate handedness-related differences in white-matter properties. The authors found that right-handers had significant asymmetries in small-world properties of white matter tracts while subjects showing the preference to use the left hand for manual skills had fewer asymmetries (Li et al., 2014). Also other studies revealed lateralization differences in connectivity dependent on handedness. For example, Saenger and colleagues found that in right-handers connectivity of the default mode

resting-state network (DMN) shows more hemispheric asymmetries compared to left-handers (Saenger et al., 2012). Interestingly, during childhood development, asymmetries in resting-state connectivity of the motor system towards the left hemisphere reflect better motor performance in right-handed children (mean age: 10 yrs), indicating that lateralization of motor networks might be a typical feature of right-handers. Developmental studies further demonstrated that right hand preference can be already observed before birth; for example, ultrasound studies revealed that about 90% of the fetuses suck the thumb of the right hand (Hepper et al., 2005a), suggesting a strong genetic influence for handedness. But also use-dependent effects may impact on asymmetry of the motor system (Haaland et al., 2000; Karni et al., 1995; Kloppel et al., 2007). This might be especially important when studying left-handers as they have learned to live in a world in which many tools and procedures are made for right-handers (Porac, 1996). In fact, left-handers were demonstrated to be more flexible in using both hands in activities of daily living (Bryden et al., 2011; Vaid et al., 1989), which might impact on lateralization of brain activity.

In conclusion, our findings indicate that right-handedness is associated with stronger interhemispheric resting-state connectivity between primary and premotor cortex as compared to left-handedness. This stronger lateralization of the motor system in right-handers might explain the behavioral notion that right-handedness is usually more lateralised than left-handedness who tend to be more flexible in the use of both the right and left hand.

4.4 Limitations of the applied methods

One limitation of the present studies pertains to the limited number of areas included in the connectivity models. While other areas in prefrontal as well as parietal cortex undoubtedly contribute to the control of even simple hand movements (Cieslik et al., 2012), we restricted the areas to include “key” regions of the motor system. In the present study, we increased the model complexity from the default value of DCM as implemented in SPM from 8 regions to 10 regions. In DCM, model complexity is penalized by conservative shrinkage priors who make it more difficult for a given connection to become significant. In other words, priors on the connectivity parameters ensure that the system remains stable (Friston et al., 2003). Hence, the number of included regions in DCM is always a trade-off between model fit and generalizability. The fact that we found significant connections despite a rather complex model (10 regions, 90 connections) highlights the robustness of the data. Furthermore, DCM also models indirect influences of a network, i.e., regions that were not included in the model are considered as well. Moreover, left-handers featured less asymmetry in effective

connectivity, despite clear preference to use their left hand for everyday life tasks. We cannot disentangle whether this effect arises from the fact that left-handers live in an environment that is rather made for right-handers (and hence they are more often forced to use their non-dominant right hand which might also affect cortical connectivity) or from prenatal disposition such as preferring the thumb of the right or left hand (Hepper et al., 2005a).

However, the relative simplicity of the motor task used in the present studies makes it rather unlikely that relevant use-dependent effects in every-day life may have influenced the differences found between right- and left-handed subjects. It is interesting to note that differences between right- and left-handers were only evident in the connectivity data but not in the "classical" BOLD activation analysis. That connectivity analyses of motor system activity can have higher sensitivity compared to activation analyses has also been shown by Sharma et al. (2009). One reason for the greater sensitivity might relate to the region of interest approach used in DCM which corrects for residual interindividual variability in the precise anatomical location of premotor areas in individual subjects. Furthermore, in DCM, the HRF is computed for each and every ROI separately (Friston et al., 2003) in contrast to the "classical" activation analysis, which uses a canonical HRF model for all voxels. Hence, DCM better accounts for variability of the HRF between regions, which might further increase its sensitivity for detecting differences between groups of subjects.

A further limitation given by our resting-state fMRI measurements is that we did not specifically measured physiological noise (e.g., respiratory oscillations and cardiac cycles) which might influence the low-frequency fluctuation signal. However, attempting to adjust fMRI resting-state time-series for the effect of confounds we used a regression model consisting of the six standard motion parameters from realignment, mean signal intensities, first-order temporal derivative of each parameter and the quadratic term of all parameters. Using this method the effects of confounds in resting-state functional connectivity can be substantially reduced (Satterthwaite et al., 2013).

4.5. Future prospects

Based on the present findings it would be an interesting approach to investigate the putative biological determinants of motor behavior in a network model of subjects with brain lesions, e.g., after stroke. A structural lesion resulting from a stroke critically disturbs the complex balance of excitatory and inhibitory influences within the motor network (Grefkes and Fink, 2014). Several studies already demonstrated that affected hand movements are associated with changes of neural activity in both hemispheres in the first weeks after stroke,

which then return to levels observed in healthy controls, particularly in patients making full motor recovery (Rehme et al., 2011b; Ward et al., 2003). Furthermore, several connectivity studies demonstrated that increases of neural coupling between distinct key motor regions, especially the influence from premotor areas towards contralateral M1, are associated with better motor performance in subjects with brain lesions (Rehme et al., 2011a; Wang et al., 2011). However, the exact mechanisms of the brain underlying the flexible adaption of the brain to an increasing motor demand in stroke patients related to motor impairment and recovery thereof are not fully understood. The question arises whether this dynamic modulation is mediated by the same areas as in healthy subjects showing different levels of neural activity when performing simple hand movements or whether there are additional areas supporting the lesioned motor network. Identifying brain regions that drive motor performance might, therefore, be of particular relevance in a neurorehabilitative setting in order to identify targets that could be modulated by brain stimulation techniques.

4.6 Summary and conclusion

In summary, the present studies reveal that the influence of an extrinsic factor like increasing motor demand on motor network connectivity is mediated by changes in neural coupling of inter- and intrahemispheric pathways from premotor areas and cerebellum towards contralateral M1. Hence, our data point to a critical contribution, especially of premotor areas and motor cerebellum, in the flexible adaption of the brain to varying motor demands in healthy right- and left-handed subjects. Furthermore, the present studies suggest that an intrinsic factor like handedness has a further systematic impact on effective connectivity within the human motor network. Our results reveal a general principle of brain organization with a prominent role of dominant SMA in right-handers and indicate a strong lateralization in the dominant hand-hemisphere system when performing dominant hand movements. Left-handers showed a weaker asymmetry in motor network connectivity implying different hemispheric mechanisms of hand motor control as compared to right-handers. Interestingly, our results revealed that handedness has also a systematic impact on interhemispheric functional connectivity between left M1 and right PMd during resting-state, i.e., in the absence of overt motor performance. Hence, our findings demonstrate that the differences in task performance between right- and left-handers reflect the impact of handedness on both functional and effective connectivity. Furthermore, enhanced connectivity between these areas serves as an individual classification marker of handedness in individual subjects. Thus, a generally higher intrinsic connectivity in right-handers might explain the

behavioral notion that right-handedness is usually more lateralised than left-handedness who tend to be more flexible in the use of both the dominant and non-dominant hand.

References

Akkal, D., Dum, R.P., Strick, P.L., 2007. Supplementary motor area and presupplementary motor area: targets of basal ganglia and cerebellar output. J Neurosci 27, 10659-10673.

Alexander, G.E., Crutcher, M.D., 1990. Functional architecture of basal ganglia circuits: neural substrates of parallel processing. Trends Neurosci 13, 266-271.

Amunts, K., Schlaug, G., Schleicher, A., Steinmetz, H., Dabringhaus, A., Roland, P.E., Zilles, K., 1996. Asymmetry in the human motor cortex and handedness. Neuroimage 4, 216-222.

Annett, M., 1985. Left, right, hand and brain: The right shift theory. Hillsdale, NJ: Erlbaum.

Babiloni, C., Carducci, F., Del Gratta, C., Demartin, M., Romani, G.L., Babiloni, F., Rossini, P.M., 2003. Hemispherical asymmetry in human SMA during voluntary simple unilateral movements. An fMRI study. Cortex 39, 293-305.

Borod, J.C., Caron, H.S., Koff, E., 1984. Left-handers and right-handers compared on performance and preference measures of lateral dominance. Br J Psychol 75 (Pt 2), 177-186.

Boudrias, M.H., Goncalves, C.S., Penny, W.D., Park, C.H., Rossiter, H.E., Talelli, P., Ward, N.S., 2012. Age-related changes in causal interactions between cortical motor regions during hand grip. Neuroimage 59, 3398-3405.

Boussaoud, D., Tanne-Gariepy, J., Wannier, T., Rouiller, E.M., 2005. Callosal connections of dorsal versus ventral premotor areas in the macaque monkey: a multiple retrograde tracing study. BMC Neurosci 6, 67.

Brodmann, K., 1909. Vergleichende Lokalisationslehre der Großhirnrinde. Leipzig: Barth.

Bryden, P.J., Mayer, M., Roy, E.A., 2011. Influences of task complexity, object location, and object type on hand selection in reaching in left and right-handed children and adults. Dev Psychobiol 53, 47-58.

Buckingham, G., Main, J.C., Carey, D.P., 2011. Asymmetries in motor attention during a cued bimanual reaching task: left and right handers compared. Cortex 47, 432-440.

Carrera, E., Tononi, G., 2014. Diaschisis: past, present, future. Brain 137, 2408-2422.

Chang, C.C., Lin, C.J., 2011. LIBSVM: A library for support vector machines. ACM Trans Intell Syst Technol. 27, 1–39.

Cheney, P.D., Fetz, E.E., Mewes, K., 1991. Neural mechanisms underlying corticospinal and rubrospinal control of limb movements. Prog Brain Res 87, 213-252.

Churchland, M.M., Shenoy, K.V., 2007. Delay of movement caused by disruption of cortical preparatory activity. J Neurophysiol 97, 348-359.

Churchland, M.M., Yu, B.M., Ryu, S.I., Santhanam, G., Shenoy, K.V., 2006. Neural variability in premotor cortex provides a signature of motor preparation. J Neurosci 26, 3697-3712.

Cieslik, E.C., Zilles, K., Caspers, S., Roski, C., Kellermann, T.S., Jakobs, O., Langner, R., Laird, A.R., Fox, P.T., Eickhoff, S.B., 2012. Is There "One" DLPFC in Cognitive Action Control? Evidence for Heterogeneity From Co-Activation-Based Parcellation. Cereb Cortex.

de la Fuente-Fernandez, R., Kishore, A., Calne, D.B., Ruth, T.J., Stoessl, A.J., 2000. Nigrostriatal dopamine system and motor lateralization. Behav Brain Res 112, 63-68.

Dettmers, C., Fink, G.R., Lemon, R.N., Stephan, K.M., Passingham, R.E., Silbersweig, D., Holmes, A., Ridding, M.C., Brooks, D.J., Frackowiak, R.S., 1995. Relation between cerebral activity and force in the motor areas of the human brain. J Neurophysiol 74, 802-815.

Dettmers, C., Lemon, R.N., Stephan, K.M., Fink, G.R., Frackowiak, R.S., 1996. Cerebral activation during the exertion of sustained static force in man. Neuroreport 7, 2103-2110.

Dum, R.P., Strick, P.L., 2002. Motor areas in the frontal lobe of the primate. Physiol Behav 77, 677-682.

Dum, R.P., Strick, P.L., 2005. Frontal lobe inputs to the digit representations of the motor areas on the lateral surface of the hemisphere. J Neurosci 25, 1375-1386.

Eickhoff, S.B., Dafotakis, M., Grefkes, C., Shah, N.J., Zilles, K., Piza-Katzer, H., 2008. Central adaptation following heterotopic hand replantation probed by fMRI and effective connectivity analysis. Exp Neurol 212, 132-144.

Eickhoff, S.B., Grefkes, C., 2011. Approaches for the integrated analysis of structure, function and connectivity of the human brain. Clin EEG Neurosci 42, 107-121.

Fogassi, L., Gallese, V., Buccino, G., Craighero, L., Fadiga, L., Rizzolatti, G., 2001. Cortical mechanism for the visual guidance of hand grasping movements in the monkey: A reversible inactivation study. Brain 124, 571-586.

Fox, P.T., Raichle, M.E., Mintun, M.A., Dence, C., 1988. Nonoxidative glucose consumption during focal physiologic neural activity. Science 241, 462-464.

Fridman, E.A., Hanakawa, T., Chung, M., Hummel, F., Leiguarda, R.C., Cohen, L.G., 2004. Reorganization of the human ipsilesional premotor cortex after stroke. Brain 127, 747-758.

Friston, K.J., 1994. Functional and Effective Connectivity in Neuroimaging: A Synthesis. Hum Brain Mapp 2, 56-78.

Friston, K.J., Harrison, L., Penny, W., 2003. Dynamic causal modelling. Neuroimage 19, 1273-1302.

Friston, K.J., Kahan, J., Biswal, B., Razi, A., 2014. A DCM for resting state fMRI. Neuroimage 94, 396-407.

Goodglass, H., Quadfasel, F.A., 1954. Language laterality in left-handed aphasics. Brain 77, 521-548.

Goodkin, H.P., Keating, J.G., Martin, T.A., Thach, W.T., 1993. Preserved simple and impaired compound movement after infarction in the territory of the superior cerebellar artery. Can J Neurol Sci 20 Suppl 3, S93-104.

Grefkes, C., Eickhoff, S.B., Nowak, D.A., Dafotakis, M., Fink, G.R., 2008. Dynamic intra- and interhemispheric interactions during unilateral and bilateral hand movements assessed with fMRI and DCM. Neuroimage 41, 1382-1394.

Grefkes, C., Fink, G.R., 2014. Connectivity-based approaches in stroke and recovery of function. Lancet Neurol 13, 206-216.

Grefkes, C., Nowak, D.A., Wang, L.E., Dafotakis, M., Eickhoff, S.B., Fink, G.R., 2010. Modulating cortical connectivity in stroke patients by rTMS assessed with fMRI and dynamic causal modeling. Neuroimage 50, 233-242.

Griffiths, P.D., Perry, R.H., Crossman, A.R., 1994. A detailed anatomical analysis of neurotransmitter receptors in the putamen and caudate in Parkinson's disease and Alzheimer's disease. Neurosci Lett 169, 68-72.

Haaland, K.Y., Elsinger, C.L., Mayer, A.R., Durgerian, S., Rao, S.M., 2004. Motor sequence complexity and performing hand produce differential patterns of hemispheric lateralization. J Cogn Neurosci 16, 621-636.

Haaland, K.Y., Harrington, D.L., Knight, R.T., 2000. Neural representations of skilled movement. Brain 123 (Pt 11), 2306-2313.

Halsband, U., Passingham, R.E., 1985. Premotor cortex and the conditions for movement in monkeys (Macaca fascicularis). Behav Brain Res 18, 269-277.

Hardiman, M.J., Ramnani, N., Yeo, C.H., 1996. Reversible inactivations of the cerebellum with muscimol prevent the acquisition and extinction of conditioned nictitating membrane responses in the rabbit. Exp Brain Res 110, 235-247.

Heeger, D.J., Ress, D., 2002. What does fMRI tell us about neuronal activity? 3, 142-151.

Hepper, P.G., 2013. The Developmental Origins of Laterality: Fetal Handedness. Dev Psychobiol 55, 588–595.

Hepper, P.G., Shahidullah, S., White, R., 1991. Handedness in the human fetus. Neuropsychologia 29, 1107–1111.

Hepper, P.G., Wells, D.L., Lynch, C., 2005a. Prenatal thumb sucking is related to postnatal handedness. Neuropsychologia 43, 313-315.

Hepper, P.G., Wells, D.L., Lynch, C., 2005b. Prenatal thumb sucking is related to postnatal handedness. Neuropsychologia 43, 313–315.

Herz, D.M., Christensen, M.S., Reck, C., Florin, E., Barbe, M.T., Stahlhut, C., Pauls, K.A., Tittgemeyer, M., Siebner, H.R., Timmermann, L., 2012. Task-specific modulation of effective connectivity during two simple unimanual motor tasks: a 122-channel EEG study. Neuroimage 59, 3187-3193.

Hoshi, E., Tanji, J., 2004. Differential roles of neuronal activity in the supplementary and presupplementary motor areas: from information retrieval to motor planning and execution. J Neurophysiol 92, 3482-3499.

Hoshi, E., Tanji, J., 2006. Differential involvement of neurons in the dorsal and ventral premotor cortex during processing of visual signals for action planning. J Neurophysiol 95, 3596-3616.

Hoshi, E., Tremblay, L., Feger, J., Carras, P.L., Strick, P.L., 2005. The cerebellum communicates with the basal ganglia. Nat Neurosci 8, 1491-1493.

Jakobs, O., Wang, L.E., Dafotakis, M., Grefkes, C., Zilles, K., Eickhoff, S.B., 2009. Effects of timing and movement uncertainty implicate the temporo-parietal junction in the prediction of forthcoming motor actions. Neuroimage 47, 667-677.

Jäncke, L., Peters, M., Schlaug, G., Posse, S., Steinmetz, H., Muller-Gartner, H., 1998a. Differential magnetic resonance signal change in human sensorimotor cortex to finger movements of different rate of the dominant and subdominant hand. Brain Res Cogn Brain Res 6, 279-284.

Jäncke, L., Shah, N.J., Peters, M., 2000. Cortical activations in primary and secondary motor areas for complex bimanual movements in professional pianists. Brain Res Cogn Brain Res 10, 177-183.

Jäncke, L., Specht, K., Mirzazade, S., Loose, R., Himmelbach, M., Lutz, K., Shah, N.J., 1998b. A parametric analysis of the 'rate effect' in the sensorimotor cortex: a functional magnetic resonance imaging analysis in human subjects. Neurosci Lett 252, 37-40.

Jäncke, L., Specht, K., Mirzazade, S., Peters, M., 1999. The effect of finger-movement speed of the dominant and the subdominant hand on cerebellar activation: A functional magnetic resonance imaging study. Neuroimage 9, 497-507.

Jenkins, I.H., Jahanshahi, M., Jueptner, M., Passingham, R.E., Brooks, D.J., 2000. Self-initiated versus externally triggered movements. II. The effect of movement predictability on regional cerebral blood flow. Brain 123 (Pt 6), 1216-1228.

Johansen-Berg, H., Rushworth, M.F., Bogdanovic, M.D., Kischka, U., Wimalaratna, S., Matthews, P.M., 2002. The role of ipsilateral premotor cortex in hand movement after stroke. Proc Natl Acad Sci U S A 99, 14518-14523.

Johnson, P.B., Ferraina, S., Bianchi, L., Caminiti, R., 1996. Cortical networks for visual reaching: physiological and anatomical organization of frontal and parietal lobe arm regions. Cereb Cortex 6, 102-119.

Karni, A., Meyer, G., Jezzard, P., Adams, M.M., Turner, R., Ungerleider, L.G., 1995. Functional MRI evidence for adult motor cortex plasticity during motor skill learning. Nature 377, 155-158.

Kawashima, R., Roland, P.E., O'Sullivan, B.T., 1994. Fields in human motor areas involved in preparation for reaching, actual reaching, and visuomotor learning: a positron emission tomography study. J Neurosci 14, 3462-3474.

Kazennikov, O., Hyland, B., Corboz, M., Babalian, A., Rouiller, E.M., Wiesendanger, M., 1999. Neural activity of supplementary and primary motor areas in monkeys and its relation to bimanual and unimanual movement sequences. Neuroscience 89, 661-674.

Kelly, R.M., Strick, P.L., 2003. Cerebellar loops with motor cortex and prefrontal cortex of a nonhuman primate. J Neurosci 23, 8432-8444.

Kiebel, S.J., Holmes, A.P., 2007. The general linear model. . In: Friston KJ, Ashburner JT, Kiebel SJ, Nichols TE, Penny WD, editors. Statistical parametric mapping: The analysis of functional brain images. London: Elsevier; 2007. p. 101-25.

Kloppel, S., van Eimeren, T., Glauche, V., Vongerichten, A., Munchau, A., Frackowiak, R.S., Buchel, C., Weiller, C., Siebner, H.R., 2007. The effect of handedness on cortical motor activation during simple bilateral movements. Neuroimage 34, 274-280.

Knecht, S., Drager, B., Deppe, M., Bobe, L., Lohmann, H., Floel, A., Ringelstein, E.B., Henningsen, H., 2000. Handedness and hemispheric language dominance in healthy humans. Brain 123 Pt 12, 2512-2518.

Kubota, K., Hamada, I., 1978. Visual tracking and neuron activity in the post-arcuate area in monkeys. J Physiol (Paris) 74, 297-312.

Kurata, K., Hoffman, D.S., 1994. Differential effects of muscimol microinjection into dorsal and ventral aspects of the premotor cortex of monkeys. J Neurophysiol 71, 1151-1164.

Li, M., Chen, H., Wang, J., Liu, F., Long, Z., Wang, Y., Iturria-Medina, Y., Zhang, J., Yu, C., Chen, H., 2014. Handedness- and hemisphere-related differences in small-world brain networks: a diffusion tensor imaging tractography study. Brain Connect 4, 145-156.

Lin, F.H., Agnew, J.A., Belliveau, J.W., Zeffiro, T.A., 2009. Functional and effective connectivity of visuomotor control systems demonstrated using generalized partial least squares and structural equation modeling. Hum Brain Mapp 30, 2232-2251.

Logothetis, N.K., Pauls, J., Augath, M., Trinath, T., Oeltermann, A., 2001. Neurophysiological investigation of the basis of the fMRI signal. Nature 412, 150-157.

Lowe, M.J., Mock, B.J., Sorenson, J.A., 1998. Functional connectivity in single and multislice echoplanar imaging using resting-state fluctuations. Neuroimage 7, 119-132.

Luppino, G., Matelli, M., Camarda, R., Rizzolatti, G., 1993. Corticocortical connections of area F3 (SMA-proper) and area F6 (pre-SMA) in the macaque monkey. J Comp Neurol 338, 114-140.

Lutz, K., Specht, K., Shah, N.J., Jancke, L., 2000. Tapping movements according to regular and irregular visual timing signals investigated with fMRI. Neuroreport 11, 1301-1306.

Macar, F., Anton, J.L., Bonnet, M., Vidal, F., 2004. Timing functions of the supplementary motor area: an event-related fMRI study. Brain Res Cogn Brain Res 21, 206-215.

Matelli, M., Luppino, G., Rizzolatti, G., 1985. Patterns of cytochrome oxidase activity in the frontal agranular cortex of the macaque monkey. Behav Brain Res 18, 125-136.

Matelli, M., Luppino, G., Rizzolatti, G., 1991. Architecture of superior and mesial area 6 and the adjacent cingulate cortex in the macaque monkey. J Comp Neurol 311, 445-462.

McGuire, P.K., Bates, J.F., Goldman-Rakic, P.S., 1991. Interhemispheric integration: I. Symmetry and convergence of the corticocortical connections of the left and the right principal sulcus (PS) and the left and the right supplementary motor area (SMA) in the rhesus monkey. Cereb Cortex 1, 390-407.

Middleton, F.A., Strick, P.L., 2000. Basal ganglia and cerebellar loops: motor and cognitive circuits. Brain Res Brain Res Rev 31, 236-250.

Nakai, T., Kato, C., Glover, G.H., Toma, K., Moriya, T., Matsuo, K., 2003. A functional magnetic resonance imaging study of internal modulation of an external visual cue for motor execution. Brain Res 968, 238-247.

Ogawa, S., Lee, T.M., Kay, A.R., Tank, D.W., 1990. Brain magnetic resonance imaging with contrast dependent on blood oxygenation. Proc Natl Acad Sci U S A 87, 9868-9872.

Oldfield, R.C., 1971. The assessment and analysis of handedness: the Edinburgh inventory. Neuropsychologia 9, 97-113.

Passingham, R.E., 1989. Premotor cortex and the retrieval of movement. Brain Behav Evol 33, 189-192.

Penfield, W., Rasmussen, T., 1950. The cerebral cortex of man. . New York: Macmillan.

Penny, W.D., Stephan, K.E., Mechelli, A., Friston, K.J., 2004. Comparing dynamic causal models. Neuroimage 22, 1157-1172.

Pool, E.M., Eickhoff, S.B., Fink, G.R., Grefkes, C., 2014b. Effects of handedness on functional resting-state connectivity within the human motor network. Abstract No 3767. OHBM 2014, Hamburg.

Pool, E.M., Rehme, A.K., Fink, G.R., Eickhoff, S.B., Grefkes, C., 2013. Network dynamics engaged in the modulation of motor behavior in healthy subjects. Neuroimage 82C, 68-76.

Pool, E.M., Rehme, A.K., Fink, G.R., Eickhoff, S.B., Grefkes, C., 2014a. Handedness and effective connectivity of the motor system. Neuroimage 99, 451-460.

Porac, C., 1996. Attempts to switch the writing hand: relationships to age and side of hand preference. Laterality 1, 35-44.

Porac, C., Coren, S., 1981. Life-span age trends in the perception of the Mueller-Lyer: additional evidence for the existence of two illusions. Can J Psychol 35, 58-62.

Pujol, J., Deus, J., Losilla, J.M., Capdevila, A., 1999. Cerebral lateralization of language in normal left-handed people studied by functional MRI. Neurology 52, 1038-1043.

Ramnani, N., 2006. The primate cortico-cerebellar system: anatomy and function. Nat Rev Neurosci 7, 511-522.

Rao, S.M., Bandettini, P.A., Binder, J.R., Bobholz, J.A., Hammeke, T.A., Stein, E.A., Hyde, J.S., 1996. Relationship between finger movement rate and functional magnetic resonance signal change in human primary motor cortex. J Cereb Blood Flow Metab 16, 1250-1254.

Rao, S.M., Mayer, A.R., Harrington, D.L., 2001. The evolution of brain activation during temporal processing. Nat Neurosci 4, 317-323.

Raos, V., Umilta, M.A., Murata, A., Fogassi, L., Gallese, V., 2006. Functional properties of grasping-related neurons in the ventral premotor area F5 of the macaque monkey. J Neurophysiol 95, 709-729.

Ratcliff, G., Dila, C., Taylor, L., Milner, B., 1980. The morphological asymmetry of the hemispheres and cerebral dominance for speech: a possible relationship. Brain Lang 11, 87-98.

Rehme, A.K., Eickhoff, S.B., Wang, L.E., Fink, G.R., Grefkes, C., 2011a. Dynamic causal modeling of cortical activity from the acute to the chronic stage after stroke. Neuroimage 55, 1147-1158.

Rehme, A.K., Fink, G.R., von Cramon, D.Y., Grefkes, C., 2011b. The role of the contralesional motor cortex for motor recovery in the early days after stroke assessed with longitudinal FMRI. Cereb Cortex 21, 756-768.

Rogers, B.P., Carew, J.D., Meyerand, M.E., 2004. Hemispheric asymmetry in supplementary motor area connectivity during unilateral finger movements. Neuroimage 22, 855-859.

Rouiller, E.M., Babalian, A., Kazennikov, O., Moret, V., Yu, X.H., Wiesendanger, M., 1994. Transcallosal connections of the distal forelimb representations of the primary and supplementary motor cortical areas in macaque monkeys. Exp Brain Res 102, 227-243.

Sadato, N., Ibanez, V., Deiber, M.P., Campbell, G., Leonardo, M., Hallett, M., 1996. Frequency-dependent changes of regional cerebral blood flow during finger movements. J Cereb Blood Flow Metab 16, 23-33.

Saenger, V.M., Barrios, F.A., Martinez-Gudino, M.L., Alcauter, S., 2012. Hemispheric asymmetries of functional connectivity and grey matter volume in the default mode network. Neuropsychologia 50, 1308-1315.

Satterthwaite, T.D., Elliott, M.A., Gerraty, R.T., Ruparel, K., Loughead, J., Calkins, M.E., Eickhoff, S.B., Hakonarson, H., Gur, R.C., Gur, R.E., Wolf, D.H., 2013. An improved framework for confound regression and filtering for control of motion artifact in the preprocessing of resting-state functional connectivity data. Neuroimage 64, 240-256.

Satz, P., 1979. A test of some models of hemispheric speech organization in the left- and right-handed. Science 203, 1131-1133.

Schlaug, G., Sanes, J.N., Thangaraj, V., Darby, D.G., Jancke, L., Edelman, R.R., Warach, S., 1996. Cerebral activation covaries with movement rate. Neuroreport 7, 879-883.

Schluter, N.D., Rushworth, M.F., Passingham, R.E., Mills, K.R., 1998. Temporary interference in human lateral premotor cortex suggests dominance for the selection of movements. A study using transcranial magnetic stimulation. Brain 121 (Pt 5), 785-799.

Schubotz, R.I., von Cramon, D.Y., 2001. Functional organization of the lateral premotor cortex: fMRI reveals different regions activated by anticipation of object properties, location and speed. Brain Res Cogn Brain Res 11, 97-112.

Schuyler, B., Ollinger, J.M., Oakes, T.R., Johnstone, T., Davidson, R.J., 2010. Dynamic Causal Modeling applied to fMRI data shows high reliability. Neuroimage 49, 603-611.

Shimazu, H., Maier, M.A., Cerri, G., Kirkwood, P.A., Lemon, R.N., 2004. Macaque ventral premotor cortex exerts powerful facilitation of motor cortex outputs to upper limb motoneurons. J Neurosci 24, 1200-1211.

Smith, S.B., 2001. Preparing fMRI data for statistical analysis. In: Jezzard P, Matthews PM, Smith SB, editors. Functional MRI: an introduction to methods. New York: Oxford University Press; 2001. p. 229-41.

Smith, Y., Bevan, M.D., Shink, E., Bolam, J.P., 1998. Microcircuitry of the direct and indirect pathways of the basal ganglia. Neuroscience 86, 353-387.

Solodkin, A., Hlustik, P., Noll, D.C., Small, S.L., 2001. Lateralization of motor circuits and handedness during finger movements. Eur J Neurol 8, 425-434.

Steinmetz, H., Volkmann, J., Jancke, L., Freund, H.J., 1991. Anatomical left-right asymmetry of language-related temporal cortex is different in left- and right-handers. Ann Neurol 29, 315-319.

Stephan, K.E., Weiskopf, N., Drysdale, P.M., Robinson, P.A., Friston, K.J., 2007. Comparing hemodynamic models with DCM. Neuroimage 38, 387-401.

Stoodley, C.J., Schmahmann, J.D., 2010. Evidence for topographic organization in the cerebellum of motor control versus cognitive and affective processing. Cortex 46, 831-844.

Strick, P.L., 1988. Anatomical organization of multiple motor areas in the frontal lobe: implications for recovery of function. Adv Neurol 47, 293-312.

Vaid, J., Bellugi, U., Poizner, H., 1989. Hand dominance for signing: clues to brain lateralization of language. Neuropsychologia 27, 949-960.

Vogt, C., Vogt, O., 1919. Allgemeinere Ergebnisse unserer Hirnforschung. J Psychol Neurol 25, 279-461.

Volkmann, J., Schnitzler, A., Witte, O.W., Freund, H., 1998. Handedness and asymmetry of hand representation in human motor cortex. J Neurophysiol 79, 2149-2154.

Wang, L.E., Fink, G.R., Diekhoff, S., Rehme, A.K., Eickhoff, S.B., Grefkes, C., 2011. Noradrenergic enhancement improves motor network connectivity in stroke patients. Ann Neurol 69, 375-388.

Ward, N.S., Brown, M.M., Thompson, A.J., Frackowiak, R.S., 2003. Neural correlates of motor recovery after stroke: a longitudinal fMRI study. Brain 126, 2476-2496.

Wise, S.P., 1985. The primate premotor cortex: past, present, and preparatory. Annu Rev Neurosci 8, 1-19.

Witt, S.T., Laird, A.R., Meyerand, M.E., 2008. Functional neuroimaging correlates of finger-tapping task variations: an ALE meta-analysis. Neuroimage 42, 343-356.

Yan, L.R., Wu, Y.B., Hu, D.W., Qin, S.Z., Xu, G.Z., Zeng, X.H., Song, H., 2012. Network asymmetry of motor areas revealed by resting-state functional magnetic resonance imaging. Behav Brain Res 227, 125-133.

List of abbreviations

ALE: activation likelihood estimation

ArS: arcuate sulcus

BOLD: blood-oxygenation-level-dependent

CBF: cerebral blood flow

CBV: cerebral blood volume

CC: corpus callosum

CgG: cingulate gyrus

CgS: cingulate sulcus

$CMRO_2$: oxygen consumption rate

CS: central sulcus

CST: corticospinal tract

BA: Brodmann area

BMS: Bayesian Model Selection

BOLD: blood-oxygenation-level–dependent

CMA: cingulate motor area

DCM: dynamic causal modeling

DMN: default mode network

DTI: diffusion tensor imaging

EEG: electroencephalography

EHI: Edinburgh Handedness Inventory

EPI: echo planar imaging

FDR: false discovery rate

fMRI: functional magnetic resonance imaging

FoV: field of view

FWE: family wise error

GLM: general linear model

HRF: hemodynamic response function

IFG: inferior frontal gyrus

IPS: intraparietal sulcus

LQ: laterality quotient

M1: primary motor cortex

PM: premotor cortex

PMd: dorsolateral premotor cortex

PMv: ventrolateral premotor cortex

ROI: region of interest

SMA: supplementary motor area

SPL: superior parietal lobe

SVM: support vector machine

TE: echo time

TMS: transcranial magnetic stimulation

TR: time of repetition

V1: primary visual cortex

VOI: voxel of interest

Personal contribution to the publications

3.1 Network dynamics engaged in the modulation of motor behavior in healthy subjects.
I designed the study under supervision of C. Grefkes, performed the experiment (together with A.K. Rehme), analysed the data and wrote the manuscript.

3.2 Handedness and effective connectivity of the motor system.
I designed the study under supervision of C. Grefkes, performed the experiment (together with A.K. Rehme), analysed the data and wrote the manuscript.

3.3 Functional resting-state connectivity of the human motor network: Differences between right- and left-handers
I designed the study under supervision of C. Grefkes, performed the experiment (together with A.K. Rehme), analysed the data and wrote the manuscript.

Danksagung

Zunächst möchte ich mich bei Prof. Dr. Christian Grefkes für all seine Unterstützung in den letzten Jahren bedanken. Lieber Christian, Du hast es mir ermöglicht, eigenverantwortlich zu arbeiten, hast mich meine (Um-) Wege gehen lassen, aus denen ich lernen konnte, und mich immer wieder vor Aufgaben gestellt, an denen ich wachsen konnte. Danke.

Bedanken möchte ich mich auch bei Prof. Dr. Ansgar Büschges und Frau Prof. Dr. Visser-Vandewalle für die Bereitschaft mich seitens der Universität zu betreuen. Ich danke Ihnen für Ihr Interesse an meiner Arbeit und für Ihre Unterstützung in allen wissenschaftlichen und organisatorischen Fragen.

Ein weiterer Dank gilt Prof. Dr. Gereon Fink und Prof. Dr. Simon Eickhoff, durch deren Kommentare und Anregungen ich meine Forschungsarbeiten immer wieder neu beleuchten, kritisch hinterfragen und weiterentwickeln konnte.

Ich möchte mich auch bei allen derzeitigen und früheren Mitgliedern der Arbeitsgruppe Neuromodulation & Neurorehabilitation bedanken, die auf vielfältige Art und Weise meine Arbeit begleitet und mich unterstützt haben. Ein großes Dankeschön gilt dabei Dr. Anne Kathrin Rehme. Danke für Deine Unterstützung, die stetige Diskussionsbereitschaft und die tolle Zusammenarbeit in den ganzen letzten Jahren.

Ich danke auch meiner Familie und ganz besonders meinen Eltern für Ihre Unterstützung während des Studiums und darüber hinaus, wodurch es mir überhaupt erst möglich war, diesen Weg zu gehen.

Ein ganz besonderer Dank gilt meinem Mann. Lieber Michael, Du hast mir stets verständnisvoll den Rücken freigehalten, mich bestärkt, wenn ich gezweifelt habe und mich immer liebevoll unterstützt. Danke.

Erklärung

Ich versichere, dass ich die von mir vorgelegte Dissertation selbständig angefertigt, die benutzten Quellen und Hilfsmittel vollständig angegeben und die Stellen der Arbeit – einschließlich Tabellen, Karten und Abbildungen –, die anderen Werken im Wortlaut oder dem Sinn nach entnommen sind, in jedem Einzelfall als Entlehnung kenntlich gemacht habe; dass diese Dissertation noch keiner anderen Fakultät oder Universität zur Prüfung vorgelegen hat; dass sie – abgesehen von unten angegebenen Teilpublikationen – noch nicht veröffentlicht worden ist, sowie, dass ich eine solche Veröffentlichung vor Abschluss des Promotionsverfahrens nicht vornehmen werde. Die Bestimmungen der Promotionsordnung sind mir bekannt. Die von mir vorgelegte Dissertation ist von Univ.-Prof. Dr. Christian Grefkes, Univ.-Prof. Dr. Ansgar Büschges und Univ.-Prof. Dr. Veerle Visser-Vandewalle betreut worden.

Köln, den 14. November 2014